ABSTRACT

Title of Document: INTERCOMPARISON AND VALIDATION OF CONTINENTAL WATER LEVEL PRODUCTS DERIVED FROM SATELLITE RADAR ALTIMETRY, MODELING AND FORECASTING TROPICAL LAKE LEVELS

Martina Ričko, Doctor of Philosophy, 2012

Directed By: Professor James A. Carton
Department of Atmospheric and Oceanic Science
And
Dr. Charon M. Birkett
Earth System Science Interdisciplinary Center

This dissertation focuses on validating the use of satellite radar altimetry products to observe and forecast water level in lakes and reservoirs.

Satellite measurements of lake and reservoir water levels complement *in situ* observations by providing stage information for ungauged basins and by filling data gaps in gauge records. Yet different satellite radar altimeter-derived continental water level products may differ significantly due to choice of satellites, geophysical corrections, etc. To explore the impacts of these differences, in the first part of this dissertation a direct comparison between three different altimeter-based lake level estimates is presented and validated with lake level gauge time series for lakes of a variety of sizes and conditions (e.g. whether they freeze seasonally). This comparison provides quantitative estimates of the error in lake levels as well as advice on product

choices to end users. The largest discrepancies among the altimeter products occur for the lakes that freeze.

In the second part of this dissertation a simple water balance model is developed relating net freshwater flux on a catchment basin to lake level. The model is constructed with two empirical parameters: effective catchment to lake area ratio and time delay between freshwater flux and lake level response. This model allows comparison of observed net freshwater flux with the lake level estimates from altimetry for a series of 12 tropical lakes distributed across three continents. The results show encouraging agreement between these independent datasets.

The third part of this dissertation uses the simple lake model, developed in the second part of this dissertation, and applies it to NOAA's Climate Forecast System (CFS) coupled model thus allowing us to produce seasonal lake level forecasts based on seasonal predictions of net freshwater flux. In the CFS net freshwater flux data bias with respect to the independent reanalysis is determined. One example of such a lake level model forecast is presented, showing promising significant results over most examined tropical lakes, but failing for reservoirs and smaller lakes. Model forecast bias with respect to altimeter observations is proposed to be further investigated for multiple lead times.

INTERCOMPARISON AND VALIDATION OF CONTINENTAL WATER LEVEL PRODUCTS DERIVED FROM SATELLITE RADAR ALTIMETRY, MODELING AND FORECASTING TROPICAL LAKE LEVELS

By

Martina Ričko

Dissertation submitted to the Faculty of the Graduate School of the
University of Maryland, College Park, in partial fulfillment
of the requirements for the degree of
Doctor of Philosophy
2012

Advisory Committee:
Professor James A. Carton, Chair
Associate Research Scientist Dr. Charon M. Birkett
Professor Rachel T. Pinker
Professor Robert Hudson
Professor Eric S. Kasischke, Dean's Representative

Preface

This work derives almost entirely from published (Chapter 3) and submitted or in preparation research articles (Chapter 2 and 4). As such, each Chapter (2-4) has its own Introduction, Methodology, Results, and Conclusion sections, as required by peer-reviewed publications. A certain amount of overlapping in the introductory sections of the first four Chapters is also inevitable, given that they investigate different aspects of the same research topic. Two Chapters connect three topics: Chapter 1 provides a general introduction and motivation of the work in the framework of current lake level research, and Chapter 5 gives an overall summary and concluding remarks.

Acknowledgements

There are a great many people to whom I wish to thank for their encouragement and support. First, I would like to thank the members of my family. Especially I thank my mom, Ivanka, for all her love and support that she has given me and for all the sacrifices that she made to help put me through my seemingly unending schooling.

I am very grateful to my advisors, Professor James A. Carton and Dr. Charon M. Birkett, for their valuable guidance and support, and for affording me the opportunity to do exciting, relevant, and novel research. I would like to thank Charon for her generously long hours of discussions, always encouraging me, and sharing her knowledge and ideas. I would like to thank Professor Robert Hudson, Professor Rachel T. Pinker and Professor Eric S. Kasischke for very pleasant and inspiring experience during our teaching sessions over past few years. Also I thank them all for reviewing my dissertation and serving on my committee.

I also acknowledge the Faculty and Staff of the Department of Atmospheric and Oceanic Science, and especially wish to thank to Tammy Hendershot for always making sure I was on top of every deadline.

I would like to thank to all collaborators who contributed to this work, Jean-François Crétaux, Jérôme Benveniste, Richard Smith, Philippa Berry, and Jiande Wang, with providing the data, and generously providing any needed information.

And finally thanks to all my friends for their friendship, and patience for not being available most of the time during my long graduate school years.

Table of Contents

List of Tables

List of Figures

Chapter 1: Introduction

1.1 Background

The water volume stored within lakes and reservoirs is a very sensitive proxy primarily for precipitation; as well as for other climatic parameters through evaporation, temperature, surface pressure, wind stress, radiation (both short and long wavelength); and for hydrologic parameters such as groundwater and runoff (Crétaux et al. 2010). Lakes are thus great targets that may be used to study the combined impact of climate change and water resources management. Water management generally directly affects the water balance parameters of a lake, through irrigation, hydropower industry, or human consumption; while climate change affects the hydrological cycle and alters the water balance of a lake through long-term changes in temperature and precipitation.

The assessment of lake water balance could provide better knowledge of regional and global climate change. In addition, a quantification of the human stress on water resources across all continents is also an important factor.

Monitoring and predicting water availability plays a critical role in most parts of the world and particularly for agrarian economies of the tropics (Glantz et al. 1991; Anyamba and Eastman 1996) as demand for water is growing because of population growth. Industrial growth and economic development may strongly influence future demand for water as well. In the past decade improvements in satellite radar altimeter estimates of river and lake levels offer an exciting additional monitoring tool to

complement declining networks of *in situ* gauges owing to cost, maintenance and agreements that address issues of water between the countries (e.g., Crétaux and Birkett 2006; Anyah et al. 2006; Birkett et al. 2011; Crétaux et al. 2011a). However, prediction systems are still limited since current climate models with their low horizontal resolution (e.g., 125-250 km) do not resolve detailed hydrologic processes at the level of individual lakes.

1.2 Statement of the Problem and Significance

This research is aimed at investigating several relevant issues relevant to continental water bodies: tropical and global lakes and reservoirs at *intraseasonal*, *interannual* to *decadal* time-scales. The topics studied in the following Chapters target the important procedures of: *validating satellite radar altimetry products*, and *modeling* and *forecasting* of water level in lakes and reservoirs. A short description of the framework, significance, and motivation for each issue follows hereafter. More comprehensive and specific background and context are provided at the beginning of each Chapter.

1.2.1 Validation of Global Lake Level Products

Satellite measurements of lake and reservoir water levels complement *in situ* observations by providing stage information for ungauged basins and by filling data gaps in gauge records (e.g., Crétaux and Birkett 2006; Berry and Benveniste 2010; Birkett et al. 2011; Crétaux et al. 2011a; Ričko et al. 2012). Yet different satellite radar altimeter-derived continental water level products may differ significantly

owing to choice of satellites, and data processing methods. To explore the impacts of these differences Chapter 2 intercompares three such available products for a set of 18 lakes and reservoirs distributed globally, and compares them against subset of 14 for which gauge data are available.

1.2.2 Modeling Tropical Lake Levels

The availability of satellite estimates of rainfall and lake levels offers exciting new opportunities to estimate and monitor the hydrologic properties of lake systems (e.g., Crétaux and Birkett 2006; Anyah et al. 2006; Calmant et al. 2008; Birkett et al. 2011; Crétaux et al. 2011a; Ričko et al. 2012). Earlier studies have focused on modeling of lake levels (e.g., Calder et al. 1995; Nicholson et al. 2000; Vallet-Coulomb et al. 2001; Kebede et al. 2006; Ricko et al. 2011), thus combined with simple basin models connections to climatic variations can then be explored with a focus on a future ability to predict changes in storage volume for water resources or natural hazards concerns. The investigation of a simple water balance model and its possibility of using rainfall to create seasonal forecasts of future lake levels and hindcasts of past lake levels is fundamental for the understanding of present-day and future variations in lake levels.

1.2.3 Forecasting Tropical Lake Levels

Current coupled climate forecast models, such as the National Centers for Environmental Prediction coupled atmosphere/ocean climate forecast model (CFSv2;

Saha et al. 2012), still do not have sufficient resolution to support full hydrologic system models. The most widely used water level forecasts are those for many of the U.S. rivers and watersheds, and especially for North American Great Lakes water levels that are typically based on more sophisticated mathematical computer simulation models. A recent assessment of one such model (the Great Lakes Advanced Hydrologic Prediction System (AHPS)), indicates that AHPS generally captures between 64 and 74% of the observed variability of Great Lakes water levels (Gronewold et al. 2011).

As an interim step, before better models are developed, the investigation in Chapter 4 supports the proposal to introduce the simple hydrologic model into such climate forecast models to forecast water levels in lakes on seasonal time scale whose spatial scales are well below that resolved by the climate model's horizontal grid. The investigation of the forecast model bias in representing hydrologic components is crucial for the understanding of present-day and future lake level variability.

1.3 Objectives

In relation to the issues described above, the major goals of this work were to:

- Assess the satellite radar altimetry-based databases: intercompare the available products, and validate them against *in situ* gauge time series where available;
- Investigate the ability of a simple basin model to estimate variations in water level for tropical lakes and reservoirs;
- Investigate the climate impacts of rainfall change over tropical lakes and reservoirs;

- Investigate biases and weaknesses of current global climate models in representing hydrological cycle;
- Investigate to advance the current seasonal climate forecasts of lake levels.

1.4 Dissertation Outline

Chapter 2 critically examines, validates and discusses three available continental water level products that derived from satellite radar altimetry. An observational analysis of the climate effects of intraseasonal to interannual variations of water levels in tropical lakes and reservoirs is presented in Chapter 3. An alternative approach to climate forecast models of the lake levels is analyzed in Chapter 4, which describes the results of experiments of lake level forecasts over tropical lakes and reservoirs. Finally, summary and concluding remarks follow in Chapter 5.

Chapter 2: Intercomparison and Validation of Continental Water Level Products Derived from Satellite Radar Altimetry[1]

2.1 Introduction

Measurement of surface water level for continental water bodies such as inland seas, lakes, and river systems presents multiple challenges, one of which is the need to compensate for the declining quantity of networks of *in situ* gauges. Recent improvements in satellite radar altimetry offers the possibility of more than compensating for this loss, and indeed providing near-global coverage of continental water levels with near-real time availability (Berry et al. 2005; Crétaux and Birkett 2006; Crétaux et al. 2011a; Birkett et al. 2011). As a result, a growing number of users are interested in applying altimetry level estimates to a wide variety of studies related to climate change, prediction of natural disasters such as floods and droughts, water resource and fishery management, navigation, sediment transport etc. These users include the climate community, who are primarily interested in historic water level estimates; and the geodetic community, who are interested in near-real time water level estimates for current alerts and predictions of water levels. The water management community also has a great interest in these altimeter products for the purpose of calculating changes in water storage necessary for water use and monitoring purpose. This study explores the use of continuous satellite radar altimeter water level estimates as applied to a reference set of 18 lakes and reservoirs, where

[1] This Chapter has been submitted to *J. Appl. Rem. Sens.* as Ričko et al. (2012).

the data generally spans a 19-year period (1992-2011), in monitoring continental surface waters.

Currently there are several altimeter water level product databases offering users a selection of water level measurements using published, but different techniques. They each provide guidelines on product accuracy, but validation studies tend to be limited to comparisons for those targets where *in situ* gauge data are available. Here, we undertake an intercomparison of products from three separate on-line databases: the National d'Etudes Spaciales (CNES) Laboratoire d'Etudes en Géophysique et Océanographie Spatiale (LEGOS) database for lakes, reservoirs, rivers and wetlands (Crétaux et al. 2011a); the Global Reservoir and Lake Monitor (GRLM) database, the United States Department of Agriculture's Foreign Agricultural Service (USDA/FAS) and National Aeronautics and Space Administration (NASA) funded product (Birkett et al. 2011); and the Global River and Lake product database produced by De Montfort University, a European Space Agency Project (ESA-DMU; Berry and Wheeler 2009). The objective for the study was to assess the three databases, i.e., intercompare the available products, and validate them against *in situ* gauge time series data where available. The findings from this study can be easily applied to research or operational programs, such as the short-term and long-term climate change studies, hydrological applications, and the operational short-term forecasts of continental water levels.

2.1.1 Satellite Radar Altimetry

Satellite radar altimeters are primarily designed to operate over oceans and ice sheets (for general information, see Fu and Cazenave 2001). As an altimeter satellite orbits the Earth, the nadir-viewing instruments continuously emit microwave pulses toward the surface. The altimetric range (the distance between the satellite antenna and surface) can be deduced from the two-way time delay between pulse emission and echo reception. This measurement, together with additional geophysical data and the known satellite orbital position, enables the topography of surface water level to be derived with respect to a single reference datum, for example a reference ellipsoid. As each satellite is placed in a repeat orbit (with the ground track accuracy of ±1 km), water level variations can be then constructed for a specific target (e.g., lake or reservoir) during the lifetime of the mission.

The main advantages of satellite microwave radar altimetry over laser altimetry in determining lake levels are: operational during day and night, and not being hindered by clouds, vegetation, or canopy cover. The fact that surface water level heights are given with respect to a common reference datum is especially useful in forming a globally consistent dataset. Altimeters can also provide water level information for targets where *in situ* gauge data are either not available at all, only intermittently available, or whose quality is suspect. The multiple samples altimetry provides of large lakes also allows for a better estimate of area-average surface height than is usual from *in situ* gauges. As a result of these advantages satellite altimetry offers a great ability to monitor monthly, seasonal, interannual and overall record

trend variations in water level (over the lifetime of the mission) for large numbers of lakes.

Altimeter height estimates have error sources that are generally independent of the errors found in gauge records. As indicated above, several factors need to be kept in mind when using satellite radar altimetry. The orbit parameters of a satellite altimeter determine both the temporal resolution (typically 10-35 day) of the water level measurements, as well as the spatial density and location of the ground tracks. The larger lakes (e.g., Lake Malawi and the Great Lakes of North America) are crossed by multiple ground tracks from multiple satellite altimeters, while the smaller lakes (e.g., Tonle Sap) only offer the option of height measurements from a single ground track from a single satellite system. The spatial sampling along each ground track (~350-660 m) also depends on the along-track sampling and averaging of the data during and after the satellite mission. The accuracy of each altimeter level product is affected by a number of factors. One important factor is the size of the lake (or the extent of water along the ground track), which determines the number of radar echoes collected that can be averaged along the satellite track. Additional factors include the complexity of the terrain surrounding the lake, the tracking logic software, and the algorithm used for processing of the echoes, all of which affect how quickly the lake surface is acquired, uniquely identified, and maintained. The surface roughness of the water (wave height), and various atmospheric and geophysical influences such as water vapor, wind, rate of precipitation, presence of ice, tides, and the corrections for these effects all play a role in product accuracy. The correction for changes in column water vapor is particularly important, and its accuracy depends on

the availability of simultaneous measurements from an onboard microwave radiometer or, if this is not available, the correction is estimated from the output of a global forecast model (Crétaux et al. 2009). A number of studies have examined the impacts of the complexity of the returned altimeter waveforms (radar echoes) and the sophistication of echo shape analysis algorithms on accuracy (Berry et al. 2005, 2007; Gommenginger et al. 2006; Frappart et al. 2006; Calmant et al. 2008).

A great number of studies have used radar altimetry to monitor water level variations of individual lakes, rivers, wetlands, and floodplains (e.g., Berry et al. 2002; 2005; Birkett 1995; 1998; 2000; Alsdorf et al. 2001; De Oliveira Campos et al. 2001; Mercier et al. 2002; Maheu et al. 2003; Bjerklie et al. 2003; Mertes et al. 2004; Coe and Birkett 2004b; Crétaux et al. 2005; Kouraev et al. 2007; Calmant et al. 2008; Medina et al. 2008; Getirana et al. 2009; Swenson and Wahr 2009; Becker et al. 2010; Birkinshaw et al. 2010; Kouraev et al. 2011; Lee et al. 2011; Ricko et al. 2011; Zhang et al. 2011), and a number of validation studies have already been performed (Crétaux et al. 2009; 2011a; Birkett et al. 2011; Frappart et al. 2006; Berry and Benveniste 2010). For the large open North American Great Lakes with wind-roughened surfaces, comparison of TOPEX/Poseidon (T/P) satellite radar altimetry with *in situ* gauge data provides a ~3-5 cm root-mean-square (RMS) difference estimate (Birkett 1995; Morris and Gill 1994; Shum et al. 2003), which we interpret as an estimate of altimeter height error. Crétaux et al. (2011a) found that for the biggest lakes (Victoria, Superior and Erie) this error is less than 10 cm. An example of an intermediate size lake, Lake Issykkul (not included in this study), gives a very low error estimate of 3 cm RMS (Crétaux et al. 2011b). Smaller lakes or sheltered

waters have larger errors due to having fewer radar echoes and poorer range resolution. In these cases the RMS difference estimates have been observed to range from tens of cm, (e.g., Lake Chad, Birkett 2000; Lake Winnebago and Lake of the Woods, Ross and McKellip 2006; Lake Kariba, Mar de Chiquita, and Titicaca, Crétaux et al. 2011a) to over a meter (e.g., narrow reservoirs such as the Lake Powell reservoir, Crétaux et al. 2011a; Birkett et al. 2011; Ross and McKellip 2006). These errors are still generally an order of magnitude smaller than that required to close the lake mass budget to first order and thus remain useful (Crétaux and Birkett 2006).

2.2 Datasets and Methods

2.2.1 Study Regions

We focus on a sample of 18 lakes and reservoirs distributed across three continents: 6 in Africa, 10 in North America, 1 in South America, and 1 in Southeast Asia (Fig. 2.1), for which altimetry products and in many cases *in situ* observations are available. The lakes have been selected to sample a range of important parameters: location, surface size, type, freezing, surrounding terrain, managed and unmanaged. Lakes smaller than (<100 km^2) generally are not sampled sufficiently by altimetry and thus are not included in this study.

On the African continent Lake Chad and the Volta Reservoir are located in central North Africa. Shallow (<7 m) Lake Chad experiences seasonal level fluctuations in the lake and surrounding marsh area, expanding in size from about 2000 km^2 to about 15,000 km^2 between dry and wet seasons. Most water loss is through evaporation and water extraction, though it has ~15% water loss through

ground seepage (Carmouze et al. 1983; Isiorho et al. 1996). The Volta Reservoir is the world's largest reservoir by surface area. It is located within the Ghana basin and is connected to the Atlantic Ocean through the Volta River. Two smaller African lakes are also included: Lake Tana, which lies in the Ethiopian Rift Valley, and the Kainji Reservoir, located to the southwest of Lake Chad. Finally, two large, deep lakes are included: Lake Tanganyika and the most southern Lake Malawi, both of which lie along the Rift Valley of eastern and central Africa.

On the North American continent we include the five Laurentian Great Lakes: Erie, Ontario, Michigan, Huron, and Superior, which are the largest group of freshwater lakes on Earth (containing roughly 22% of the world's fresh surface water). The smallest of these by area is Lake Ontario, while the shallowest and the smallest by volume is Lake Erie. The largest and deepest is Lake Superior. The Lake Michigan-Huron system, considered hydrologically as a single lake, exhibits the greatest range of level fluctuation of all the Great Lakes (Argyilan and Forman 2003). Lake Winnebago in the eastern region of the Wisconsin State, Lake of the Woods in Minnesota, and the northern Canadian Lake Athabasca are also included. The two largest reservoirs in the United States: Mead and Powell are examined as well. While Lake Mead is formed by water impounded by the Hoover Dam, Lake Powell is formed by the Glen Canyon Dam.

In Southeast Asia we include Lake Tonle Sap in Cambodia. This is the largest lake in Southeast Asia, and an important part of the Mekong hydrological system. With the start of the monsoon season in late May, Lake Tonle Sap begins to flood, and its shallow terrain means that its surface area rapidly expands as its level rises at a

rate of ~1000 km^2 per meter rise of level (Magome et al. 2004; Mekong River Commission 2005). In South America we consider Lake Guri, a reservoir whose dam and generator is a major source of hydroelectric power for Venezuela.

Eight lakes and reservoirs are located in the tropics and subtropics and do not experience the effects of an annual freeze and thaw cycle. In contrast, the North American lakes we consider except Powell and Mead freeze at least partially during the northern winter season. The freezing period for the Great Lakes starts in December and lasts until March, with maximum freezing area during February and March. For some lakes ice can last through whole northern spring season until May (especially smaller Great Lakes such as Erie and Ontario). Lakes Winnebago, Woods, and Athabasca can start freezing early in late November. The duration and extent of the freezing period varies from year to year.

Most of the lakes and reservoirs are controlled to some extent. However, the impact of management is probably largest for the reservoirs: Guri, Mead, Powell, Volta and Kainji. Most reservoirs are multipurpose; for irrigation, hydropower, flood control, water supply, navigation, fishing, and recreation (Avakyan and Iakovleva 1998). All lakes and reservoirs used for this study are freshwater and are permanent.

2.2.2 Satellite Radar Altimetry Products

There have been a number of satellite radar altimetry missions that have been used to construct water level products. The suite of NASA and CNES satellite missions consist of: TOPEX/Poseidon (T/P) (1992-2002), Jason-1 (2002-2008), and Jason-2/Ocean Surface Topography Mission (OSTM; 2008-present), all having a

9.92-day exact repeat cycle with a track spacing of 350 km at the equator, and operating at two frequencies (13.6 GHz in the Ku band and 5.3 GHz in the C band). These satellites have near-polar orbits spanning ±66^{o} latitude. The future Jason-3 satellite is scheduled to follow Jason-2 with an expected launch in 2013. This NASA/CNES suite is complemented by the ESA Earth Resources Satellite radar altimeters: ERS-1 (1991-1996) and ERS-2 (1995-2002), and the Environmental Satellite ENVISAT (2002-present). These all have a 35-day exact repeat cycle with 70 km equatorial track spacing, and an orbit spanning ±82^{o} latitude. ERS-1/2 operate in Ku band (13.8 GHz), while ENVISAT operates also at additional frequency 3.2 GHz (S band). The Naval Research Laboratory (NRL) GeoSat Follow-On (GFO) Mission satellite (2000-2008) is somewhat different from either of these satellite suites in that it had a 17.05-day exact repeat cycle with 170 km equatorial track spacing, and an orbit spanning ±72^{o} latitude, using a single frequency (13.5 GHz). In general, most of these satellites require a minimum target area >100 km^{2} or width >500 m to achieve sufficient data quality (Crétaux and Birkett 2006). The more recent Jason-2/OSTM and ENVISAT missions were specifically developed for monitoring continental water level as well as ocean and ice surfaces. A summary of the derivation of altimetric heights and their associated errors can be found in Appendix A. Here we examine three widely available products developed from these satellite datasets: (a) the LEGOS multi-satellite product; (b) the NASA and USDA/FAS product based on the GRLM database; and (c) the ESA-DMU Global River and Lake product (Crétaux et al. 2011a; Birkett et al. 2011; Berry and Wheeler 2009).

(a) LEGOS

The multi-satellite LEGOS product is available for 17 of the 18 lakes and reservoirs we consider and spans the period late-September/early-October 1992 until 2011. This product merges data from six satellites (T/P, Jason-1, Jason-2, ERS-2, ENVISAT, and GFO) and is updated once or twice per year. The product has been created using all standard corrections (orbit, ionospheric, wet and dry tropospheric corrections, polar and solid Earth tides, and sea state bias). For small reservoirs LEGOS uses also data from the Ice-1 retracker on ENVISAT and Jason-2, but for the lakes used in this study they were all calculated with 1 Hz data, except for the Powell and Mead reservoirs. Depending on the lake's size, the satellite data may be averaged over very long distances (spanning the lake), and for large lakes the data is corrected for the slope of the geoid. Because the reference geoid provided with the altimetry measurements (e.g., EGM96 for T/P data) may not be accurate enough for lake level estimation, LEGOS have computed a mean lake level by averaging the altimetry measurements over time. If different satellites cover the same lake, the lake level is computed in a 3-step process, in which each dataset is processed independently, then inter-satellite radar instrument range biases are removed using the T/P data as a reference (Crétaux et al. 2011a). The LEGOS product is distributed with approximately monthly time-resolution. For a few lakes, such as Bangweulu and Titicaca, the product begins in 2000, coincident, most probably, with the start of GFO in 2000. For Lake Tonle Sap the LEGOS product ends in 2002, most probably coincident with the demise of T/P. Crétaux et al. (2011a) notes that lake level accuracy is enhanced when multiple satellites are available.

The numerical values of the water level time series with associated standard deviations from the ensemble mean height (estimated from individual radar echoes) are referenced relative to the new improved resolution gravity model GRACE GGM02C (Tapley et al. 2005), and are freely accessible. In addition, the LEGOS database provides classification and division of the target type by separating reservoirs and river basins from lakes, but currently provides no information about ice presence. The LEGOS database currently covers 160 lakes and reservoirs and about 1300 river sites. Users can also visualize the geographic location of the lake and the multi-satellite ground track locations by utilizing Landsat imagery. A new updated version of the LEGOS database gives additional time series of surface and volume variation, with hypsometry and surface snapshots available for users interested in hydrological studies. Validation comparisons of the LEGOS products with *in situ* daily gauge data show that the product RMS accuracy ranges from a minimum of 3 cm for Lake Issykkul (Crétaux et al. 2011b), and 4-5 cm for the Great Lakes: Superior and Erie, to a maximum of 80 cm for small Lake Powell (Crétaux et al. 2011a).

(b) GRLM

GRLM provides both archived and near real time products for 16 of the 18 lakes and reservoirs considered in this study, spanning the period late-September/early-October 1992 until 2011 for most of the lakes. The main GRLM product has 10-day resolution and is derived from the three NASA/CNES satellites: T/P, Jason-1, and Jason-2/OSTM. The Jason-2/OSTM near real time observations are

obtained from the Interim Geophysical Data Records, available at a delay of 1-3 days after the satellite overpass and added to the existing time series on a weekly basis, and was the first to utilize near-real time radar altimetry data over inland water bodies in an operational manner (Birkett et al. 2011). Currently for some lakes GRLM also gives 17-day resolution data from the NRL/GFO mission satellite, but we do not use this product in our product comparison. All lakes and reservoirs (currently ~75 lakes >100 km^2) covered by GRLM are located within major agricultural regions. Because the original USDA/FAS requirements demanded only relative water level variations, the GRLM heights are given relative to a reference ellipsoid rather than a geoid-based datum.

GRLM relative lake level variations are provided with respect to a 9-year mean level derived from the first 9 years of T/P altimetry observations. Both the raw and smoothed versions of the time series are available. In addition to height information, the raw data contain an error estimate (discussed below) and a mean value of the strength of the radar backscatter coefficient. The latter serves as an indicator of surface roughness or potential for icy conditions (Birkett 1998; 2000). Large error estimates may denote interference from land (coastlines, islands) or dry lake-bed conditions. To the user the exact position along the satellite track where the heights were obtained, and the Jason-1 and Jason-2 inter-mission height bias (with respect to T/P) that was applied to merge the three satellite datasets, can be of importance as well. A second smoothed GRLM product uses a median type filter to eliminate outliers and reduce high frequency noise. The smoothed GRLM product

serves as a visual aid to identify significant lower frequency features in the unsmoothed GRLM product.

Product users must note that due to the filtering built into the on-board data processing software many radar echoes were lost over the surfaces of small or calm lake waters during the Jason-1 mission. In these cases the GRLM database offers an alternative product that incorporates height variations from the GFO mission. This alternative combined product has proved a mixed success in that it allows many gaps to be filled, but adds additional errors due to differences in the location of the ground tracks and instrumentation of the different missions. Validation of the NASA/CNES-based GRLM products with daily gauge data shows that RMS errors are smaller than 10 cm for the North American Great Lakes and other large and open lakes such as African Lakes Victoria and Tanganyika (Ross and McKellip 2006; Birkett et al. 2011). Smaller lakes that experience more wind sheltered conditions are expected to have RMS accuracies lower than 20 cm (e.g., Lake Chad, Sarch and Birkett 2000). Satellite passes that cross over narrow reservoir extents in severe terrain will result in RMS values of many tens of centimeters (e.g., ~1.6 m for Lake Powell, Birkett et al. 2011). A validation exercise by Birkett et al. (2002) of the height of rivers throughout the Amazon basin using just the T/P dataset provided RMS errors ranging from tens of centimeters to several meters with an average error of 1.1 m.

(c) ESA-DMU

The ESA-DMU River and Lake database covers 14 of the lakes and reservoirs examined in this study. These products are based on only two satellite radar

altimeters: i) the historical data from ENVISAT (2002-2010) available at approximately monthly resolution (35 days), and ii) the more recent near real time data from Jason-2/OSTM (2009-2011) available at 10-day resolution. The products are available with delays ranging from 3 days up to 4 months after the satellite overpass. Additional ERS-2 data (1995-2003) (courtesy of Richard Smith, De Monfort University) was provided to the authors at 35-day resolution and has been utilized in this study for five of the African lakes (Chad, Kainji, Tana, Tanganyika, Malawi) and for the Asian Lake Tonle Sap.

Processing of the ESA-DMU altimetry products starts by identifying ENVISAT and Jason-2 tracks sampling the chosen set of river and lake targets (Berry and Wheeler 2009). Individual waveform shapes are identified and passed on to the retracking system to determine the altimetric height. In order for the processor to identify more correctly the boundaries of continental water bodies and to recombine crossings over a single target, a box algorithm is used with pre-calculated database boxes holding the allowable coordinates for a given altimetric pass. After all the standard range and height corrections are applied (e.g., orbit corrections, atmosphere delays of radar pulses, instrument and surface related corrections), the altimetry range data is referenced to the EGM96 geoid model to construct sea level orthometric heights. For an easier direct comparison between different targets, the orthometric height products are referenced to a climatological mean computed by averaging over the full time period, thus creating a set of relative mean orthometric height time series.

Besides the time series of relative mean orthometric heights, to a climate user the most important information from the ESA-DMU products are the mean latitude and longitude, the total number of data points, and the number of good quality data (for most targets these two numbers coincide), along with the time series of standard deviations of the samples in the crossing. Variations in the ground track location, caused by the slight movement of the geographic position of satellite orbit tracks from cycle to cycle and the differences in the horizontal extent of the water at different times, are given as well.

The ESA-DMU product monitors a large number of targets: for ENVISAT the number is about 750, while for the recent Jason-2 the number is about 57 (Berry and Wheeler 2009). The product is freely accessible from the River and Lake web site for ENVISAT, and for some targets for Jason-2 as well. Users need to register and access the River and Lake web site via a login process. It is interesting to note that for several lakes, the ESA-DMU product is available on a grid point system, with multiple product options over the lake depending on the location. A user can therefore choose a record closest to the point of interest (e.g., close to *in situ* gauge station for validation), or take the mean of all given targets for a chosen lake or area. Large lakes can have several targets (Great Lakes each have 15-31), while smaller lakes such as Lake Tana can have only one target over the entire lake.

Several gauge validation comparisons have been performed for the ENVISAT Radar Altimeter 2 for river and lake targets in the Amazon basin showing RMS differences in the range of 25-53 cm (25–53 cm, Frappart et al. 2006; 36 cm, Benveniste et al. 2007; and 30 cm, Berry 2007). A recent extensive validation for

targets in the Amazon basin by Berry and Benveniste (2010) has shown that ENVISAT consistently has the lowest RMS error among the radar altimeters (0.47 m versus: ERS-2 0.63 m, TOPEX 1.84 m, and Jason-1 1.22 m). Da Silva et al. (2010) have shown that the use of recently improved retracking algorithms (e.g., Ice-1 and Ice-2) have allowed refined data selection, and when combined with other corrections these changes have lowered RMS errors to less than 20 cm. They have also improved the performance of ENVISAT, reducing errors to less than 30 cm. However, these generic retrackers work only under optimal conditions and have not been adjusted to obtain a lot of data over targets experiencing higher RMS errors, whereas more sophisticated ESA-DMU retrackers can process data over all targets.

2.2.3 In situ Gauge Data

Many *in situ* gauge networks have been reduced in density over the last few decades owing to geographical, political or economic constraints, and data is not publically released for many that are still operating (Alsdorf et al. 2003). Other limitations include the fact that gauges are generally located along the lake shore or near the outlets of the lakes and thus may not be representative of a lake area average. For some gauges the absolute location and its sampling rate are unknown. For most gauges, including those used in this study, no estimate of the measurement error is provided. It is generally thought that gauge measurement error ranges from 0.3 cm for continuous-record gauging stations up to about 1 cm depending on the location or position of the gauge site (e.g., slope, wind sheltered position) (WMO, 1994). No estimates are generally available for the error of representativeness, which is likely to

be larger than the measurement error. Most gauges are maintained for reasons other than climate monitoring, and thus are subject to problems such as interruptions and occasional reciting.

From online sources or by personal contact, we have obtained gauge time series for 14 of the case study lakes listed in Table 2.1. For example, water level data for the North American Great Lakes are given in the International Great Lakes Datum (IGLD, 1985). The distances between the gauge locations and the center position of the altimeter crossings varies between 9 and 444 km (see Table 2.1). The gauge observations are daily (except for Lake Tana for which we have monthly data) and each spans a portion or all of the period 1992-2011. For most lakes presented here a reference datum is not known, while for some (Lake Mead and Powell) elevation is given relative to sea level. For climate studies this fact is not relevant, though it is important to maintain the same gauge datum for the duration of the data time series.

2.2.4 Analysis Approach

Here we review the processing of the altimeter and *in situ* time series at the gauge locations. The following method was employed to adjust for differences in data product time spans and datums, and data gaps. First, data outliers (identified subjectively using the smoothed version of GRLM time series as a visual aid) were removed. Overall, the GRLM dataset had the most outliers and also had several gaps of missing data especially during Jason-1 (2002-08).

The GRLM products that consist of three separate satellites (T/P, Jason-1, and Jason-2/OSTM) are combined into one time series, such that overlapped data of

Jason-1 with T/P at the beginning and Jason-2/OSTM at the end of Jason-1 period are removed (due to gaps and larger errors) and replaced by T/P and Jason2/OSTM. Similarly, for the period of overlap between the ERS-2 and ENVISAT (2002-03), the ERS-2 overlapped data are removed. The altimeter time series are then aligned with the gauge time series. For lakes that experience large gaps of gauge data altimeter datasets are aligned with respect to the LEGOS data.

After outliers and overlapped data are removed, the products are interpolated to a uniform 1-day time interval. To quantify possible interpolation error arising from this method, the gauge data and altimetry products have been compared with an alternative method of constructing the latter that uses paired raw altimetry data from the closest ±5 days. The two methods result in only small differences when applied to a case study of the five Great Lakes. For the rest of this study we use the daily interpolated time series exclusively.

2.3 Results

2.3.1 Product Error Estimates

An important concern arises for the users when trying to deduce the total height error from the error estimates provided by each of the three radar altimetry products. Interestingly, estimates from different products need not agree, owing to the varying instruments and processing methods among the product datasets. We are interested to see if the internal error estimates are consistent with the differences between altimeter-based and gauge level estimates. Also, users want to know which parameters contribute the most and how they are estimated.

To evaluate the consistency of error estimates, a comparison of the error estimates provided by the three products (LEGOS, GRLM, and ESA-DMU) with the RMS differences between the products and gauges for 14 lakes and reservoirs follows (Fig. 2.2). For LEGOS the largest product error occurs for Lake Tonle Sap (0.81 m) followed by reservoirs Powell, Kainji, Guri, Mead, and Volta (0.20-0.36m). For GRLM the largest error values are observed for Powell reservoir (0.74 m) followed by Kainji, Guri, Tonle Sap, and Volta (0.19-0.29m); while for ESA-DMU the largest error values are for the Kainji reservoir (0.92 m) followed by Lake Woods, Tana, Tonle Sap, and Athabasca (0.21-0.38m). The smallest error estimates occur for the Great Lakes in all three products (0.04-0.05 m for GRLM, 0.06-0.07 m for LEGOS, and 0.08-0.11 m for ESA-DMU). We conclude that although the order of which lakes have the lowest error varies among the altimetry products, reservoirs and smaller lakes tend to have the largest product internally estimated errors.

The RMS differences between altimeter and gauge water level compare well to all GRLM and ESA-DMU median internal error estimates, with the largest discrepancy occurring for Guri (0.82 m vs 0.20 m for GRLM; 1.08 m vs 0.01 m for ESA-DMU) and Volta reservoir (0.35 m vs 0.07 m for GRLM; 0.36 m vs 0.20 m for ESA-DMU). They tend to be larger than the internal LEGOS error estimates, mostly lying in the upper 75 percentile of LEGOS internal errors except for Lake Chad and Lake Ontario.

2.3.2 Validation of Altimetry Water Level Products using In situ Observations

First, in order to estimate the error in the gauge data itself, due, for example, to the representativeness of a single gauge station interpreted as a lake average, water level heights from four gauge stations located along the shores of Lake Ontario (at Eolcott, Cape Vincent, Oswego, and Rochester) have been compared for our base period 1992-2009. The average RMS difference among those 4 gauge stations is 3 cm (varying between 2 and 4 cm). The average RMS difference between gauge and altimetry height for this lake is 6 cm (Table 2.3). If we assume the errors are uncorrelated and that the former provides an estimate of the gauge observation error (actually it should be a 40% over-estimate if the errors are uncorrelated), then we may conclude that the RMS error in the altimetry itself is $(36-9)^{1/2} \approx 5.2cm$. Thus in this case at least, it is evident that the RMS difference between altimeter and gauge heights is a reasonable estimate of the RMS error in the altimeter height itself.

For our set of lakes for which both the ERS-2 and ENVISAT data are available (Chad, Tana, Kainji, Tanganyika, Malawi, and Tonle Sap) a comparison of the two data sets shows that ENVISAT has up to a 33% lower error, consistent with previous studies (Berry and Benveniste 2010; Da Silva et al. 2010). For Lake Tana, for example, we find RMS differences with respect to the gauge heights of 9 cm for ENVISAT, but 24 cm for ERS-2 (although we need to bear in mind that the two instruments were not contemporaneous and conditions may have changed).

Overall, the comparison of the altimeter products with gauge heights shows good agreement for 14 lakes and reservoirs (Table 2.2 shows correlation with a 95% confidence level interval and Table 2.3 shows RMS difference with standard error

interval that can be insignificant when error is rounded and given as 0). Interestingly, all reservoirs show excellent correlations among the three altimeter products (r between 0.93 and 1.00 significant at a probability level of 0.05). All of the Great Lakes have low RMS differences ≤ 10 cm, with the smallest difference of only 4-7 cm for Lake Superior. This result confirms previous studies reviewed above (e.g., 5-7 cm, Ross and McKellip 2006; ≤ 10 cm, Birkett et al. 2011; 4-5 cm for Superior and Erie, Crétaux et al. 2011a). We find the largest RMS differences for reservoirs, especially Powell (1.41 m for LEGOS), Guri (1.08 m for ESA-DMU), and Mead (0.59 m for LEGOS). These RMS difference estimates are also similar to published estimates (e.g., for Powell: 0.80 m by Crétaux et al. (2011a), 1.40 m by Ross and McKellip 2006, ~1.60 m by Birkett et al. (2011); and for Amazon basin: 1.10 m by Birkett et al. (2002)).

Figure 2.3 shows examples of 10 lakes and reservoirs for which gauge data is available illustrating the agreement between altimeter products and gauge time series (for compactness we include only one of the Great Lakes, Ontario, in this figure). At Lake Chad, the gauge data lag all three altimetry products by ~40 days. This is likely due to the fact that the gauge station at Bol is located in a seasonally inundated marsh region ~50 km northeast of the permanent waters of the lake. This time lag is somewhat comparable to a previous estimate of a 20 day lag (Coe and Birkett 2004b). In contrast, at Lake Tana gauge data leads the products by ~20 days when computed during the interval from late 2002 to 2011. Tana experienced an increase in the amplitude of its seasonal cycle from 16 cm to 21 cm in 2002 as seen in the gauge observations. This sudden increase in amplitude raises the question of the validity of

this gauge data, for example, whether gauge data before and after 2002 are from two different locations, or whether some other change in instrumentation is influencing these differences. The Guri reservoir, which appears to have a steady seasonal variation of ~6 m, reveals in its time series the effect of active water management. (Notice the seasonal maximum height is constant with time. Any additional water is spilled. When the water level drops below about -24 m, the power-generation at Guri would stop. When water levels approach this value water conservation is imposed).

Interestingly, the lakes that freeze (Great Lakes, Lake of the Woods, and Lake Athabasca) show higher mean correlations (0.86-0.92) and lower RMS differences (13-16 cm) among the altimetry products during summer (June-August), while during winter (December-February) mean correlations are slightly smaller (0.81-0.90) with larger RMS differences (16-21 cm). Lake Athabasca shows erroneously large differences between the altimetry products and the gauge data during the seasonal minima of certain years (e.g., 1995, 2001, 2004, 2005, 2007, and 2008), where these differences for LEGOS can range up to 1.69 m in 1995. Similar differences between the altimetry products and the gauge data during seasonal minima are observed in the Lake of the Woods time series during several years as well (maximum of 1 m in 2007 for the ESA-DMU product). These differences are most probably due to the poor performance of radar altimeters during those periods when Lake Athabasca and Lake of the Woods freeze. The information about what the *in situ* gauge at the lake is measuring and where the gauge is located (for example, how deep under the ice) during lake's freezing period is unknown, but could help explain for some of the observed differences.

Even though many data outliers in the GRLM product water level time series for Lake of the Woods have been removed prior to the comparison with the gauge data, and the gauge dataset for Lake of the Woods experiences a 3-year gap during 1994-1997, those two datasets correlate better during the shorter overlapped time period (1992-2002, r = 0.90) than during the full time period (1992-2011, r = 0.86). Only the GRLM (T/P) dataset complements the missing gauge observations during that time, as both the LEGOS and ESA-DMU products for Lake of the Woods begin from the end of 2002. RMS differences between the altimetry products and the gauge data range from 19-27 cm, comparable to Ross and McKellip's (2006) value of 26 cm. Many data outliers in the GRLM product water level time series for Lake Winnebago also had to be removed prior to comparison with the gauge data. GRLM shows many data gaps, and the other two altimetry products cover this lake reflecting a lack of data from ESA satellites, thus it is not surprising that the GRLM product for Lake Winnebago has the lowest correlation with gauge time series (r = 0.73). The RMS difference between GRLM and gauge time series (11 cm) is significantly lower than Ross and McKellip's (2006) value of 27 cm, probably due to the greater length of our dataset and our removal of outliers.

Because the time range of the ESA-DMU data product is shorter than the other products, comparisons among the three altimeter products are restricted to 2002-2010 when all three altimetry data are available. The comparison is limited to 10 lakes and reservoirs (Chad, Volta, Tana, Guri, Woods, and five Great Lakes) for which most products and gauge data are available (Fig. 2.4; Tables 2.2 and 2.3). We find that LEGOS has insignificantly higher median correlation between the gauge and

altimetry data (0.97) than GRLM and ESA-DMU (0.96 and 0.94), with an insignificantly smaller spread of all correlation values (0.93-0.97) versus GRLM (0.93-0.98) and ESA-DMU (0.92-0.98). The slightly larger spread of RMS differences (6-34 cm) is observed between the GRLM and gauge data, while LEGOS and ESA-DMU follow closely (7-28 cm and 7-23 cm).

The median correlation between any two altimetry products shows excellent agreement (r = 0.95-0.97). Slightly larger spread of correlation values (0.92-0.98) is seen between GRLM and ESA-DMU than between LEGOS/ESA-DMU (0.94-0.99) and LEGOS/GRLM (0.93-0.97). Somewhat larger RMS differences (7-25 cm) observed between LEGOS and GRLM indicate that these two altimetry products differ more than any other two (LEGOS/ESA-DMU 7-15 cm and GRLM/ESA-DMU 7-23 cm). Lower correlations are evident (Fig. 2.4a) for Lake of the Woods and Lake Chad, while the largest RMS differences (Fig. 2.4b) occur for the reservoirs Guri and Volta.

Overall, the altimetry products (LEGOS, GRLM, and ESA-DMU) are in excellent agreement with the gauge observations (median correlations >0.95), and the correlations among the products are even slightly higher (0.97). A closer examination shows that the most accurate altimeter product with respect to the gauges varies for a given lake and during any period of time. We also acknowledge that our sample of 10 lakes is small, and their choice likely impacts the results.

The comparisons above have concentrated on relative lake level, but the question arises: as datum requirements of the various end-users vary, which datum should be provided? Here, we consider a special case, Lake Ontario, which has

accurate altimeter level estimates (RMS altimetry minus gauge difference is 6-7 cm). Figure 2.5 compares the orthometric heights directly. Since GRLM is not based on an orthometric system an approximation is made via calculating the mean reference ellipsoid height (38.08 m) across the reference ground track and subtracting the mean geoid height (-35.95 m using the Earth Gravitational Model 1996) at this geographical location (Brian Beckley, personal communication, 2011). The altimetry products are offset from the International Great Lakes Datum, for ESA-DMU (0.11 m), LEGOS (0.61 m), and GRLM (0.81 m). For climate studies this issue of the choice of datum does not impact the types of studies that interest most users. For other users the choice may be important.

2.3.3 Seasonal Cycle and Trends

Lake and reservoir water levels generally have distinct seasonal cycles due to seasonal cycles in thermal expansion, ice formation, and net water flux (Fig. 2.3). Because they are a periodic feature of these records the amplitude and phase of the seasonal cycle is an easy feature to identify and a useful feature to compare even if the time series do not completely overlap in time. Also, any sudden unexplained changes or trends in the observed seasonal cycle or systematic differences between the altimeter and gauge seasonal cycles may suggest a problem with the measurements or observing strategy, while trends that appear in both and are thus clearly real, are particularly interesting.

For most lakes and reservoirs the altimetric and gauge estimates of the seasonal cycle match quite well. Two exceptions are the reservoirs Powell and Guri,

both of which have significantly higher seasonal cycles in the gauge time series than in the altimeter time series (Table 2.4), perhaps reflecting local effects of the gauge placement. In contrast, Woods and Athabasca both have lower amplitudes in the gauge time series than in the altimeter product time series. For these lakes the differences may result from the impact of winter freezing on the altimeter returns, although the weak amplitudes may be affected by sampling errors as well.

Some lakes have multi-year changes in their seasonal cycles of water level. Lake Tana's seasonal amplitude has increased with time from 1.31 m prior to 2002 to 1.50 m in later years (apparent in both LEGOS and the gauge time series). In contrast, GRLM and LEGOS altimetry data confirm the observation of Ricko et al. (2011) that the seasonal cycle at Lake Chad has decreased in amplitude from in excess of 1.33 m prior to 2002 to 0.55 m according to GRLM; or from 1.42 m to 1.12 m according to LEGOS. Interestingly, ESA-DMU altimeter heights are low prior to 2002 and thus the change in amplitude in the early 2000s is not evident. Gauge data, in contrast, shows a slight increase in amplitude from 1.17 m to 1.21 m. These differences in estimates of the amplitude of the seasonal cycle could result from the use of varying satellites with different track locations, and different applied corrections, and the end-users should be aware of this.

In addition to seasonal variability the time series also show responses to distinct weather and climate events. For example, the Volta reservoir experienced extreme minima related to drought episodes during 1998, 2003-2004, and 2007. Heavy rainfall in 2010 led to a record high water level and forced the opening of the Volta dam spillway resulting in flooding events downstream (Gana News Agency

2010; Gana Media News 2010). Some lakes and reservoirs also experience long-term trends (here what we mean by long term is limited to the length of our 19 year records). These latter include the reservoirs in the drought-stricken and rapidly growing southwestern United States: Powell (-1.06 m yr^{-1}) and Mead (-3.03 m yr-1), according to the gauge time series. The altimeter data give similar trends for both (for Powell, LEGOS gives -1.13 m yr-1, and GRLM -0.69 m yr-1; for Mead, LEGOS m yr-1gives -2.70 m yr-1). For Powell the trend is somewhat misleading in that it is the result of a dramatic 35 m decrease in water level in the middle years of the record (1999-2005). The story is very different for Volta Reservoir where flooding, mostly since 2007, has caused an increase of nearly 10 m, evident in the altimeter time series as well. Also a significant positive trend is confirmed in water levels of Lake Malawi (0.11 m yr^{-1} according to all three altimetry products) due to an increase in rainfall (Ngondgondo et al. 2011). Some of the variations in the trends as observed in different products appear to be due to differences in satellite coverage, ground track position, and corrections applied, but for climate analysis purposes these variations in trend estimates are acceptably small.

2.4 Discussion and Conclusions

This study presents a validation exercise utilizing the freely accessible, LEGOS, GRLM and ESA-DMU operational lake products spanning almost two decades (19 years) of altimetry observations. The three products differ in the methodology used to estimate lake level. LEGOS (Crétaux et al. 2011a) combines more satellite datasets than the others. ESA-DMU performs a retracking of

waveforms of ERS and ENVISAT altimeters with their more complex surface tracking capabilities (Berry et al. 2005; 2007; Gommenginger et al. 2006; Frappart et al. 2006), as well as LEGOS for some small lakes.

All three radar altimetry products perform well for our sample of 18 lakes and reservoirs of varying latitude, size, surface roughness, and surrounding terrain. This conclusion is based on treating *in situ* gauges as accurate estimators of lake and reservoir levels and thus differences between the altimeter products and the gauge time series provide estimates of the error in the altimeter time series. However, as Crétaux et al. (2011b) points out for Lake Issykkul: technical problems with gauges, data gaps, as well as unrepresentative siting can easily increase the gauge error level to 4-5 cm, making them an unreliable source of ground truth if variations at the few cm level are required. Also, gauge time series are not publically available for many lakes and reservoirs, and if available are likely undocumented.

Examination of the internal error estimates based on comparison of multiple echoes shows some consistent patterns and reassuringly similar results from the three altimetry products. The North American Great Lakes have the smallest errors (<10 cm). The largest errors as determined by comparison to gauge time series occur for the lakes that freeze (Lake Athabasca and Lake of the Woods). For these lakes the RMS differences between the three products and gauge data are ≥50% of the lake level variability itself, most probably due to reduced performance of the radar altimeters when ice is present. Comparisons to gauge time series also show the lowest errors of only few cm (4-10 cm) again occur for the Great Lakes, while the errors increase to more than a meter for narrow Powell and Mead reservoirs, all consistent

with previously published studies (Ross and McKellip 2006; Birkett et al. 2011; Crétaux et al. 2011a). However, even for these smaller lakes the error levels appear to be sufficiently low to detect climate variability in the two-decade record.

The seasonal cycle of water level, which is a distinct and generally stable feature of most lakes and reservoirs, allows us to compare records that may not completely overlap in time. In doing so we find that agreement among different products varies for a given lake, perhaps due to differences in satellite ground track locations. In addition, differences in overpass time and mean reference frames might contribute to these differences. Thus, our assessment of the most accurate altimeter product varies for a given lake and period of time.

Finally, we examine the linear trends of water level. Some lakes and reservoirs, such as Mead, exhibit clear trends over the period of this study. For others, such as Powell, multi-year variability exists, but is not well-represented by a linear trend. These trends provide interesting insights into the changing climates and regional demands. The water level decrease for Mead reflects the persistent drought in the Southwestern United States and growing demand for water. Positive trends are evident for Volta (0.37 m yr-1) and Lake Malawi (0.11 m yr-1) due to an increase in frequency of rainfall events in these regions. However, whether or not a linear trend is appropriate, the individual estimates for the three altimeter products agree well.

For the climate community each of the products has their own advantages and limitations. For example, a useful option offered by ESA-DMU is the water level time series on a grid point system allowing multiple spatial averaging options for a single lake, so users can choose a time series closest to the geographical point of

interest. Even though LEGOS merges multiple satellites into one time series, the performance of LEGOS is similar to the other two altimetry products (up to ~80 cm RMS differences in case of Volta reservoir, which for climate studies is acceptable). Recently updated, LEGOS provides additional information in the form of surface and volume variation, with a time sequence of surface imagery for some lakes and reservoirs. GRLM does not reference water level heights to the orthometric system, as the other two products. However, the fact that the three products use different reference datums is not a concern for climate studies.

2.5 Recommendations and Future Plans

Both the World Meteorological Organization and the Global Climate Observing System identify lake and reservoir levels as forming a key climate reference dataset. In particular water level changes for a group of 79 lakes, including Chad and several Great Lakes, have been designated Essential Climate Variables (ECVs) as part of the Global Terrestrial Network for Lakes (GTN-L). A data center called HYDROLARE (www.hydrolare.ru) has been created by the State Hydrological Institute of St. Petersburg, Russia under the sponsorship of Global Climate Observing System and Global Terrestrial Observing System. The main purpose of HYDROLARE is to develop web-based delivery of the ECVs for the GTN-L lakes based on a combination of in situ gauges and remote sensing data, principally radar altimetry. This comparison between the *in situ* data and the three radar altimetry products is a step towards developing the regular comparisons required by HYDROLARE to fulfill its mission.

Our comparison of the three altimeter product water levels shows that there is still significant room for improvement. The error levels are still too large for some smaller lakes and reservoirs (e.g., Powell and Mead reservoir) where they exceed 0.5 m. We believe a key source of this higher error lies in ineffective atmospheric corrections used in the processing of altimeter data, and thus further efforts to improve atmospheric corrections are highly recommended. Even though some recent studies have shown considerable improvements in quality from current altimeters due to improvements in processing (Birkett and Beckely 2010), there is still additional room for improvement in waveform tracking logic and retracking methods to better identify the signal response of very small lakes in regions of highly varying terrain. Studies of data filtering options and the estimation of time series error estimates, including further checks on range corrections, are all still needed.

We encourage development of multi-satellite products as they allow coverage of a wider set of lakes and reservoirs, especially smaller ones, over longer periods. GRLM has already started and will continue in the future to incorporate data from the ERS and ENVISAT altimeters, thus allowing expansion of coverage to ~600 lakes. In addition, new geoid model implementation and corrections are under further development, and ESA-DMU plans to replace the current model EGM96 by a newer version of EGM09 or GOCE derived model solution. The ESA-DMU products involving ENVISAT and Jason-2 are available only since 2002, thus we recommend inclusion of the earlier ERS-2 dataset in ESA-DMU regardless of its poorer performance.

We encourage inclusion of ancillary information of interest to end-users such as ice presence, wind conditions, calm waters, storms/floods events, as well as additional information about lake basin parameters (e.g., surface areal extent, volume, temperature and salinity, surrounding soil moisture, land cover, precipitation, etc.). Indeed, for lakes at higher latitudes with seasonal ice cover, it is essential that products provide information on ice related parameters (e.g., ice and snow cover time, ice thickness). Currently, of the three products we examine only GRLM gives some information about the presence of ice, obtained from the backscatter coefficient. However, we note that LEGOS is developing a similar dataset and plans to apply the methodology to large seasonally-frozen lakes, in order to provide duration of ice appearance, and specific dates of ice events (e.g., the first appearance of ice, the formation of stable ice cover, the first appearance of open water, and the complete disappearance of ice) for each lake or sub-region of the lake that freezes (Crétaux et al. 2011a). LEGOS plans to update its database for these products every year after winter time, and give to users both remote sensing data (radar altimetry and SSM/I) and ice related *in situ* data.

Recent and upcoming technological improvements should greatly enhance the capability of satellite altimetry. Satellite laser altimetry (Lidar) could offer water level information at better spatial resolution and accuracies under cloud-free conditions, with additional information on the surface gradient and extent of surface waters. The Ice, Cloud, and Land Elevation Satellite (ICESat) 2003-09 mission, providing measurements of ice sheet mass balance, cloud and aerosol heights, and land topography and vegetation characteristics, offers some height retrieval capability that

has not been included in the products considered here. Soon an ICESat-2, a micro-pulse multi-beam (Yua et al. 2010) follow-on mission that provides denser cross-track sampling to resolve surface slope on an orbit basis, with improved elevation estimates over high slope areas and very rough areas, and sea ice estimates, will replace ICESat. Additional improvements will be gained with the next generation of satellite radar altimeters that will utilize enhanced technologies, such as the high inclination altimeters. Future missions include the Indian Space Research Organization's (ISRO)/CNES SARAL (Satellite with ARgos and ALtiKa) mission and the ESA Sentinel-3. Both altimeters should improve tracking, and have smaller footprints and finer range precision, ensuring continuity of the altimetry service currently available from ENVISAT and Jason-1/-2. A Ka-Band Radar Interferometer (KaRIn) is proposed by NASA/CNES for the Surface Water and Ocean Topography (SWOT) mission acquiring high-resolution elevation measurements (Fu et al. 2003; Alsdorf et al. 2007). The already operating CryoSat-2 mission carries a sophisticated radar altimeter SIRAL (SAR Interferometric Radar Altimeter) designed to improve measurements of icy surfaces. It provides high-resolution measurements of the thickness of floating sea ice and the surface of ice sheets accurately enough to detect small changes. Cryosat-2, and the future SARAL and Sentinel-3 missions, will be included in the future processing of the LEGOS product as well.

2.6 Tables

Table 2.1 Lakes and reservoirs used in this study. Columns show gauge station name, source, time period of data available, and distances between the gauge station and the middle position of the satellite radar altimeter track crossing over or near lake and reservoir (km) for LEGOS, GRLM and ESA-DMU.

				Distance (km)		
Lake	Gauge station	Source	Time period	Gauge - LEGOS	Gauge - GRLM	Gauge - ESA-DMU
Chad	Bol	Personal contact, J.-F. Crétaux	1992-2008	9	52	59
Volta	Akosombo	Volta River Authority	1999-2010	164	49	54
Tana	unknown	Personal contact, J. Ratsey	1992-2006	–	–	–
Mead	Hoover Dam	Lake Mead Water Database[a]	1992-2011	67	–	–
Powell	Glen Canyon Dam	Lake Powell Water Database[a]	1992-2011	126	83	–
Erie	Cleveland	NOAA[b]	1992-2011	82	82	102
Ontario	Oswego	NOAA[b]	1992-2011	88	76	153
Michigan	Milwaukee	NOAA[b]	1992-2011	119	80	35
Huron	Harbor Beach	NOAA[b]	1992-2011	169	174	111
Superior	Marquette	NOAA[b]	1992-2011	76	110	147
Winnebago	Oshkosh	USGS[c]	1992-2011	–	10	–
Woods	Warroad	USGS[c]	1992-2011	53	53	79
Athabasca	Crackingstone point	Environment Canada	1992-2009	89	–	75
Guri	Central Hidroelectrica Simon Bolivar	OPSIS[d]	2002-2010	444	10	21

[a]U.S. Bureau of Reclamation.
[b]National Oceanic and Atmospheric Administration (NOAA) Tides and Currents Database.
[c]U.S. Geological Survey (USGS) Database.
[d]Venezuelan electricity grid system operator (OPSIS), Boletin Estadistico Mensual del Sistema Electrico Nacional, 2008.

Table 2.2 Correlations among gauge and altimeter product time series of water level. Correlations have been computed over full time period for which both time series are available. 95% confidence intervals are included.

Lake	GRLM vs Gauge	LEGOS vs Gauge	ESA-DMU vs Gauge	LEGOS vs GRLM	LEGOS vs ESA-DMU	GRLM vs ESA-DMU
Chad	0.90 ± 0.02	0.91 ± 0.02	0.91 ± 0.02	0.94 ± 0.02	0.95 ± 0.02	0.91 ± 0.02
Kainji	–	–	–	0.95 ± 0.09	0.98 ± 0.08	0.93 ± 0.09
Volta	0.99 ± 0.10	0.98 ± 0.09	1.00 ± 0.11	0.98 ± 0.07	0.97 ± 0.10	0.99 ± 0.12
Tana	0.97 ± 0.02	0.97 ± 0.02	0.96 ± 0.02	0.99 ± 0.02	0.97 ± 0.02	0.97 ± 0.02
Tanganyika	–	–	–	0.99 ± 0.01	0.96 ± 0.01	0.95 ± 0.01
Malawi	–	–	–	0.99 ± 0.02	0.97 ± 0.02	0.98 ± 0.02
Mead	–	1.00 ± 0.31	–	–	–	–
Powell	0.99 ± 0.31	0.99 ± 0.26	–	0.98 ± 0.30	–	–
Erie	0.97 ± 0.01	0.95 ± 0.01	0.86 ± 0.01	0.95 ± 0.01	0.91 ± 0.01	0.93 ± 0.01
Ontario	0.98 ± 0.01	0.98 ± 0.01	0.96 ± 0.01	0.96 ± 0.01	0.96 ± 0.01	0.96 ± 0.01
Michigan	0.98 ± 0.01	0.98 ± 0.01	0.93 ± 0.01	0.97 ± 0.01	0.91 ± 0.01	0.91 ± 0.01
Huron	0.99 ± 0.01	0.99 ± 0.01	0.93 ± 0.01	0.99 ± 0.01	0.96 ± 0.01	0.93 ± 0.01
Superior	0.97 ± 0.01	0.97 ± 0.01	0.95 ± 0.01	0.96 ± 0.01	0.97 ± 0.01	0.96 ± 0.01
Winnebago	0.73 ± 0.01	–	–	–	–	–
Woods	0.86 ± 0.01	0.81 ± 0.01	0.81 ± 0.01	0.89 ± 0.01	0.93 ± 0.02	0.87 ± 0.01
Athabasca	–	0.91 ± 0.01	0.85 ± 0.02	–	0.92 ± 0.02	–
Guri	0.99 ± 0.20	0.99 ± 0.21	0.99 ± 0.23	0.99 ± 0.13	0.99 ± 0.21	0.99 ± 0.19
Tonle Sap	–	–	–	0.99 ± 0.09	0.98 ± 0.10	0.98 ± 0.10

Table 2.3 RMS difference among satellite and gauge observations of water level (m). RMS difference computed over full time period for which data is available. Standard error intervals are included.

Lake	GRLM vs Gauge	LEGOS vs Gauge	ESA-DMU vs Gauge	LEGOS vs GRLM	LEGOS vs ESA-DMU	GRLM vs ESA-DMU
Chad	0.29 ± 0.01	0.28 ± 0.01	0.29 ± 0.01	0.20 ± 0.01	0.19 ± 0.01	0.24 ± 0.01
Kainji	–	–	–	0.93 ± 0.04	0.73 ± 0.04	1.06 ± 0.05
Volta	0.54 ± 0.05	0.53 ± 0.04	0.20 ± 0.06	0.56 ± 0.03	0.61 ± 0.05	0.49 ± 0.06
Tana	0.18 ± 0.01	0.17 ± 0.01	0.21 ± 0.01	0.09 ± 0.01	0.17 ± 0.01	0.19 ± 0.01
Tanganyika	–	–	–	0.05 ± 0.01	0.14 ± 0.01	0.15 ± 0.01
Malawi	–	–	–	0.08 ± 0.01	0.17 ± 0.01	0.16 ± 0.01
Mead	–	0.59 ± 0.16	–	–	–	–
Powell	0.82 ± 0.16	1.41 ± 0.13	–	1.41 ± 0.15	–	–
Erie	0.06 ± 0	0.10 ± 0	0.10 ± 0	0.10 ± 0	0.10 ± 0.01	0.07 ± 0.01
Ontario	0.06 ± 0	0.06 ± 0	0.07 ± 0	0.08 ± 0	0.07 ± 0.01	0.07 ± 0
Michigan	0.08 ± 0	0.11 ± 0	0.07 ± 0.01	0.11 ± 0	0.08 ± 0.01	0.08 ± 0.01
Huron	0.06 ± 0	0.08 ± 0	0.07 ± 0.01	0.08 ± 0	0.05 ± 0.01	0.06 ± 0.01
Superior	0.05 ± 0	0.06 ± 0	0.05 ± 0	0.07 ± 0	0.04 ± 0	0.05 ± 0
Winnebago	0.11 ± 0.01	–	–	–	–	–
Woods	0.19 ± 0	0.27 ± 0.01	0.24 ± 0.01	0.20 ± 0.01	0.16 ± 0.01	0.21 ± 0.01
Athabasca	–	0.28 ± 0.01	0.28 ± 0.01	–	0.22 ± 0.01	–
Guri	0.82 ± 0.10	0.87 ± 0.11	1.08 ± 0.12	0.63 ± 0.06	0.76 ± 0.11	0.66 ± 0.10
Tonle Sap	–	–	–	0.44 ± 0.05	0.58 ± 0.05	0.68 ± 0.05

Table 2.4 Seasonal cycle amplitude (m) based on gauge and altimetry time series, computed over full time period for which data is available.

	Amplitude (m)			
Lake	Gauge	LEGOS	GRLM	ESA-DMU
Chad	1.20	1.32	0.98	1.11
Volta	3.01	3.34	2.94	3.40
Tana	1.34	1.42	1.45	1.44
Mead	3.82	1.21	–	–
Powell	5.33	3.25	4.18	–
Erie	0.36	0.35	0.31	0.29
Ontario	0.54	0.55	0.56	0.43
Michigan	0.30	0.32	0.34	0.30
Huron	0.29	0.30	0.31	0.28
Superior	0.27	0.27	0.24	0.25
Woods	0.38	0.74	0.60	0.67
Athabasca	0.60	0.95	–	0.90
Guri	10.07	8.46	6.99	8.86

2.7 Figures

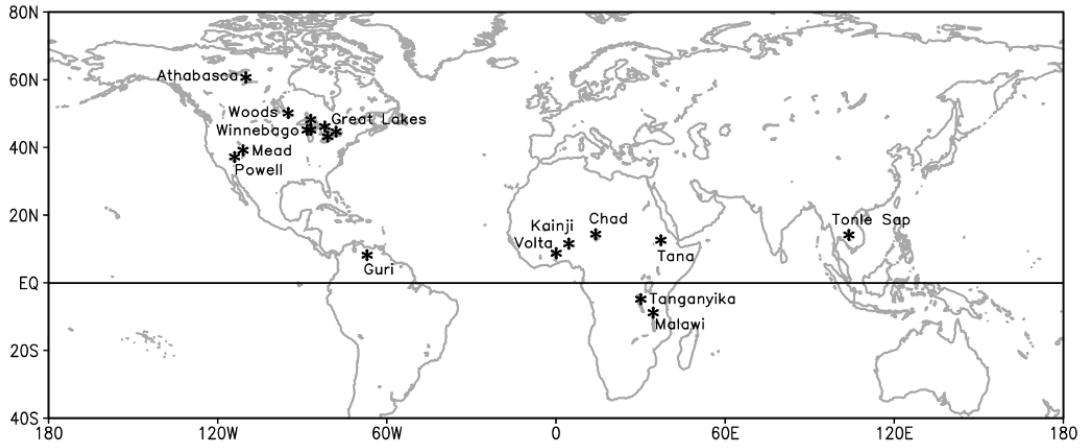

Figure 2.1 Locations of selected lakes and reservoirs (stars). The Laurentian Great Lakes consist of five lakes: Erie, Ontario, Michigan, Huron, and Superior.

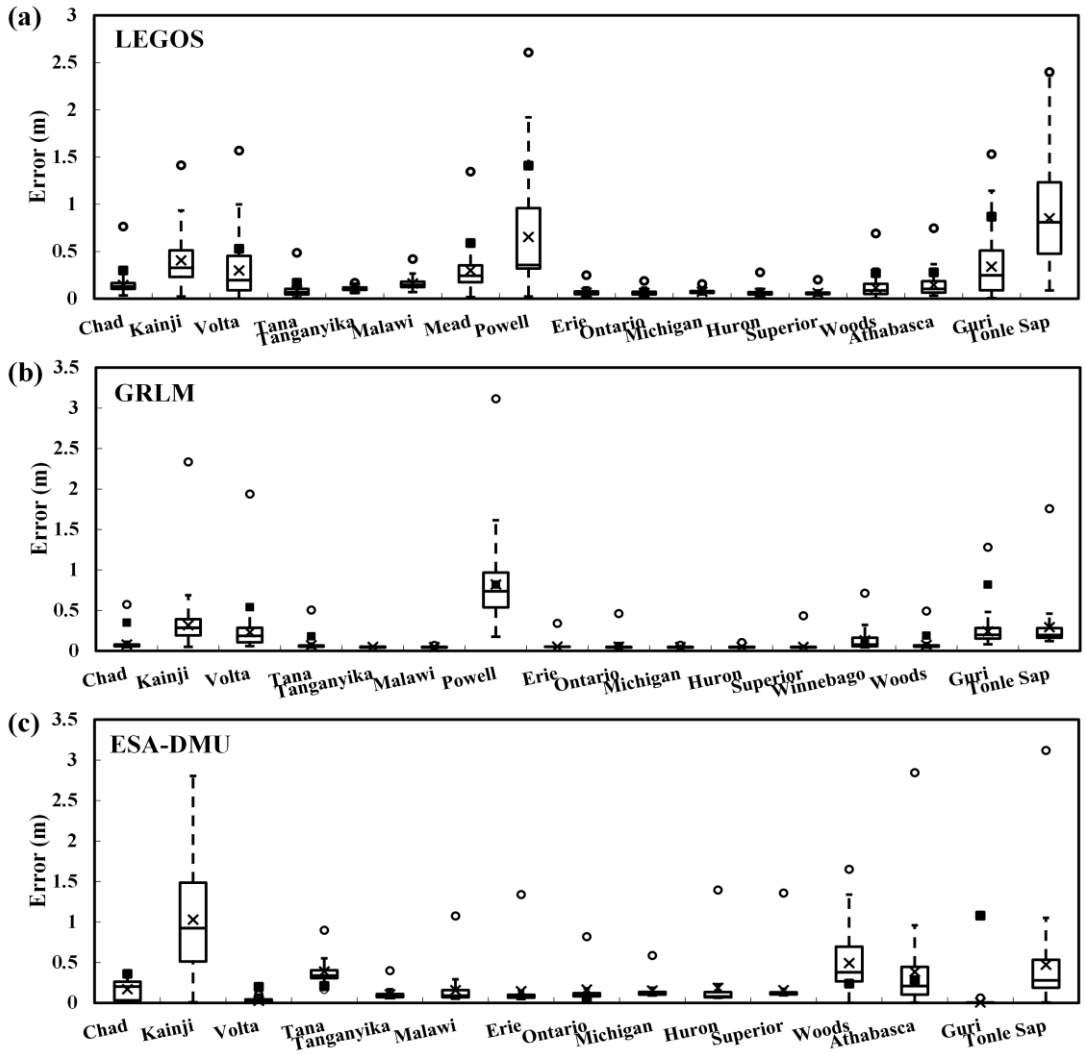

Figure 2.2 Box plots of error bars (m) given by: (a) LEGOS, (b) GRLM, and (c) ESA-DMU. The crosses show the mean of the errors for each lake or reservoir. Each box represents the 25th and 75th percentiles of the error, and the line in the middle of the box represents the median error (50th percentile). The ‘‘whiskers’’ extend to the farthest outlying errors that are no more than 1.5 times the interquartile range (difference between the 75th and 25th percentiles) away from the median. The open circle symbols beyond the whiskers denote outliers in altimetric errors, which are farther than 1.5 times the interquartile range from the median. The black boxes represent the observed RMS difference between the altimetry and gauge data.

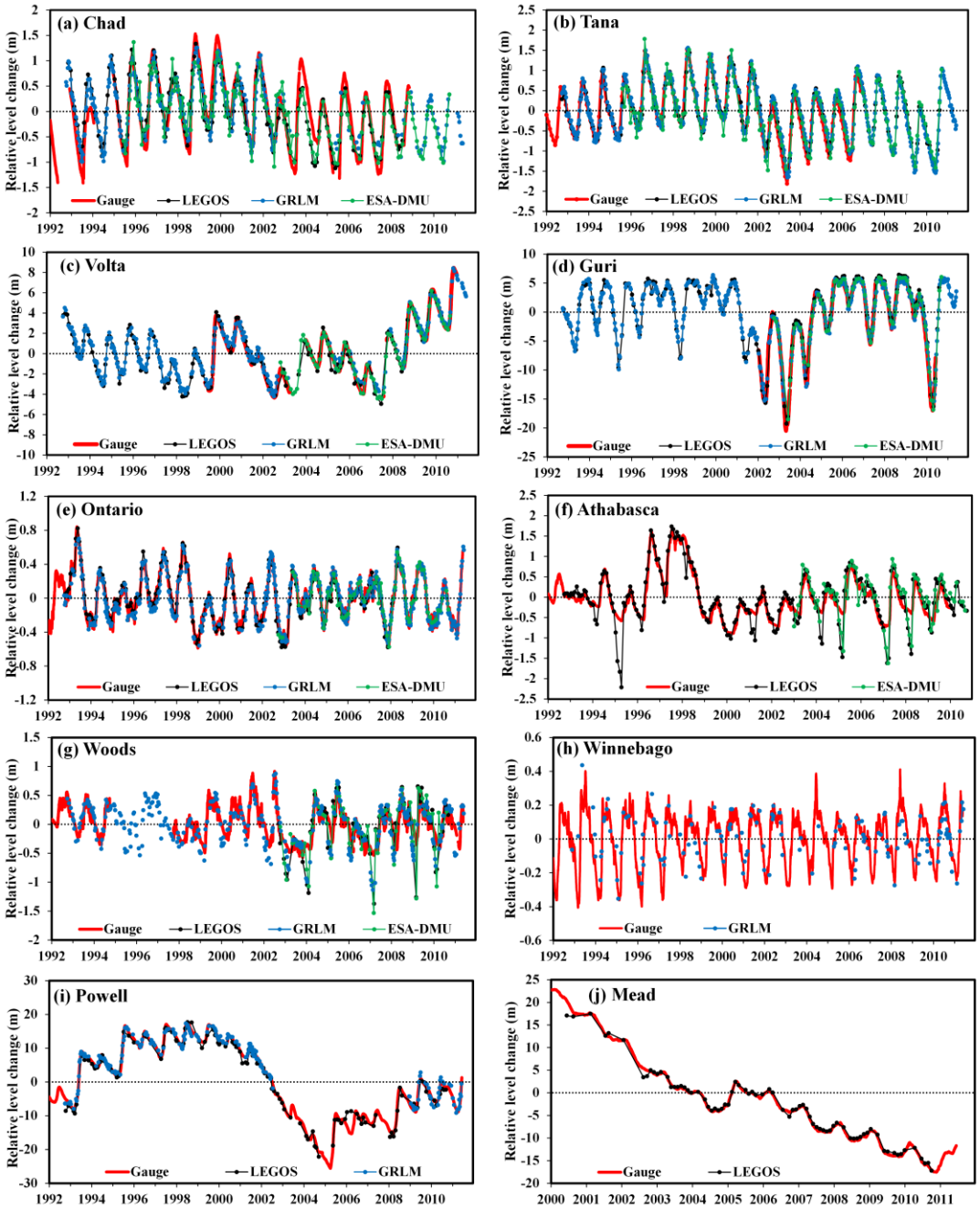

Figure 2.3 Comparison of the gauge observations (red) and altimetry products: LEGOS (black), GRLM (blue), and ESA-DMU (green) for ten lakes: (a) Chad, (b) Tana, (c) Volta, (d) Guri, (e) Ontario, (f) Athabasca, (g) Woods, (h) Winnebago, (i) Powell, and (j) Mead during 1992-2011.

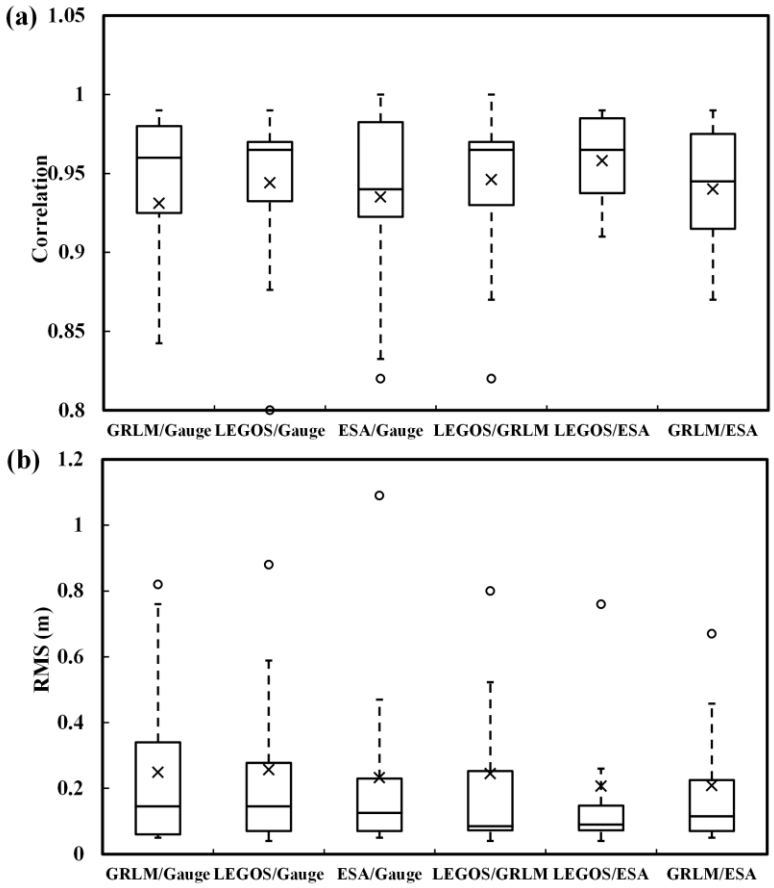

Figure 2.4 Box plots of (a) correlations and (b) RMS differences among altimetry water level products and gauge data for 10 lakes and reservoirs containing all three altimetry products (Chad, Volta, Tana, Guri, Ontario, Erie, Huron, Michigan, Superior, and Woods) during 2002-10. The crosses show the mean value of the correlation/RMS. Each box represents the 25th and 75th percentiles of the correlations/RMS, and the line in the middle of the box represents the median (50th percentile). The ‘‘whiskers’’ extend to the farthest outlying correlation or RMS difference that is no more than 1.5 times the interquartile range (difference between the 75th and 25th percentiles) away from the median. The circle symbols beyond the whiskers denote observed correlations/RMS, which are farther than 1.5 times the interquartile range from the median. Units of RMS errors are m.

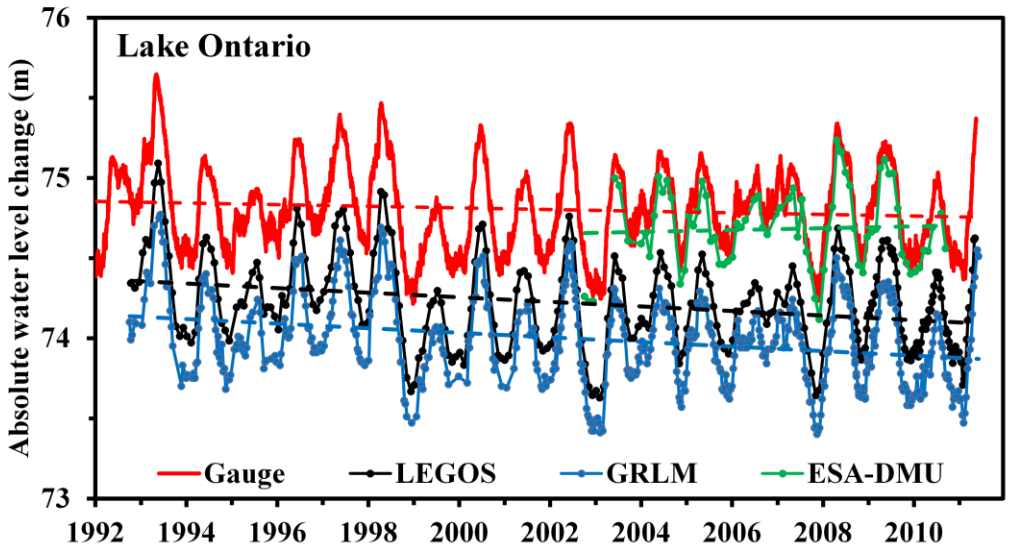

Figure 2.5 Absolute water level orthometric height (m) and linear trends for Lake Ontario during 1992-2011. Time series include Oswego station gauge observations (red), and altimetry products: LEGOS (black), GRLM (blue), and ESA-DMU (green). Dashed lines show linear trends computed from the time series. The height offset with respect to gauge observations is 0.61 m for LEGOS, 0.81 m for GRLM (which uses a different reference system), and 0.11 m for ESA-DMU.

Chapter 3: Climatic Effects on Lake Basins. Part I: Modeling Tropical Lake Levels[2]

3.1 Introduction

Monitoring and predicting water availability plays a critical role in most parts of the world and particularly for the agrarian economies of the tropics (Glantz et al. 1991; Anyamba and Eastman 1996). In the past decade improvements in satellite radar altimeter estimates of river and lake levels offer an exciting additional monitoring tool to complement declining networks of in situ gauges (Crétaux and Birkett 2006; Anyah et al. 2006). However, prediction systems are currently limited since current climate models do not resolve detailed hydrologic processes at the level of individual lakes. Here we exploit the simultaneous availability of estimates of net surface freshwater flux and lake levels during a 16-year altimetric satellite observation period (1992-2007) to develop simple models of water level variation for a sample of tropical lakes. The results of this study provide information on the values of the effective catchment to lake ratios and the time delay between freshwater flux and lake level response, allowing us to compare the consistency of independent rainfall and lake level observations. While we focus on tropical lakes, because of their strong seasonal and interesting interannual variability, the approach should be applicable to lakes at higher latitudes as well.

[2] This Chapter has been published as Ricko, Carton, and Birkett (2011).

Net surface freshwater flux is the difference between precipitation and evaporation over the catchment area. In the tropics net freshwater flux varies strongly seasonally, mainly as a result of seasonal variations in rainfall rather than evaporation. On monthly time scales the spatial distribution of rainfall is concentrated in atmospheric convergence zones where rainfall exceeds 10 mm day^{-1}. The principal convergence zones are the Intertropical convergence zone (ITCZ), and its intersection with tropical continents, the South Pacific and Atlantic convergence zones. Of these, the narrow zonally oriented ITCZ gives rise to the most striking variations in rainfall as it follows the seasonal shift of solar declination northward in boreal summer and southward in austral summer (Charney 1969), and its movements are thus responsible for the wet and dry seasons in the tropics.

Near the annual mean position of the ITCZ (generally a few degrees north of the equator) freshwater input reaches a peak twice a year in boreal spring and boreal fall, as the ITCZ passes overhead on both its northward and southward migrations. The distribution of regions with these semiannual rainy seasons is somewhat irregular spatially, particularly in the Amazon region (Sombroek 2001; Marengo et al. 2008). Farther poleward the seasonal rainfall is characterized by one wet season in the northern tropics during boreal summer and in the southern tropics during boreal winter.

In addition to seasonal variations, ITCZ rainfall exhibits strong interannual variability, notably associated with ENSO. During the northern winter of the warm El Niño phase of ENSO rainfall is enhanced in the central and eastern tropical Pacific as well as eastern tropical Africa, while drought conditions prevail in maritime

Australasia and in eastern equatorial South America (Ropelewski and Halpert 1996; Nicholson and Kim 1997). By northern summer of an El Niño year dry conditions extend throughout northern tropical South America, while the Indian Monsoon is reduced in strength. During the cool La Niña phase precipitation patterns are approximately reversed, with dry conditions in the central and eastern tropical Pacific and eastern Africa and anomalously wet conditions in maritime Australasia in northern winter. By the following summer anomalously wet conditions span northern South America as well as India (due to a strengthening of the Indian monsoon). During our 16-year period of interest there were five El Niño events: a strong and long-lasting event in 1997-98, substantial events in 1992-93 and 2002-03, less substantial events in 1994-95 and 2006-07, and three La Niña events in 1998-99, 1999-2000, and 2007-08.

In addition to ENSO, the tropics support several other identifiable sources of climate variability affecting rainfall distributions. The Indian sector undergoes zonal shifts of rainfall on interannual time scales forming a dipole pattern in anomalous rainfall (Ashok et al. 2001). An extremely strong negative phase of this pattern occurred in 1997-98 during which East African rainfall, usually only slightly higher during an El Niño event, was very severe, while Indonesia experienced droughts. Indeed, the anomalous weather patterns during 1997-98 had a striking impact on the Rift Valley lakes of East Africa with an anomalous rainfall increase of 20%-160% during the rainy season (Birkett et al. 1999; Murtugudde et al. 2000; Mercier et al. 2002).

Rainfall in the tropical Atlantic sector is also subject to interannual and decadal variations. The Nordeste region of Brazil, located at the latitude of the southernmost position of the seasonal ITCZ, in certain years can be subject to extreme drought or rainfall anomalies (Xie and Carton 2004). Extreme rainfall years for this region include 1993, 1995 (high) and 1998 (low). Likewise, changes in the northernmost seasonal migration of the ITCZ leads to years of anomalous rainfall in the Sahel region of central and western North Africa (Janowiak 1988). Since 1991 this region has been anomalously dry, with only occasional years of above average rainfall including 1994, 1999, and 2003. This drying trend is evident at Lake Chad in central North Africa, where altimetry observations, reviewed below, show that the water level has declined by more than 0.5 m during the past nine years.

Beginning in the early 1990s the launch of a succession of satellite radar altimeters has opened up the potential of remote sensing of levels for those lakes crossed by satellite repeat tracks. Initially poor signal-to-noise ratios limited the use of this data. However, improvements in processing techniques have dramatically improved the accuracy of this data (Birkett 1995), and the availability of multiple satellites in different orbits has increased the number of lakes covered as well as the number of measurements.

In this study we focus on tropical lakes and reservoirs in the band of latitudes swept seasonally by movements of the ITCZ. In addition to providing strong rain-induced level variations, their tropical locations preclude concerns about radar scattering by ice and level changes due to seasonal thermal expansion. We focus on a sample of 12 tropical lakes and reservoirs distributed across three continents: 8 in

Africa, 3 in Central and South America, and 1 in Southeast Asia (Table 3.1) for which acceptable multidecadal records are available. Most of these lakes and reservoirs are controlled to some extent. However, the impact of management is probably largest for the three reservoirs (Kainji, Bangweulu, and Balbina). Indeed, most reservoirs are multipurpose; as well as for irrigation, hydropower, and flood control, they are used for water supply, navigation, fishing, and recreation (Avakyan and Iakovleva 1998). Unfortunately, small lakes (<100 km^2) generally are not sampled sufficiently by the altimetry and thus cannot be included in this study.

Hydrologic models developed for lake hydrological systems are of two types. The first includes the complex physically-based models developed as a result of considerations of detailed hydrology, storage, and transport mechanisms. The second type, considered here, are simplified empirical linear models, estimating lake level as a function of net freshwater flux into the catchment basin. In this study our simple basin model contains two parameters: effective catchment to lake area ratio and time delay, both of which are determined by linear regression based on the simultaneous availability of lake level and rainfall. Successful application of this type of model opens up the possibility of deriving lake levels from water flux observations or forecast models, extending the link between these different components of the hydrologic system.

3.2 Study Regions

Many of the African lakes that we consider here (listed in Table 3.1) lie in the Rift Valley of eastern and central Africa, including Turkana, Tanganyika, Mweru,

Bangweulu, and Malawi. Three Western Rift Valley lakes - Tanganyika, Mweru, and Bangweulu - are part of the Congo River basin. Lake Tanganyika is the world's second or third largest lake by volume and second in depth, with major inputs from the Ruzizi and Malagarasi Rivers and major outflow into the Lukuga River. Bangweulu Reservoir has many sources, of which the Chambeshi River (the source of the Congo River) is the largest, but drains through the Luapula River. The Luapula River, together with the Kalungwishi River, provides water to tiny Lake Mweru. For all three of these Southern Hemisphere lakes the main rainy season is in boreal winter (Fig. 3.1).

Two deep lakes, Malawi and Turkana, lie in the Eastern Rift Valley. Lake Malawi is 580 km long and is the most southern of the great African Rift Valley lakes. Located within the Zambezi River basin it is the second largest and second deepest lake in Africa. Supplied primarily by the Ruhuhu River, Lake Malawi drains into the Shire River. The smaller closed Lake Turkana has several source rivers in the Nile River basin. The main water input (90%) is from the Omo River, which enters the lake from the north. The second largest input is from the Turkwel River, which is in the process of being dammed for hydroelectric power generation. Lake Turkana water loss is through evaporation owing to its arid climate. It is the world's largest permanent closed desert lake and the world's largest alkaline lake. By volume it is also the world's fourth largest salt lake. Seasonal rainfall for Malawi resembles that of the Western Rift Valley lakes described above, while Lake Turkana shows only weak seasonal rains due to shadowing by the surrounding terrain, with the highest rainfall coming during the "long rains" of March-June.

The last three African lakes we consider are Lake Tana, which lies north of Turkana in the Ethiopian Rift Valley; Lake Chad, in central North Africa; and Kainji Reservoir, positioned southwest from Lake Chad, with the main rainy season in boreal summer (Fig. 3.1). Lake Tana, the source of the Blue Nile, is fed by four rivers and numerous seasonal streams. With a mean depth of only 8 m, the strong seasonal cycle of rain drives a 25% seasonal variation in depth; however, construction of a weir in 1996 has limited fluctuations of the level of this lake (Kebede et al. 2006).

Shallow (<7 m) Lake Chad experiences seasonal level fluctuations in the lake and surrounding marsh area, expanding in size from about 2,000 km^2 to about 15,000 km^2 between dry and wet seasons. Lake Chad receives most of its water (95%) from the Chari/Logone River system, which connects Chad to the seasonally rainy highlands to the south with similar timing but half the amplitude of Kainji Reservoir and Lake Tana (Van Campo and Gasse 1993). Most water loss is through evaporation and water extraction, though it has ~15% water loss through ground seepage (Carmouze et al. 1983; Isiorho et al. 1996). Declining rains and excess water extraction have been held jointly responsible for the shrinkage of the lake over the past half century.

Lake Chad was the subject of earlier altimeter level studies by Coe and Birkett (2004a) who developed a predictive model based on correlating upstream water levels in the Chari River with downstream levels in the lake. Estimates of phase lags across the basin varied from 20 days to 5 months (Birkett 2000; Coe and Birkett 2004a); however, a one-month phase lag between the lake and the Chari River was explored as a potential warning tool of high flows.

The Kainji Dam was commissioned in December 1968, forming the Kainji Reservoir for the purpose of generating electricity. Incidentally, there are problems associated with its operation. During high September inflows there is often annual flooding of the lower Niger plains as the spillways are opened. During periods of low inflows (March-May), the water level is often well below the desired operational level (Jimoh 2008).

In Central and South America we consider three lakes: Lake Titicaca, the largest freshwater lake in South America; Balbina Reservoir in central Amazonia; and Lake Nicaragua, the largest lake in Central America. Lake Titicaca is fed by rainfall and meltwater from mountain snowfields. Most water loss is through evaporation, although about 10% is lost through the Desaguadero River (Roche et al. 1992). The water level of Lake Titicaca undergoes decadal variations of 1-2 m owing to changes in rainfall. For example, it experienced low water levels in the 1940s but rising elevations in recent years (Guyot et al. 1990). Lake Titicaca, because of its Southern Hemisphere location, experiences a rainy season in boreal winter (Fig. 3.1).

The shallow Balbina Reservoir was created in 1987 by damming the Uatumã River in the Amazon basin to supply hydroelectric power. Reservoir level variations reflect variations of rainfall into the Amazon basin with highest rain from February through May (with peak rain in March-April). It contains 1500 islands and innumerable stagnant bays where the water's residence time can exceed the 1-yr average (Fearnside 1989).

Lake Nicaragua, located in Central America and affected by rainfall from the Eastern Pacific ITCZ, experiences two rainy seasons per year and a relative minimum

of rainfall during July and August known as the midsummer drought (Magaña et al. 1999). In response, Lake Nicaragua has a twice-yearly peak of lake level (Fig. 3.1).

Lake Tonle Sap in Cambodia is the largest lake in Southeast Asia and a key part of the Mekong hydrological system. It has only one major inlet/outlet – the Mekong River. Water drains from Lake Tonle Sap into the Mekong River through Tonle Sap River beginning in September. By spring Lake Tonle Sap has an average depth of only 1 m. The onset of the monsoon season in late May and the resulting rise in Mekong River water levels reverses the direction of Tonle Sap River and Lake Tonle Sap begins to flood, quadrupling its surface area and deepening it to up to 9 m. Large changes in the area of Lake Tonle Sap mean that its volume depends on both lake level and surface area with the area expanding at a rate of ~1000 km^2 m^{-1} rise of level (Magome et al. 2004; Mekong River Commission 2005). The lake is also subject to year-to-year variations. For example, Inomata and Fukami (2008) point out that 1998 was a year of unusually low rainfall, which consequently resulted in an anomalously low lake level.

3.3 Datasets

This study utilizes five different datasets focusing on two main parameters: lake level and rainfall. Lake level variability is determined by satellite radar altimeters. *TOPEX/Poseidon* (T/P) (1992-2002) and *Jason-1* (2002-08) have a 10-day repeat cycle with a track spacing of 350 km at the equator. Validation exercises with ground-based gauge data have shown that the time series of lake level variations can be accurate to 3 cm root-mean-square (RMS). The *Geosat Follow-on* (GFO) Mission

(2000-08) has a 17-day repeat cycle and 170-km equatorial track spacing with accuracies 3.5 cm RMS. The altimeters carried by the Earth Resources Satellites *ERS-1* (1991-96), *ERS-2* (1995- 2002), and *ENVISAT* (2002 - present) follow a 35-day repeat cycle with 80-km equatorial track spacing and accuracies generally 9 cm RMS. All satellites require a minimum target area >100 km^2 or width >500 m to achieve sufficient data quality (Crétaux and Birkett 2006). Some lakes such as Lake Malawi are crossed by multiple tracks (Fig. 3.2). Others, such as Lake Tonle Sap, are crossed only by one track, in this case near the outlet to the south of the lake.

In addition to the availability of tracks, data retrievals over lakes are subject to coastline and island interference. The accuracy of the altimetric height lake level is also affected by lake size and the number of available radar echoes collected, the surface roughness of the water (wave height), as well as atmospheric parameters such as water vapor. Due to the presence of on-board radar echo filtering software, lake level observations from *Jason-1* are particularly poor for the smaller or more sheltered lakes with calm waters. A full discussion of the error budget terms for radar altimeters is provided in Crétaux and Birkett (2006) and Calmant et al. (2008). We note here that, in general, comparison of the combined altimeter record to gauges and intercomparison of measurements between instruments suggest the level estimates for large lakes are generally accurate to within 5 cm, but this level of accuracy may degrade to tens of centimeters (e.g., Lake Chad, Birkett 2000) to over a meter (e.g., narrow reservoirs such as Lake Powell) depending on the target (Birkett et al. 2009).

For 11 of our 12 lakes and reservoirs we use the merged-satellite product of the Laboratoire d'Etudes en Géophysique et Océanographie Spatiales (LEGOS)

(Crétaux et al. 2011a). This merged product includes data from the remote sensing system carried by the six satellites (T/P, *Jason-1*, *ERS-1–2*, *ENVISAT*, and *GFO*) with each dataset processed independently and intersatellite height biases removed using T/P data as a reference. The merged product is available at approximately monthly resolution starting in late September or early October 1992 for most lakes. For a few lakes, such as Bangweulu and Titicaca, the product begins in 2000. For Balbina Reservoir and Lake Tonle Sap the LEGOS product ends in 2002 coincident with the demise of T/P. We explore uncertainties due to altimeter sampling and processing by comparing the LEGOS data for eight of the lakes with corresponding level estimates available from the U. S. Department of Agriculture Foreign Agriculture Service, Global Reservoir and Lake Monitor (GRLM) (Birkett et al 2010). The GRLM product is based only on three satellites – T/P, *Jason-1*, and *GFO* – but is available at a finer 10-day resolution. For the comparison we interpolate both products to a uniform 5-day interval starting on the same dates, remove data outliers (identified subjectively) and fill short gaps in the time series by linear interpolation.

In this study we consider three rainfall products: the updated European Centre for Medium Range Weather Forecasts (ECMWF) ERA-Interim reanalysis (Simmons et al. 2007a,b; Uppala et al. 2008), the Global Precipitation Climatology Project (GPCP) pentad rainfall (Xie et al. 2003), and the Tropical Rainfall Measurement Mission (TRMM) 3B42 (V6) daily precipitation index (Adler et al. 2000). ERA-Interim rainfall, derived here from the 3-h time step forecasts from the 0000 UTC analysis at 1.5^{o} spatial resolution, represents an update of the earlier 40-yr ECMWF Re-Analysis (ERA-40) (Uppala et al. 2004), created to address systematic errors in

this earlier reanalysis. Over tropical land areas the ERA-Interim rainfall is slightly higher (in general up to 3 mm day^{-1}) than in the previous reanalysis (Uppala et al. 2008). In particular Betts et al. (2009) reports significant improvements of ERA-Interim rainfall over the Amazon basin, showing more rainfall in all seasons than ERA-40 (up to 1 mm day^{-1}), but with an annual cycle that is still too weak.

The two observation-based products that we consider, GPCP and TRMM, both include satellite-based observations. GPCP is a combined surface rain gauge-satellite analysis available as a 5-day (pentad) average product at 2.5^{o} spatial resolution. TRMM Multisatellite Precipitation Analysis (TMPA) is an adjusted satellite analysis combining active and passive observations from the TRMM satellite together with more frequent geostationary IR measurements to obtain a calibrated product with high temporal sampling, available daily at 0.5^{o} spatial resolution. GPCP is available for our full period of interest, while TRMM begins in 1998. Although TRMM and GPCP have very similar spatial and temporal patterns, over land TRMM has higher amplitude (Adler et al. 2000). A 1-yr comparison to rain gauges in northwest Africa by Nicholson et al. (2003) suggests that TRMM is nearly unbiased with a RMS error, when smoothed to monthly resolution, comparable to GPCP. The differences among the rainfall products are illustrated in Fig. 3.3 for Lake Malawi. It is evident that the intraseasonal variations of GPCP and TRMM are larger than those of ERA-Interim; however, the seasonal cycles are similar to within 10%-20%.

We consider only a single evaporation product, that of the ERA-Interim reanalysis. In the tropics evaporation has much weaker variations than precipitation (Yoo and Carton 1990), as illustrated at Lake Malawi (Fig. 3.3); thus, in the tropics

seasonal and interannual estimates of net freshwater flux are insensitive to the precision of the evaporation estimates.

3.4 Model

Here we introduce a simple water balance model similar to those used elsewhere (e.g., Calder et al. 1995; Nicholson et al. 2000; Vallet-Coulomb et al. 2001; Kebede et al. 2006). Invoking conservation of mass for a lake catchment system leads to an approximate relationship between the lake level anomaly from its time mean (H), lake area (A_L), catchment area (A_C), anomalous net freshwater flux ($\tilde{P} - \tilde{E}$), and anomalous water loss (ε_t) through a variety of processes (e.g., evaporation, groundwater and surface stream outflow) at any given time (t) and space (x,y):

$$\frac{d}{dt}\left[\iint H(x,y,t)dA_L\right] = \iint [\tilde{P}(x,y,t-\delta t) - \tilde{E}(x,y,t-\delta t)]dA_C - \varepsilon_t . \qquad (3.1)$$

Here we assume a single constant delay (δt) between the time of freshwater flux and the accumulation of water in the lake. Thermal expansion effects are neglected as are the effects of changing salinity on evaporation rates. If we assume water level does not vary spatially within the lake (which could occur owing to wind effects for example), compute the time average of (3.1), subtract that time average equation from (3.1), neglect water loss ($\varepsilon_t = 0$), and assume A_C and A_L are constant, then (3.1) reduces to the following predictive equation:

$$\tilde{H}(t) = \frac{A_c}{A_L} \int_{\tau=-\delta t}^{t-\delta t} [\tilde{P}(\tau) - \tilde{E}(\tau)] d\tau + \tilde{H}(t=0), \qquad (3.2)$$

where $\left[\tilde{P}(t) - \tilde{E}(t)\right] = A_C^{-1} \iint (\tilde{P} - \tilde{E}) dA_C$ is the time-fluctuating anomaly of net freshwater flux from its time mean, averaged over the catchment basin, and similarly $\tilde{H}(t)$ represents the time-fluctuating lake level anomaly about its mean [$\tilde{H}(t) = H(t) - \overline{H}$, see Appendix B]. We ignore anthropogenic influences, as we have no information to guide us on accounting for these effects.

The model contains two parameters: effective catchment to lake ratio, defined as the ratio of catchment area to lake area $(A_C/A_L)_{eff}$ computed by fitting (3.2) using observed height and freshwater flux data for each lake, and time delay between freshwater flux and lake level response (δt). These two parameters, determined separately, allow us to construct model estimates of lake level based solely on freshwater flux estimates. Any unmodeled drainage (e.g., groundwater seepage) is also folded into the definition of $(A_C/A_L)_{eff}$. Note that $(A_C/A_L)_{eff}$ in general will differ from (A_C/A_L) as estimated from hydrologic drainage maps and the difference will provide information about the magnitude of unmodeled effects. The second parameter δt is estimated based on simultaneously maximizing the correlation between the model lake level and altimetric observations. Its uncertainty is determined by identifying the range of time delays spanned by the 95% confidence interval of the correlation. The resulting models are designated Model-I, Model-G, and Model-T for those developed using the three rainfall products (ERA-Interim, GPCP and TRMM, respectively). Since the emphasis in this study (and the validity of the empirical

model) is on interannual and shorter timescales, all time series are filtered to remove a least squares quadratic trend. Such trends could be introduced by unmodeled effects such as changes in land cover. However, the integral nature of the relationship between freshwater flux and lake level means that spurious trends in lake level may also be the result of white noise random errors in freshwater flux. By removing the trend we reduce the impacts of both model limitations and random error in the forcing.

For two shallow lakes, Chad and Tonle Sap, lake area increases dramatically with increasing lake level owing to the flooding of surrounding marshes. If instead of assuming a constant A_L we assume a proportional relationship $A_L = QH$, where Q is an empirical constant, then Eq. (3.2) leads to a square root relationship between the integral of freshwater flux and lake level:

$$\tilde{H}(t) + \frac{\tilde{H}^2(t)}{2\overline{H}} = \frac{A_C}{A_{Lo}} \int_0^t [\tilde{P}(\tau - \delta t) - \tilde{E}(\tau - \delta t)] d\tau + \tilde{H}(t=0) + \frac{\tilde{H}^2(t=0)}{2\overline{H}}, \quad (3.3)$$

where $A_{Lo} = 2Q\overline{H}$ (see Appendix B). When it is small compared to the variability of lake level we expect (3.3) to yield a quadratic relationship between $\tilde{H}(t)$ and the right-hand side of (3.3). But, for deeper or more slowly expanding lakes we regain a linear relationship similar to that expressed in (3.2). For Lake Chad the scatter diagram in Fig. 3.4 presents the right-hand side of (3.3) plotted along the ordinate versus $\tilde{H}(t)$ along the abscissa. The positive curvature in this relationship suggests that for this lake the second term on the left-hand side of (3.3) is not negligible

compared to the first. However, the relationship remains approximately linear for the observed range of $\tilde{H}(t)$. Because of the appropriateness of a linear approximation for all lakes considered here we will only explore the linear model described by (3.2).

3.5 Results

3.5.1 Altimetry Validation

Construction of lake-level time series involves a complex set of decisions regarding the choice of satellite, ground track, noise filtering algorithms, geophysical corrections, height reference datum, and application of intermission height bias. Since rather different choices have been made for LEGOS and GRLM, we begin by comparing the lake-level time series from the two different products for the eight lakes for which both altimetry datasets are available.

The comparison (after trend removal, described below) shows that the agreement is quite good for most lakes (Tables 3.2 and 3.3 show correlation significant at a probability level of 0.05 and RMS difference). Malawi, for example, shows excellent agreement with a correlation in excess of $r = 0.99$ significant at a probability level of 0.05 (Fig. 3.5a) and a RMS difference of 0.11 m. The worst agreement between the two lake level estimates occurs for Kainji Reservoir ($r = 0.87$ Fig. 3.5b), the smallest lake for which both datasets are available. Kainji Reservoir also has the largest RMS difference between the estimates of 1.45 m, which is about half of the observed variability. In this respect it resembles Lakes Tana and Chad. The Lake Chad level is known to be difficult to estimate owing to the presence of shallow

low-lying near-shore areas and islands. The causes of level error at Tana are less obvious. Determining the causes of these differences is complicated by the fact that LEGOS and GRLM use data from some of the same altimeters (but the estimates with range errors from individual satellites are not available for direct comparison). Thus, we are left to conclude simply that for most large lakes the products are in excellent agreement, but in the case of Kainji, Tana, and Chad there are significant differences between the LEGOS and GRLM estimates.

3.5.2 Validation of Model-based Lake Level Estimates

We have pointed out that freshwater input to northern and southern tropical lakes peak in different seasons. Figure 3.1 shows the seasonal cycle of GPCP rainfall ranging from 0 to 12.5 mm day^{-1} with the standard deviation of climatological monthly rainfall (shaded in the background), in general, less than 2 mm day^{-1} for our selected tropical lakes and reservoirs. Rainfall is averaged over lake catchment areas defined and given in Table 3.1. Published estimates of the catchment and lake areas may vary with season and are different for different sources (the values we report in Table 3.1 are obtained from comparison of International Lake Environment Committee and LakeNet databases, with individual lake studies). For our catchment basins freshwater flux associated with GPCP rainfall is similar to TRMM and generally larger than ERA-Interim.

To illustrate our procedure for determining two model parameters (see Table 3.4) we consider Lake Malawi. For Lake Malawi setting δt = 15 day gives a correlation between left-hand and right-hand terms in Eq. (2) of r = 0.79 using GPCP

rainfall, increasing to r = 0.95 when using ERA-Interim flux with δt = 25 day (Fig. 3.6a,b, Fig. 3.7). The uncertainty in the correlation associated with the relatively short data records leads to an estimate of the uncertainty in the time lag of ±10 day. RMS differences are also lower when using ERA-Interim rainfall rather than GPCP (0.24 m versus 0.33 m). During the shorter 11-yr period 1998 through 2007 when TRMM rainfall is available, TRMM flux gives r = 0.75, while GPCP leads to a better fit with r = 0.85 (Fig. 3.6c,d), and lower RMS differences (0.24 m versus 0.32 m). Minimization of the RMS differences leads to an effective catchment to lake area ratio of 3 regardless of the rainfall product used.

This procedure, carried out separately for each model, leads to time lag estimates of 0-15 days for Tana, Titicaca, and Nicaragua; 15-35 days for Tanganyika, Malawi, Chad, and Bangweulu; 45-100 days for Turkana, Mweru, and Kainji; while for Balbina and Tonle Sap there is no evident time lag between anomalous level rise and rainfall (Table 3.4).

Some specific characteristics of the lakes might be used as explanations for these values of the empirical parameters: arid versus moist region, high versus low elevation, open versus closed basin, absolute size of the catchment basin (water coming to the lake from farther away takes longer), etc. Uncertainty in the estimate of time delay can be an important source of error as well. Our estimates of time lags are comparable to previous estimates where available. For example, for Lake Chad time lag varies from 20 days to 5 months according to Coe and Birkett (2004a) and Birkett (2000), whereas our models show values ranging from 25 to 35 days.

Time series of lake levels and corresponding model estimates are shown in Fig. 3.8a,b. The variability of the lake-level height time series ranges over one order of magnitude among lakes because of differences in configurations and morphological characteristics of both the lakebeds and the catchment basins as well as rainfall variability.

In response to the seasonal variations in rainfall, all lake levels, except for Lake Turkana, have prominent seasonal cycles. However, a few interesting differences between rainfall and lake level at seasonal timescales do occur. The seasonal cycle of ERA-Interim rainfall onto the Lake Chad catchment basin decreases in amplitude by 50% with time from 2001 to 2007 (0.64 to 0.33 m) in a way that is inconsistent with either the seasonal Lake Chad level variations or with either GPCP or TRMM rainfall, suggesting that ERA-Interim rainfall has an erroneous trend there. At Mweru, in contrast, seasonal ERA-Interim rainfall appears to increase in amplitude with time, especially during the recent period 2003-07 (increasing from 0.53 to 0.72 m). Lake Titicaca, high in the Andes, shows a reduced seasonal input of freshwater in the past few years, which does appear to be reflected in all rainfall estimates. At the Kainji Reservoir the modeled level has a very brief seasonal peak in rainfall in late summer (September). In contrast, the observed level remains high throughout the summer, perhaps as a result of active water management.

We next consider the accuracy of the three lake-level models (Tables 3.2 and 3.3). Because record lengths are shorter for Model-T, a version of Model-G (called Model-G2) is created, which is based on parameters determined from the same length record as Model-T and thus can be directly compared (Fig. 3.8b). The median

correlation between the observed and modeled lake levels is slightly higher for Model-G than for Model-I (0.78 versus 0.70), and the median RMS differences between observation and model are the same (0.45 m). Model-G2 has significantly higher correlation with observations than Model-T (0.84 versus 0.74), while the median RMS difference is lower (0.30 m versus 0.41 m). However, a closer examination shows that the best model for a given lake varies. For Lake Chad and three Southern Rift Valley lakes – Tanganyika, Mweru, and Malawi – Model-I provides the better results (mean difference of 0.23) most of the time. For the remaining Southern Rift Valley Bangweulu Reservoir, all models do well overall (with correlations greater than 0.85). In contrast, for the Northern Rift Valley lakes Tana and Turkana, as well as the Central and South American lakes Nicaragua and Titicaca, Model-G provides the best results (mean difference of 0.39), while Model-T is slightly superior overall (mean difference of 0.05) for Balbina, Tonle Sap, and Kainji.

3.5.3 Effects of Climate Variability on Tropical Lake Levels

To focus on year-to-year changes, we filter out the seasonal cycle by removing the annual and semiannual Fourier harmonics from both observed and modeled lake levels (experiments show these harmonics capture almost all the energy in the seasonal cycle)[3]. The anomaly time series are shown in Fig. 3.9a,b. With the seasonal cycle removed, the East African Rift Valley lakes – Turkana, Tanganyika, Mweru, and to a lesser extent Malawi – show pronounced rises of lake level in 1997-

[3] Because the seasonal cycle of Model-I Lake Chad level weakens with time, Fourier filtering this model leaves residual seasonal cycles at the beginning and end of the record that are out of phase.

98 in response to the combined effects of El Niño and the positive phase of the Indian Ocean dipole, confirming results from direct lake level observations (Birkett et al. 1999; Murtugudde et al. 2000; Mercier et al. 2002). Western African Rift Valley lakes, such as Mweru and Tanganyika, also experience enhanced lake level rise of 140%-190% during this anomalous rainy season. Interestingly, ERA-Interim shows a corresponding increase in rain into the Tanganyika and Mweru basins, which is not evident in GPCP, while GPCP shows an increase in rain into the Turkana catchment basin, that is not evident in ERA-Interim.

Lake Tonle Sap on the eastern side of the Indian Ocean dipole shows a corresponding decrease in level. We also confirm earlier observations of Alsdorf et al. (2001), showing that the South American Balbina Reservoir and the Central American Lake Nicaragua have 2-m and 1-m decreases in lake level during the spring and summer of 1998 resulting from the decrease in rainfall associated with the 1997-98 El Niño. Interestingly, the lake level responses to the 2002-03 El Niño are much less pronounced than the 1997-98 El Niño for most lakes. For example, Lake Nicaragua had peak values 0.47 m lower than the long-term average of height level. An exception was Lake Malawi, which had greater peak values (0.73 m) during the latter event perhaps because of climate variability in the Indian Ocean sector.

Strong tropical cyclones and hurricanes, as well as droughts, are noticeable in the lake level records. For example, Lake Nicaragua shows a dramatic 1-m increase in early November 1998 as a result of rainfall input from Hurricane Mitch (evident in GPCP and TRMM but not in ERA-Interim). Lake Nicaragua and much of Central America experienced a drought during late 2006 and early 2007. Similarly, the

catchment basins of Lake Turkana and Lake Tana experienced major drought events during 2005 and 2007. Lake Nicaragua experienced a level drop during 2001 due to drought. Most lakes and reservoirs are also subject to active and variable water management, which likely plays a significant to dominant role in regulating water level.

3.6 Conclusions

This paper explores the use of a simple empirical model in deriving lake level estimates from rainfall. This type of model has a number of potential applications, including providing level estimates for basins where no ground-based or satellite-based level data is available and in developing lake level hindcasting/forecasting capabilities. It can be used by climate modelers and by the water management community, and thus potentially represents a significant contribution to earth system modeling. The model parameters (delay time and catchment to lake area ratio) also provide information regarding the hydrological properties of the lake basin.

We apply the model to compare the model-derived and altimeter lake-level time series for a sample set of 12 tropical lakes and reservoirs distributed across Africa, Asia, and the Americas, which lie in a band of strong seasonal monsoonal rainfall. The time series of the model and altimeter datasets span most or all of the 16-yr period 1992-2007. For eight of the lakes two different altimeter-based level products are available. One, LEGOS, is based on a combination of up to six altimeters, while the other, GRLM, is based on just three. The use of different altimeters and different ways the geophysical corrections and spatial filtering are

carried out may affect the accuracy of the products. Yet, despite these differences the results from LEGOS and GRLM are reassuringly similar. The largest discrepancies between the two estimates occur for the two smallest lakes, Kainji and Tana, where the correlations dip slightly below 90%. For these two lakes the RMS differences between the two level products are about half as large as the lake level variability itself, while for many of the other lakes the RMS differences are less than 20% of the level variability.

All lake levels, except of Lake Turkana, have pronounced seasonal cycles with the largest amplitudes occurring for the lakes in high rainfall regions: Kainji in Africa, Balbina in South America, and Lake Tonle Sap in Southeast Asia. The lack of a seasonal cycle at Lake Turkana is due to its location in the rain shadowed region of the Chalbi Desert basin, blocked from the seasonal rains by its surrounding mountains. For the other lakes comparison of the timing and amplitude of the seasonal rainfall and level allows us to estimate model parameters, such as the time delay between freshwater input and level, and the effective catchment to lake area ratio. The ability to estimate these parameters is important since there are few published estimates of the former and published estimates of the latter vary widely. The lakes and reservoirs have time delays that range widely between 0 and 105 days with uncertainties of up to 35 days and effective catchment to lake ratios that range between 2 and 27.

The effective catchment to lake area ratios are generally larger than the estimated catchment to lake area ratios because of the presence of unresolved processes such as groundwater seepage, which is not otherwise accounted for in the

simple model that we propose. An extreme example of groundwater seepage is Lake Chad, which has an estimated catchment to lake area ratio of 647 but an effective ratio of 10. Similarly, Lake Turkana has an estimated ratio of 20 but an effective ratio of 3.

For each lake or reservoir we construct a simple model of level anomaly forced by observed anomalous freshwater flux falling onto the associated catchment basin. Since freshwater flux variability in this latitude band is largely driven by rainfall variability, and analyses differ, we compare three: ERA-Interim reanalysis (Model-I), a combined rainfall analysis, GPCP (Model-G), and a purely satellite rainfall analysis, TRMM (Model-T). All three analyses are available at 5-times-daily resolution; however, the TRMM rainfall is only available from 1998, while the other two span our full time period of interest (1992-2007). Either of the rainfall analyses provides reasonable lake level estimates for most lakes much of the time, but in some years the model fails at some locations. Many lakes show decadal trends, which may be caused by nonrainfall-related changes such as deforestation, growth of cultivated farming, irrigation, etc. To focus only on the (hopefully more rainfall-related) intraseasonal-to-interannual signals all records are filtered to remove a quadratic trend.

When the seasonal cycle is also removed, some of the time series reveal striking nonseasonal variability. The Rift Valley lakes, Turkana, Tanganyika, Mweru, and Malawi, all show a dramatic rise in response to the combined 1997-98 El Niño and Indian Ocean dipole events. In contrast, the Central and South American lakes, Nicaragua and Balbina, show significant level decreases for the same time period.

Interestingly, other ENSO events do not show nearly as pronounced a response. Other climate events, such as tropical cyclones and hurricanes and episodic droughts, also show up in lake level records. Changes in the effective catchment area because of irrigation, and other human intrusions, are important and have their influence on model results as well.

The development of lake-level models driven by rainfall also gives us a way to evaluate the accuracy of the rainfall products by using the lake catchment basins as if they are giant rain gauges. For some lakes the ERA-Interim reanalysis rainfall provides the most successful model estimates, for example Lake Malawi (r = 0.95). However, for most other lakes the best results are obtained using the observation-based products: GPCP or TRMM. For most of these lakes GPCP seems to produce superior results (with the median correlation of 0.78 versus 0.70 for ERA-Interim and 0.84 versus 0.74 for TRMM at two examined periods). The comparison of modeled and observed level allows us to identify weaknesses in the reanalysis rainfall estimates for particular catchment basins such as the weakening of the seasonal cycle with time at Lake Chad and the spurious interannual variability at Kainji Reservoir (ERA-Interim).

Simplifications inherent in the simple empirical model used here likely explain much of the mismatch between the model predictions and observations. To give just a few examples, this model neglects the possibility of multiple time scales associated with the delay between rainfall and changes in lake level. It assumes that the catchment basin remains static with time and neglects thermal expansion and ice formation, as well as the possibility of seasonal changes in land use. Many lakes and

reservoirs are actively managed and yet this model provides no mechanism to reflect such management. The model is inherently linear and thus cannot adequately represent processes that are flow dependent such as lake discharge and groundwater seepage. Another important simplification is the lack of any model of the changing slope of water across the lake itself, important because the altimeter coverage may be quite limited for a given lake or, worse, may change with time as the satellite altimeters used in the analyses change. And of course the quality of the results will depend on the quality of surface flux estimates. Evaluating the impact of these simplifications and developing more sophisticated models should open up new avenues for research.

Still, despite the many simplifications associated with this two-parameter model, the reasonable values it produces suggests that historical rainfall estimates can provide an interesting way of evaluating past lake level variability, the reverse of Nicholson et al. (2000) use of Lake Victoria gauge measurements to infer historical rainfall. Examination of the model errors may help to quantify anthropogenic effects like changing deforestation or irrigation where other sources of information may be limited. Finally, as noted in the introduction, the success of the models suggests their potential use for forecasting of lake levels in the medium range (1-3 week) based on output from weather prediction center forecast models. Exploring this possibility is the subject of our current research.

3.7 Tables

Table 3.1 Geographical characteristics of the lakes and reservoirs considered in this study. Surface and volume areas are variable with time and seasons.

Lake	Countries	Lat	Lon	Alt (m)	Lake area (km^2)	Catchment area (km^2)	Volume (km^3)	Depth (mean – max) (m)
				Africa				
Chad (Tchad)	Chad, Nigeria, Cameroon, Niger	13.20°N	14.10°E	280[a,b]	1540[a,b] 1600[c,d] 25 000[d]	1 035 000[c] 2 000 000[d] 2 426 370[a]	6.3[a] 72[b,c,d]	1.5[c] – 8[c] 4.1[a,b,d] – 10.5[a,b]
Kainji	Nigeria	10.40°N	4.55°E	—	1000[b,c]	—	—	11[c] – 59[e]
Tana	Ethiopia	11.40°N	37.20°E	1788[a,b] 1830[f]	158.8[c] 3050[f] 3600[a,b,d]	5.9[c] 10 000[a] 15 000[d] 16 500[f]	1.56[c] 28[a,b,d]	8[f]–14[f] 9[a,b,d] – 14[a,b]
Turkana (Lake Rudolf)	Ethiopia, Kenya	4.00°N	36.00°E	360.4[a,b]	6500[c] 6750[a,b,d]	130 860[a,d]	187[c] 203.6[a,b,d]	7[c] – 73[c] 30.2[a,d] – 109[a]
Tanganyika (Tanganika)	Tanzania, RDC,[g] Zambia, Burundi	6.00°S	30.10°E	773[a,b]	32 000[a,b,d] 32 600[c]	220 000[c] 263 000[a,d]	17 800[a,d] 17 890[b] 19 000[c]	572[a,b,c] –1471[a,b,c]
Mweru	RDC, Zambia	9.00°S	28.45°E	922[a,b]	4350[a,b] 4500[d] 5000[c]	—	32[a,b,d]	7[a,b,d] – 37[a,b]
Malawi (Nyasa, Niassa)	Mozambique, Malawi, Tanzania	10.00°S	34.50°E	500[a,b]	6400[b] 29 500[c] 30 000[d]	6593[a] 100 500[c] 130 000[d]	7775[c] 8400[a,b,d]	264[c] – 706[c] 292[a,b] – 706[a,b]
Bangweulu	Zambia	11.05°S	29.45°E	1140[a,b]	1510[a] 9840[c] 15 100[b]	100 800[c]	5[a,b,c]	4[a,b,c] – 10[a,b,c]
				Central and South America				
Nicaragua (Cocibolca)	Nicaragua	11.30°N	85.30°W	32[a,b]	8150[a,b,c]	23 844[c]	108[a,b,c]	13[c] – 45[c] ?–70[a,b]
Balbina	Brazil	1.80°S	59.50°W	50[a,b]	507.6[c] 2360[a,b]	55[c] 10 000[a]	17.53[a,b,c]	7.4[a,b] – 30[a,b]
Titicaca	Peru, Bolivia	15.80°S	69.40°W	3812[a,b]	8372[a,b] 8400[c]	56 270[c] 58 000[a]	893[a,b] 932[c]	107[a,b] – 281[a,b] 107[c] – 304[c]
				Southeast Asia				
Tonle Sap (Boeng Tonle Chhma)	Cambodia	12.98°N	103.90°E	5[a]	2500[h] 13 000[c] 16 000[h] 30 000[a]	70 000[c]	40[a,c]	1[c] – 10[c] ?–12[a]

[a] International Lake Environment Committee (1986).
[b] Crétaux et al. (2011).
[c] LakeNet (1997).
[d] Mercier et al. (2002).
[e] Hughes and Hughes (1992).
[f] Vijverberg et al. (2009).
[g] Republique Démocratique du Congo (RDC), Democratic Republic of Congo (DRC), previously Zaire.
[h] Tonle Sap Biosphere Reserve Secretariat (2006).

Table 3.2 Correlation coefficient between observational and modeled height levels after removing the quadratic trend from the LEGOS observations and modeled height levels; and correlation coefficient between the two observational lake level analyses.

Lake	Obs vs Model-I	Obs vs Model-G	Obs vs Model-T	Obs vs Model-G2	LEGOS vs GRLM
Chad	0.78	0.56	0.73	0.88	0.93
Kainji	0.45	0.57	0.69	0.66	0.87
Tana	0.30	0.87	0.70	0.86	0.89
Turkana	-0.21	0.76	0.53	0.71	0.99
Tanganyika	0.89	0.68	0.80	0.78	0.99
Mweru	0.71	0.40	0.69	0.83	0.97
Malawi	0.95	0.79	0.75	0.85	0.99
Bangweulu	0.85	0.93	0.90	0.93	–
Nicaragua	0.61	0.88	0.85	0.92	0.98
Balbina	0.10	0.47	0.38	0.32	–
Titicaca	0.74	0.90	0.86	0.90	–
Tonle Sap	0.68	0.85	0.87	0.82	–*

* LEGOS's satellite tracks cover Tonle Sap lake area and GRLM's cover only area near the outlet, so no comparison is made here.

Table 3.3 RMS difference between observational and modeled height levels (m), after removing the quadratic trend from the observations and modeled height levels; RMS difference between the two observational lake-level analyses with the RMS variability of the LEGOS lake levels.

Lake	Obs vs Model-I	Obs vs Model-G	Obs vs Model-T	Obs vs Model-G2	LEGOS vs GRLM	Obs 1992-2007	Obs 1998-2007
Chad	0.36	0.55	0.36	0.26	0.22	0.54	0.51
Kainji	3.76	2.70	2.27	2.40	1.45	3.07	3.13
Tana	1.00	0.35	0.45	0.33	0.34	0.62	0.63
Turkana	1.12	0.59	0.47	0.39	0.12	0.87	0.59
Tanganyika	0.19	0.31	0.16	0.17	0.06	0.40	0.28
Mweru	0.48	0.65	0.47	0.37	0.16	0.66	0.66
Malawi	0.24	0.33	0.32	0.24	0.11	0.54	0.45
Bangweulu	0.27	0.17	0.22	0.17	–	0.43	0.43
Nicaragua	0.41	0.22	0.23	0.17	0.09	0.44	0.44
Balbina	2.33	1.94	1.35	1.38	–	2.18	1.40
Titicaca	0.26	0.18	0.18	0.18	–	0.33	0.33
Tonle Sap	2.68	2.04	1.48	2.02	–	2.92	2.70

Table 3.4 Model parameters: time lag δt (with uncertainty resulting from 95% confidence interval estimates) between lake level and integrated freshwater flux (in days), the effective catchment area to lake area ratio $(A_C/A_L)_{eff}$, for the three models (Model-I, Model-G, and Model-T), and the actual ratio between catchment area to lake surface area (A_C/A_L). The A_C and A_L values for calculating A_C/A_L ratio are from Table 3.1.

	Time lag δt (days)				$(A_C/A_L)_{eff}$			
Lake	Model-I	Model-G	Model-T	Model-G2	Model-I	Model-G	Model-T	A_C/A_L
Chad	25 ± 5	35 ± 5	30	30	10	10	10	647[a] – 1575[b] 80[c] – 1250[c]
Kainji	70 ± 10	80 ± 5	80	80	15	20	20	–
Tana	0 ± 10	5 ± 5	0	5	2	3	3	3[b] – 4[c]
Turkana	55 ± 20	100 ± 35	90	55	3	3	3	19[b,c]
Tanganyika	15 ± 10	20 ± 10	20	30	2	2	2	7[a] – 8[b,c]
Mweru	45 ± 5	55 ± 10	50	60	4	4	4	–
Malawi	25 ± 10	15 ± 10	15	15	3	3	3	3[a] – 4[c]
Bangweulu	25 ± 5	30 ± 5	30	30	3.5	3.5	3.5	10[a]
Nicaragua	15 ± 10	10 ± 10	5	10	2	2	2	3[a]
Balbina	0 ± 5	0 ± 0	0	0	4	4	4	4[b]
Titicaca	15 ± 5	5 ± 10	0	5	2	4	4	7[b,a]
Tonle Sap	0 ± 5	0 ± 5	0	0	27	16	15	5[a] – 28[d]

[a] LakeNet (1997).
[b] International Lake Environment Committee (1986).
[c] Mercier et al. (2002).
[d] Tonle Sap Biosphere Reserve Secretariat (2006).

3.8 Figures

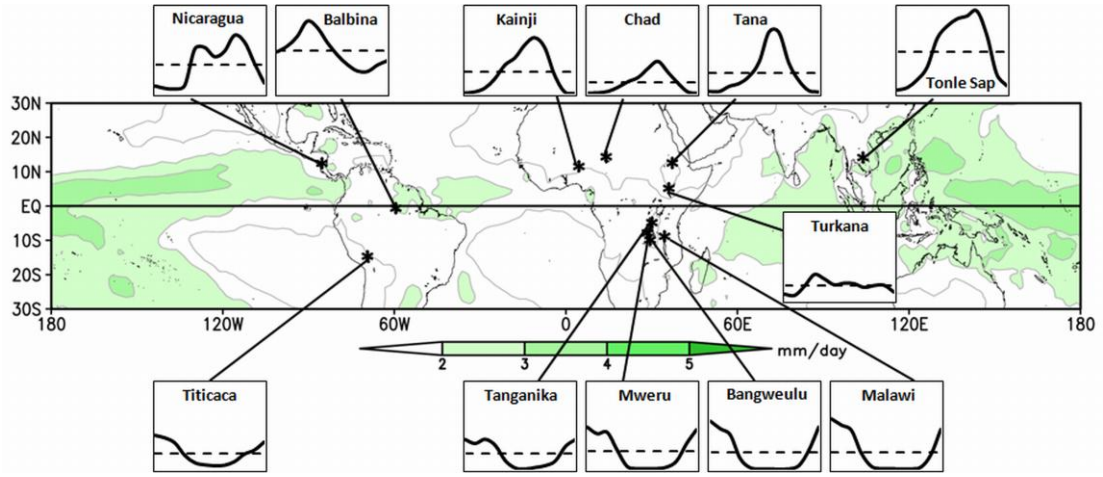

Figure 3.1 Monthly distribution of rainfall (mm day^{-1}) for selected tropical lakes and reservoirs (stars), with the standard deviation of climatological monthly rainfall shaded in the background. Solid black lines show climatological monthly GPCP rainfall averaged over the entire lake catchment basin, where vertical axes span 0-12.5 mm day^{-1}, and horizontal axes span January–December. Dashed lines show annual mean of rainfall.

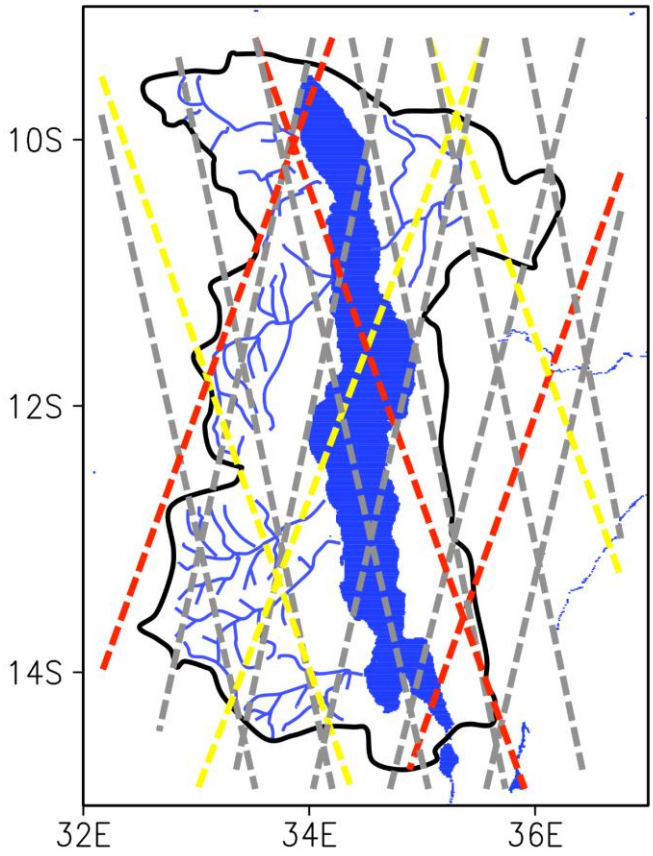

Figure 3.2 Lake Malawi with many of its rivers (blue) and catchment basin (black) delineated. Outflow is through the Shire River at the southern end. Altimeter ground tracks overlaid: *ENVISAT* and ERS (gray); *TOPEX/Poseidon* (yellow); *Jason-1* (red).

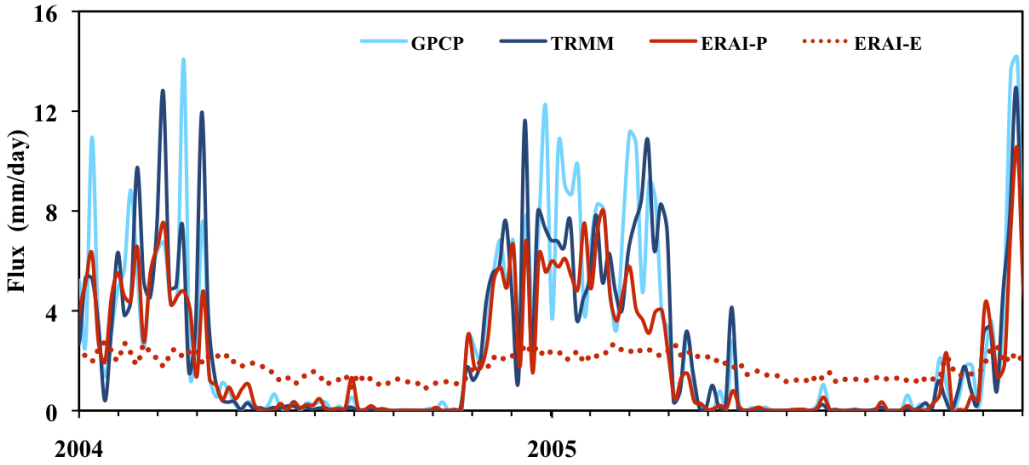

Figure 3.3 Rainfall and evaporation (mm day^{-1}) estimates averaged over the Malawi catchment area for two years 2000-01: TRMM (dark blue), GPCP (light blue), and ERA-Interim rainfall (red), and ERA-Interim evaporation (red dotted).

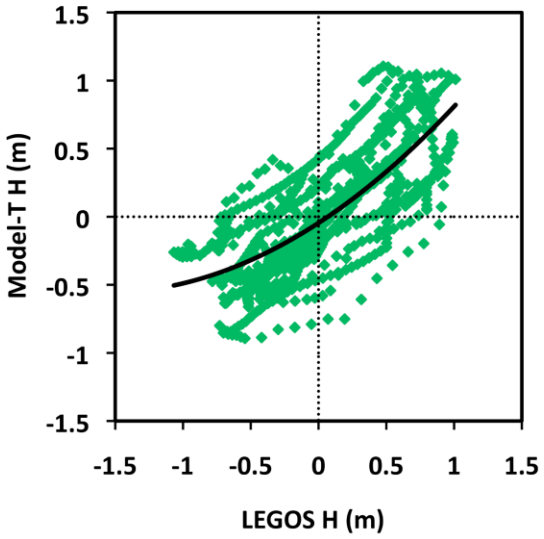

Figure 3.4 Scatter diagram of 5-day-average observed and modeled Lake Chad during 1997-2007 (when available) using TRMM rainfall with a 30-day lag. The scatter diagram clearly shows a quadratic component to the relationship predicted by Eq. (3.3) as the result of expansion of the lake surface area with rising lake level. The best-fit relationship, Model-T = $0.21H^2$ + 0.65H - 0.05, however, remains predominantly linear.

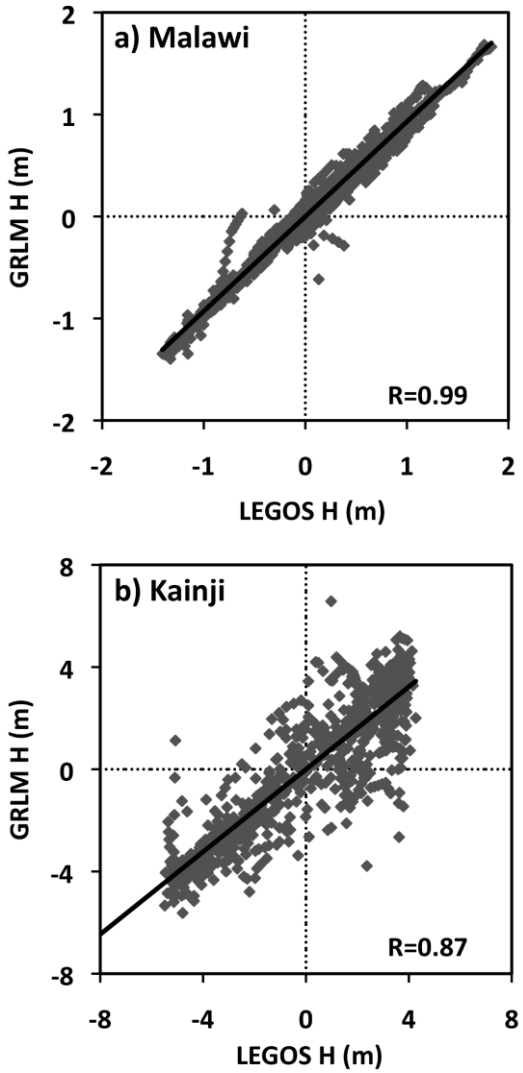

Figure 3.5 Scatter diagram of 5-day-average observed lake level during 1993-2007 (when available): LEGOS vs GRLM lake-level estimates (m) for (a) Lake Malawi, correlation $r = 0.99$, and for (b) Reservoir Kainji, correlation $r = 0.87$.

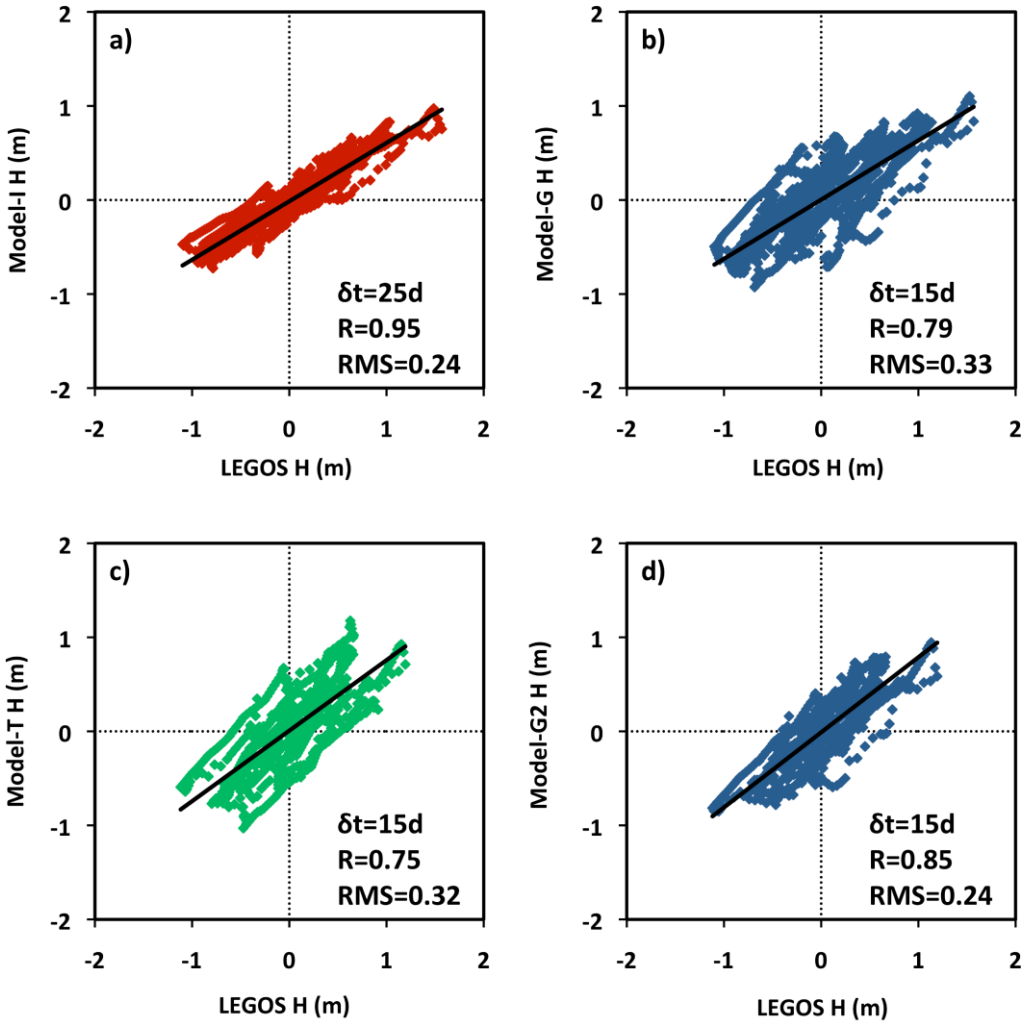

Figure 3.6 Scatter diagram of 5-day-average observed LEGOS vs modeled lake level (m) for Lake Malawi using rainfall from (a) ERA-Interim with a 25-day lag, (b) GPCP with a 15-day lag during 1993-2007, (c) TRMM, and (d) GPCP both with a 15-day lag during 1998-2007. At Malawi Model-I provides the best fit with the highest correlation r = 0.95.

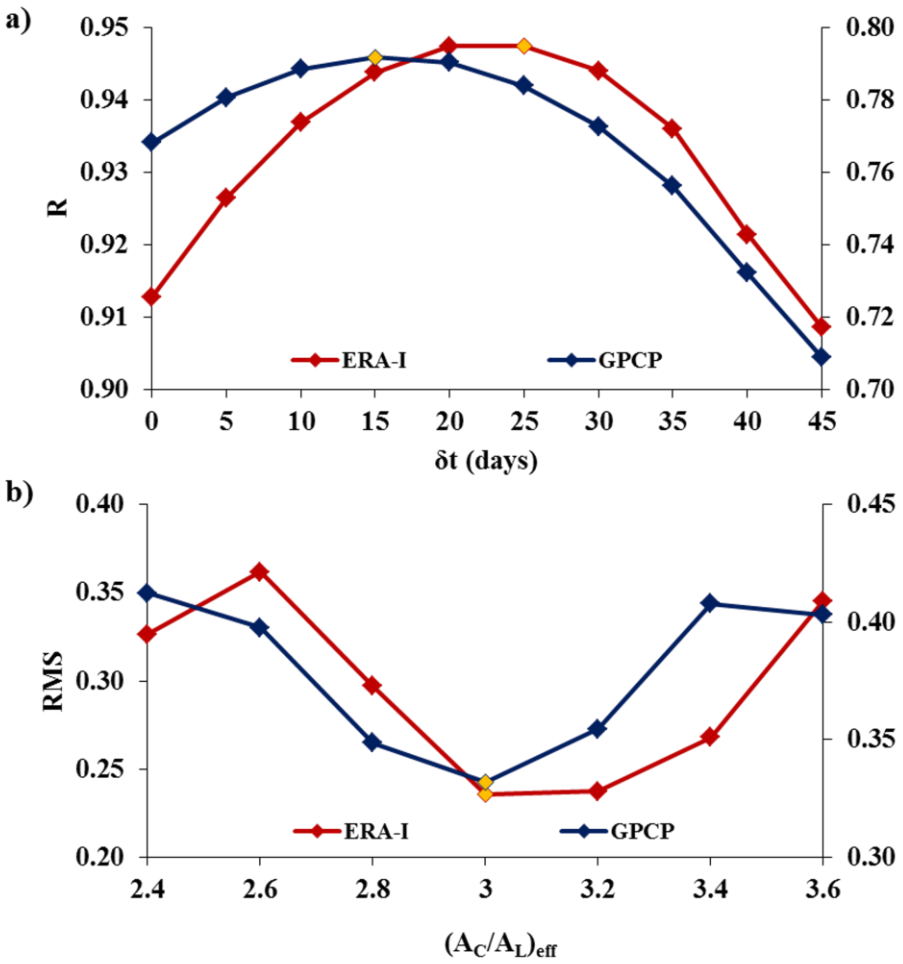

Figure 3.7 Using rainfall from ERA-Interim (red line) and GPCP (blue line) for Lake Malawi, (a) relationship between time delay of freshwater input and level rise (days) and correlation coefficient values, *r*, and (b) relationship between the effective catchment to lake area ratio and RMS values during 1993-2007: (left) *r* values for ERA-Interim and for (right) GPCP. In (a) the maximum correlation is at 25-day lag for ERA-Interim and 15-day lag for GPCP, and in (b) the lowest RMS for the effective catchment to lake ratio of $(A_C/A_L)_{eff}$ is ~3.

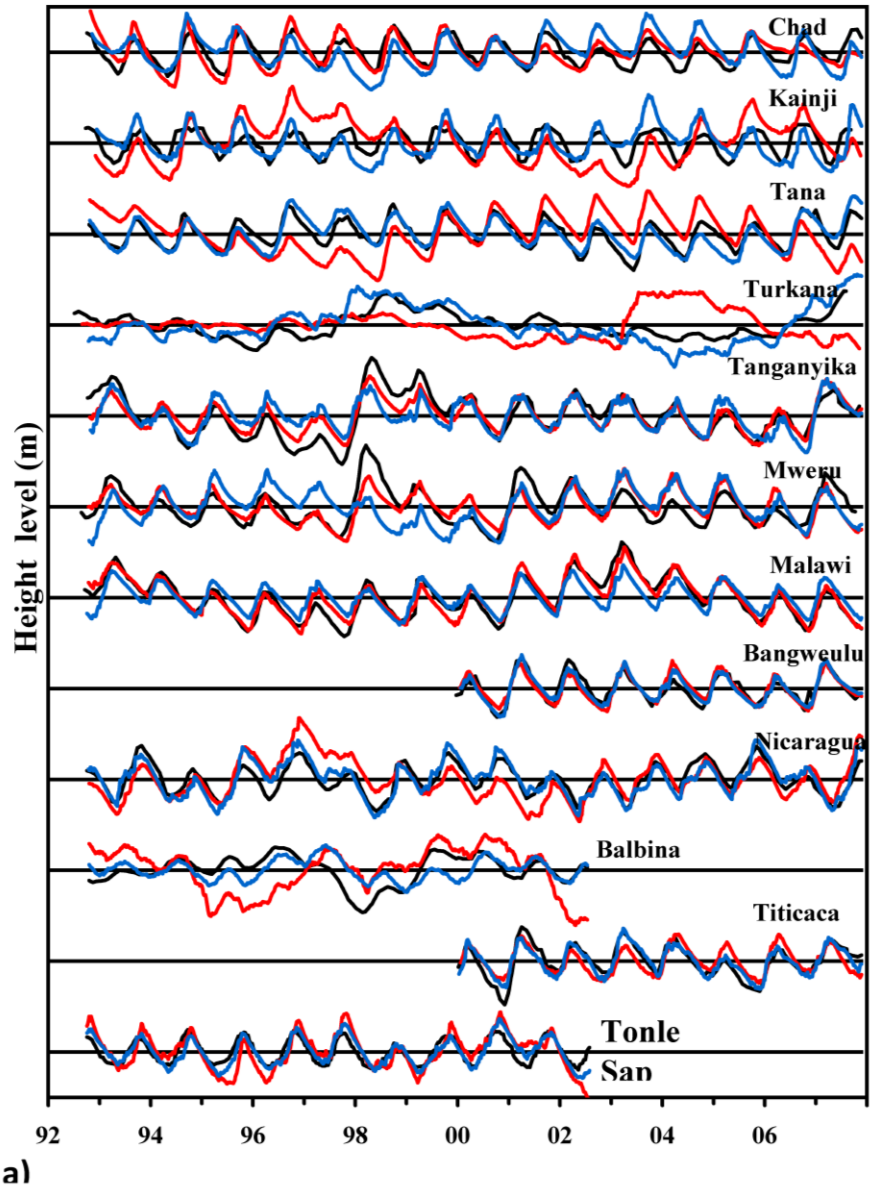

Figure 3.8 Observed LEGOS (black) and modeled lake level (colored) for 12 lakes and reservoirs considered in this study: (a) ERA-Interim (red) and GPCP (blue) for time period 1992-2007 and (b) TRMM (red) and GPCP (blue) for time period 1998-2007. Displacement between horizontal lines is 3 m. Levels for two lakes, Turkana and Balbina, have been reduced in amplitude by a factor of 3 and 2, respectively, so as to include them in the same figure. A quadratic trend has been removed from each time series.

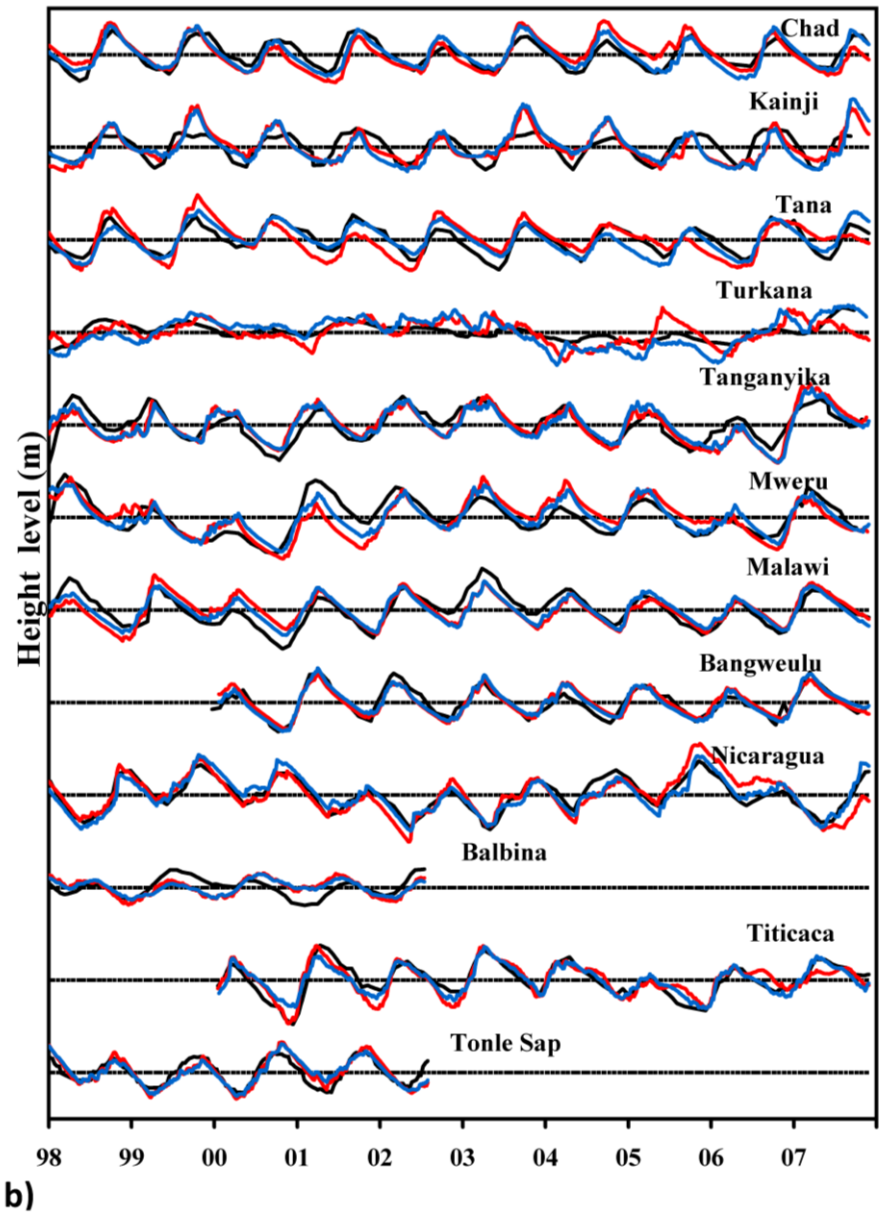
Chad
Kainji
Tana
Turkana
Tanganyika
Mweru
Malawi
Bangweulu
Nicaragua
Balbina
Titicaca
Tonle Sap
Height level (m)
98
99
00
01
02
03
04
05
06
07

b)

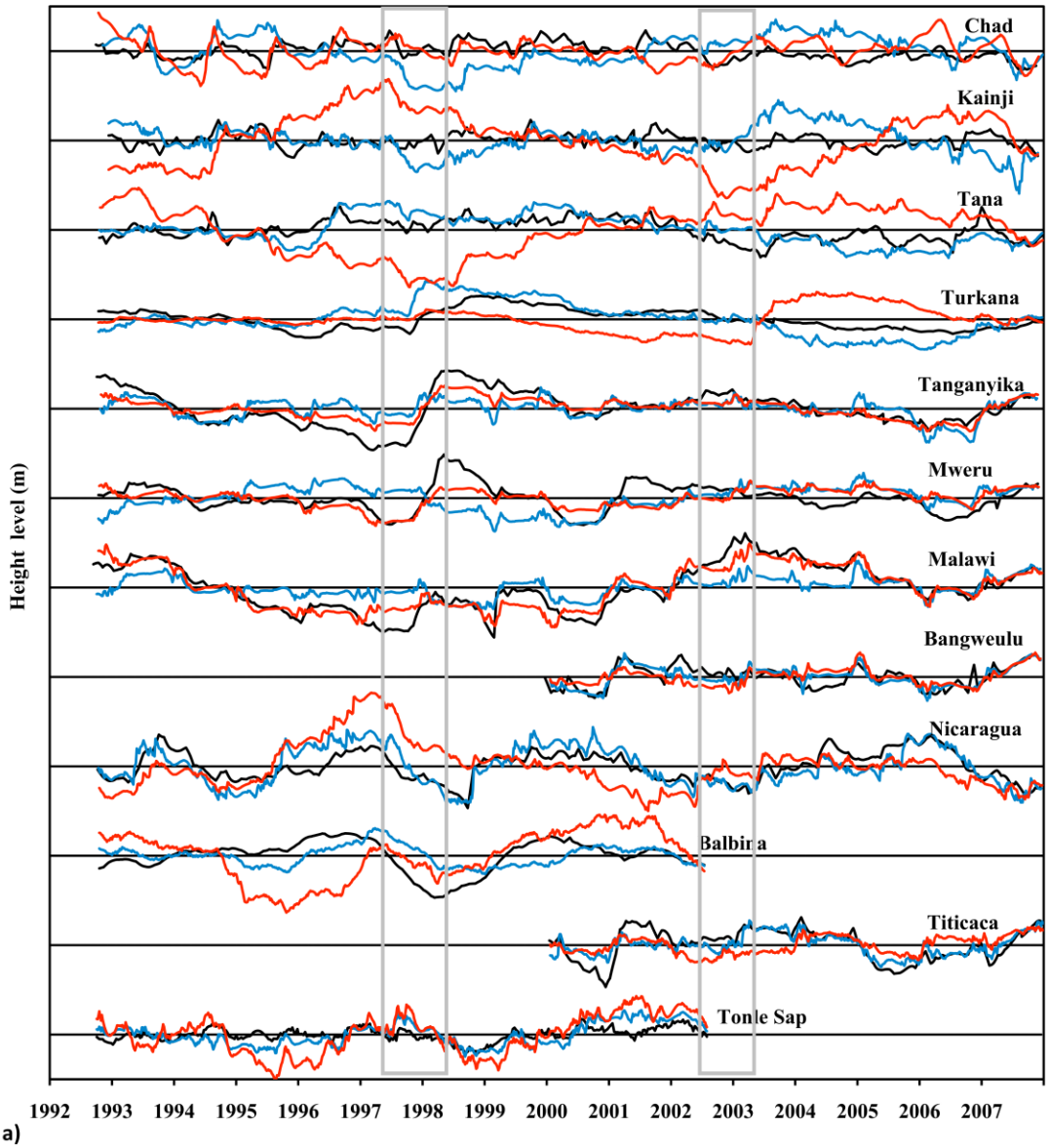

Figure 3.9 Similar to Fig. 3.8, but with the annual and semiannual Fourier harmonics filtered out. Displacement between horizontal lines is 2 m. Levels for four lakes, Turkana, Tanganyika, Mweru, and Balbina, have been reduced in amplitude by a factor of 5, 1.5, 1.5, and 2.5, respectively, to include them in the same figure. Grey boxed areas identify two El Niño periods (1997-98, 2002-03).

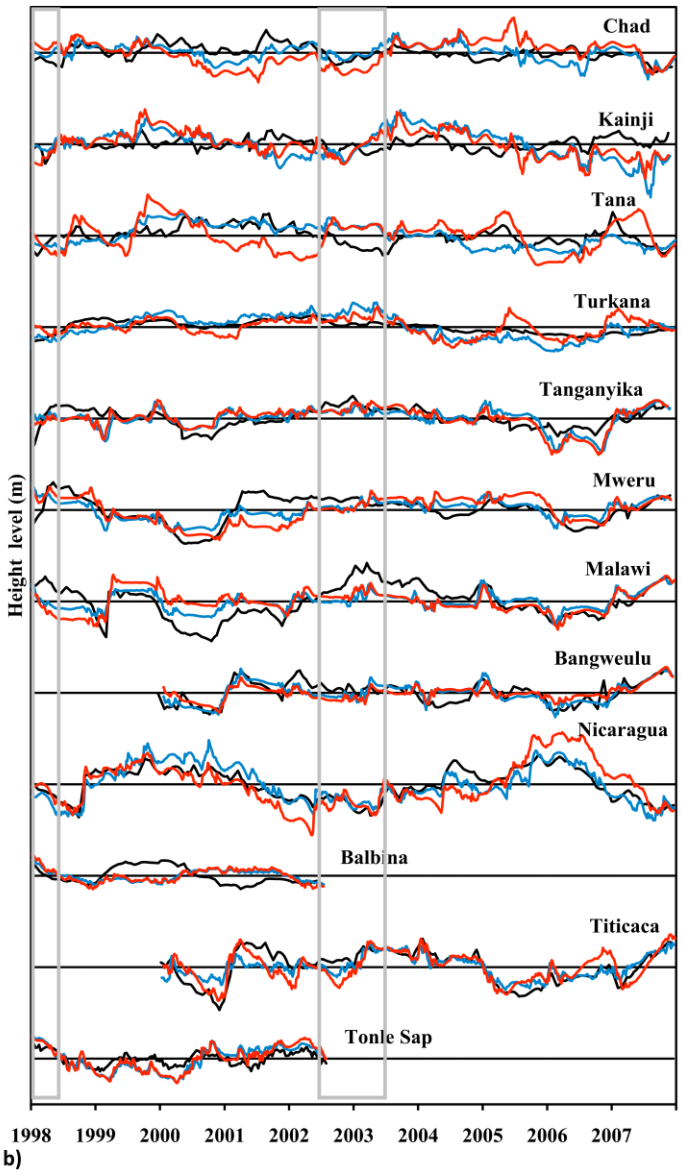
Chad
Kainji
Tana
Turkana
Tanganyika
Mweru
Malawi
Bangweulu
Nicaragua
Balbina
Titicaca
Tonle Sap
Height level (m)
1998
1999
2000
2001
2002
2003
2004
2005
2006
2007
b)

Chapter 4: Forecasting Tropical Lake Levels[4]

4.1 Introduction

Tropical lakes and reservoirs provide much needed water resources, but the supply varies depending on prevailing climatic conditions. Many studies have shown that satellite radar altimeter estimates of lake levels offer an additional monitoring tool to complement declining networks of *in situ* gauges (e.g., Crétaux and Birkett 2006; Anyah et al. 2006; Calmant et al. 2008; Birkett et al. 2011; Crétaux et al. 2011a; Ričko et al. 2012). In addition, earlier studies have focused on modeling of lake levels (e.g., Calder et al. 1995; Nicholson et al. 2000; Vallet-Coulomb et al. 2001; Kebede et al. 2006; Ricko et al. 2011). More sophisticated prediction systems offering seasonal-to-interannual lake level forecasts are very few and limited since current climate models still do not resolve detailed hydrologic processes at the level of individual lakes. Forecast skill remains a primary concern among all climate and hydrologic forecast producers and users, and still needs much improvement.

The most widely used water level forecasts are those for many of the U.S. rivers and watersheds, and especially for North American Great Lakes water levels that are typically based on computer simulation models. One example is the Great Lakes Advanced Hydrologic Prediction System (AHPS), run by The National Oceanic and Atmospheric Administration's (NOAA's) Great Lakes Environmental Research Laboratory (GLERL), which combines historical meteorological data with a series of

[4] Manuscript in preparation for *Geophys. Res. Lett*.

sophisticated mathematical models and climatological forecasts from NOAA's Climate Prediction Center (CPC) to simulate lake levels from one to 9 months in advance. A more quantitative assessment based on the percentage of observations within 90% prediction intervals, however, indicates that AHPS generally captures between 64 and 74% of the observed variability of Great Lakes water levels (Gronewold et al. 2011). This first complete study provides an assessment of the AHPS forecast model's error estimate with respect to *in situ* gauge data over Great Lakes and tries to fill the research gap related to yet undefined acceptable accuracies in 1-6 months forecasts of lake levels. Other agencies that give 6-month lake level predictions for Great Lakes every month are: the International Coordinating Committee on Great Lakes Basic Hydraulic and Hydrologic Data by Environment Canada, Great Lakes-St. Lawrence Regulation Office in Cornwall, and the U.S. Army Corps of Engineers. Similarly, these forecast values are based on their best estimate of current conditions (computed from available meteorological data), climatological forecasts and physical process models.

Besides for these large lakes, no routine predictions of lake levels for smaller lakes are available on a regular basis. This study investigates and offers an alternative method for forecasting lake level, a simple 2-parameter water balance model that can easily be incorporated into climate predictive models to forecast water level in lakes whose spatial scales are well below that resolved by the climate model's horizontal grid (e.g., typical coupled climate models are of 100-250 km). A linear hydrologic model that estimates lake level as a function of net freshwater flux into the catchment basin (see Chapter 3) is considered here for six tropical lakes and reservoirs. This

simple basin model contains two parameters: effective catchment to lake area ratio and time delay, both determined independently by linear regression based on the simultaneous availability of lake level and rainfall. Despite its obvious simplicity and limitations, this model is expected to show comparable 90-days forecast estimates with altimeter observations for lake levels.

Datasets used in this study include: the National Centers for Environmental Prediction (NCEP) retrospective forecast (reforecast) from the coupled atmosphere–ocean Climate Forecast System version 2 (CFSv2) (Saha et al. 2012), the European Centre for Medium Range Weather Forecasts (ECMWF) ERA-Interim reanalysis (Simmons et al. 2007a,b; Uppala et al. 2008), and one satellite-based observational dataset the Tropical Rainfall Measurement Mission (TRMM) Multi-Satellite Precipitation Analysis (TMPA) (Huffman et al. 2007). Forecast model estimates of lake level are validated with the radar altimetry-derived water level observations from the Global River and Lake product database produced by De Montfort University, a European Space Agency Project (ESA-DMU) (Berry and Wheeler 2009). These model estimates depend on the input net freshwater flux data; thus, another objective of this Chapter is to compare three available rainfall products and to determine the bias in hydrologic model of CFSv2 product.

Jury (2009) has shown that the climate forecast system of the earlier NCEP CFS version 1 (CFSv1; Saha et al. 2006) rainfall gives reasonably good results, with 83% good representation of studied features in the Caribbean region. Another study has shown that the CFSv1 forecast of cumulative precipitation at subseasonal scale over the Sahel has a 1 mm day^{-1} dry bias during the peak periods with respect to the

observations (Vintzileos and Thiaw 2006). However, the analysis of CFSv1 seasonal hindcast of the interannual variability over Nordeste in Brazil (Misra and Zhang 2007) indicates that the model has a large-scale error in the tropical Atlantic Ocean, and that the mean precipitation errors in the CFSv1 over Nordeste depend on lead time. In addition, variations in southwest US regional rainfall by using CFSv1 simulations show overestimates and underestimates of rainfall over different parts of the United States (Yang et al. 2009).

The assessment of the initial version, CFSv1, and its upgrade, CFSv2, could be important for understanding its performance in climate predictions and simulations. Yuan et al. (2011) has shown a first look at the capability of CFSv2 on surface air temperature and precipitation predictions based on analyzing the 28-year (1982–2009) reforecasts. Averaged globally, CFSv2 increases the predictive skill for month-1 land surface air temperature and precipitation from the CFSv1 by 37% and 29%, respectively, and has comparable performance to the latest ECMWF model. Though there is limited skill beyond month-1, CFSv2 shows promising features for advancing hydrological forecast and application studies.

4.2 Study Regions

In this study we focus on a sample of six lakes and reservoirs distributed in tropical latitudes: five in Africa and one in Southeast Asia. Lake Tanganyika is one of the world's largest lakes by volume and second in depth. Its major inputs are from the Ruzizi and Malagarasi Rivers and major outflow into the Lukuga River. Deep and long Lake Malawi is located within the Zambezi River basin and it is the second

largest and second deepest lake in Africa. Supplied primarily by the Ruhuhu River, Lake Malawi drains into the Shire River. Both lakes experience the main rainy season in boreal winter.

The other three African lakes we consider all experience the main rainy season in boreal summer: Lake Tana, Lake Chad, and Kainji Reservoir. Lake Tana is fed by four rivers and numerous seasonal streams. Shallow Lake Chad experiences seasonal level fluctuations in the lake and surrounding marsh area between dry and wet seasons. It receives most of its water from the Chari/Logone river system, which connects Chad to the seasonally rainy highlands to the south with similar timing but half the amplitude of Kainji Reservoir and Lake Tana (van Campo and Gasse 1993). Most water loss is through evaporation and water extraction, though it has ~15% water loss through ground seepage (Carmouze et al. 1983; Isiorho et al. 1996).

Lake Tonle Sap in Cambodia, the largest lake in Southeast Asia, has only one major inlet/outlet – the Mekong River. Water drains from Lake Tonle Sap into the Mekong through Tonle Sap River beginning in September, and by spring it has an average depth of only 1m. The onset of the monsoon season in late May and the resulting rise in Mekong River water levels reverses the direction of Tonle Sap River, so Lake Tonle Sap begins to flood, quadrupling its surface area, and deepening it to up to 9 m. Large changes in the area of Lake Tonle Sap mean that its volume depends on both lake level and surface area (Magome et al. 2004; Mekong River Commission 2005).

4.3 Datasets

This study has a focus on three parameters: lake level, rainfall, and evaporation. Lake level variability is determined by satellite radar altimeter observations. The available satellite radar altimetry products can contain data from several satellite radar altimetry missions. Here we utilize one altimeter water level product, the Global River and Lake product database produced by De Montfort University, a European Space Agency Project (ESA-DMU) (Berry and Wheeler 2009). This product is based on data from the Environmental Satellite ENVISAT altimeter, that follows a 35-day repeat cycle with 70 km equatorial track spacing, and has a root mean square (RMS) accuracy on the order of 9 cm on average over most lakes (Crétaux and Birkett 2006). Uncertainties due to altimeter sampling and processing among available altimeter products have already been explored (see Chapter 2). In general, comparison of the combined altimeter record to gauges and intercomparison of measurements between instruments suggest the level estimates for large lakes are generally accurate to within 5 cm, but may degrade to tens of cm (e.g., Lake Chad, Birkett 2000) to over a meter (e.g., narrow reservoirs such as Lake Powell) depending on the target (Birkett et al. 2011; Crétaux et al. 2011a; Ričko et al. in review).

Three rainfall products considered here are: the NCEP seasonal retrospective forecast from the coupled atmosphere–ocean CFSv2 (Saha et al. 2012), the updated ECMWF ERA-Interim reanalysis (Simmons et al. 2007a,b; Uppala et al. 2008), and the TRMM 3B42 (V6) daily precipitation product (Huffman et al. 2007). First, a 6-hourly resolution CFSv2 reanalysis from a full coupled atmosphere, ocean, land surface models, and data assimilation system. The CFSv2 used in the reforecast

consists of the NCEP Global Forecast System at T126 (~0.937°) horizontal resolution, the Geophysical Fluid Dynamics Laboratory Modular Ocean Model version 4.0 at 0.25–0.5° grid spacing coupled with a two-layer sea ice model, and the four-layer NOAH land surface model. In addition to the various improvements in the model physics, 9-month CFSv2 forecasts are initialized every 5 days apart from observations and four times per day from CFS reanalysis (Saha et al. 2010). Here we utilize only one 6-hourly reforecast of rainfall from a 9-month run that begins on January 1st 2010. Second rainfall product, ERA-Interim reanalysis, is derived here from the 3-h time step model forecasts from the 0000 UTC global analysis at 1.5^{o} spatial resolution, and represents an update of the earlier 40-yr ECMWF Re-Analysis (ERA-40) (Uppala et al. 2004), created to address systematic errors in this earlier reanalysis. The main advances in the ERA-Interim are in data assimilation (e.g., improved model physics, data quality control, bias handling, higher horizontal resolution) and use of recent observations. Over tropical land areas the ERA-Interim rainfall is slightly higher (in general up to 3 mm day^{-1}) than in the previous reanalysis (Uppala et al. 2008). In particular Betts et al. (2009) reports significant improvements of ERA-Interim rainfall over the Amazon basin, showing more rainfall in all seasons than ERA-40 (up to 1 mm day^{-1}), but with an annual cycle that is still too weak. Third, the observation-based TMPA product is an adjusted satellite analysis combining active and passive observations from the TRMM satellite together with more frequent geostationary IR measurements to obtain a calibrated product with high temporal sampling, available daily at 0.25^{o} spatial resolution.

Lastly, we consider two evaporation products, one from the CFSv2 reforecast

and one from the ERA-Interim reanalysis. These two reanalysis data are used here primarily for the purpose of evaluating the bias in net freshwater flux between them. In the tropics evaporation has much weaker variations than precipitation (Yoo and Carton 1990), also illustrated for our 6 lakes (Fig. 4.1). Even though evaporation may contribute to final error significantly at some regions, here we consider in the tropics seasonal and interannual estimates of net freshwater flux to be insensitive to the precision of the evaporation estimates.

4.4 Methods

All datasets are interpolated to a uniform 1-day interval for comparison purpose. In altimeter product, data outliers have been removed (identified subjectively) and short gaps filled in the time series by linear interpolation.

Bias observed in rainfall and evaporation given by CFS reforecast data with respect to ERA-Interim reanalysis is determined and used to correct CFS data. Then, linear trend in the net freshwater flux data, as well as in the raw altimeter observations of water level, is removed prior comparison of model result and altimeter observations over a 3-month period.

For the model calculations, two model parameters, effective catchment to lake ratio and time delay between freshwater flux and lake level response, are taken from the results derived in Chapter 3 and used as constants for a set of six lakes and reservoirs (see Chapter 3, Table 3.4). The resulting model explained in the following section is then used for the forecast model calculations and initialized with respect to the ESA-DMU altimeter observations.

4.5 Forecasting Model

Here we use a simple water balance model previously explained in Chapter 3, and similar to those used elsewhere (e.g., Calder et al. 1995; Nicholson et al. 2000; Vallet-Coulomb et al. 2001; Kebede et al. 2006). This predictive model gives an approximate relationship between lake level anomaly from its time mean (H), lake area (A_L), catchment area (A_C), and anomalous net freshwater flux ($\widetilde{P} - \widetilde{E}$). Assumptions used for the model are: a single constant delay (δt) between the time of freshwater flux and the accumulation of water in the lake, no spatial variations in water level within the lake, and A_C and A_L are constant. We neglect thermal expansion effects, the effects of changing salinity on evaporation rates, all water loss, and we ignore anthropogenic influences.

$$\widetilde{H}(t) = \frac{A_c}{A_L} \int_{\tau=-\delta t}^{t-\delta t} [\widetilde{P}(\tau) - \widetilde{E}(\tau)] d\tau + \widetilde{H}(t=0), \tag{4.1}$$

The predictive equation (4.1) (derived in Chapter 3) then gives the time-fluctuating anomaly of net freshwater flux from its time mean, averaged over the catchment basin, and similarly represents the time-fluctuating lake level anomaly about its mean.

The model contains two parameters: effective catchment to lake ratio defined as the ratio of catchment area to lake area $(A_C/A_L)_{eff}$, and time delay between freshwater flux and lake level response (δt). These parameters allow us to construct model estimates of lake level based solely on freshwater flux estimates. Any unmodeled

drainage (e.g., ground water seepage) is folded into the definition of $(A_C/A_L)_{eff}$.

The simple hydrologic model described in Chapter 3 is explored here with net freshwater flux parameter averaged over the lake catchment basins for our set of six lakes and reservoirs.

4.6 Results

4.6.1 Intercomparison of Rainfall and Evaporation Products

Variations in rainfall and evaporation time series are illustrated in Fig. 4.1 for the six lakes used in this study. As noted above, in the tropics evaporation has much weaker variations than rainfall, thus we focus more on rainfall variations between the products. It is shown that CFSv2 experiences the largest rainfall variations than observed in other two rainfall products (ERA-Interim and TRMM) during the peak of rainy season specifically at Kainji, Malawi and Tanganyika. Similarly, variations of TRMM are larger at times than those of ERA-Interim and CFSv2 for some lakes (Malawi, Tonle Sap and Chad), while for other lakes (Tana, Tanganyika and Kainji) TRMM variations are much smaller.

The CFSv2 reforecast rainfall experiences larger values (wet bias) with respect to other two rainfall products for most lakes and reservoirs (Table 4.1), except for Lake Malawi and Lake Tonle Sap at which CFSv2 rainfall experiences smaller values (drier bias) with respect to TRMM rainfall (up to ~1 mm day^{-1}). Overall, smaller biases are observed between CFSv2 and ERA-Interim than between CFSv2 and TRMM, except for Lake Chad that shows the smallest bias of 0.06 mm day^{-1} between CFSv2 and TRMM. TRMM experiences wet bias with respect to ERA-Interim at

Tana, Tanganyika and Kainji, while for other lakes has a dry bias. We note that bias values between rainfall products are rather small, no larger than ~1 mm day^{-1} for a given lake or reservoir, while biases between CFSv2 and ERA-Interim evaporation can be double of those of rainfall (up to ~2 mm day^{-1} at Kainji reservoir). Overall, this result of wet bias in net freshwater flux between the two products, CFSv2 and ERA-Interim, can range up to ~3 mm day^{-1} at Kainji reservoir (Table 4.1). Only Lake Tana experiences a dry bias of -0.75 mm day^{-1} in net freshwater flux. Both rainfall and evaporation experience errors in the reanalysis datasets. At times they may compensate each other thus final net freshwater flux error can vary significantly between the datasets during specific times over some locations. Figure 4.2 shows mean 9-month distribution of net freshwater flux over a full band of tropical latitudes, both for CFSv2 and ERA-Interim product. These differences are equally positive and negative over land, indicating that any conclusion drawn from results obtained from a small set of lakes and reservoirs above is specific and limited to geographical locations. Differences between net freshwater flux obtained from the two products show wetter biases (up to ~8 mm day^{-1}) over the west African Sahel, southern regions of South America, and in most parts of Indonesia; while drier biases (up to -10 mm day^{-1}) are observed mostly over northern Brazilian regions, Central America, and some regions of southern Asia.

After accounting for the model bias correction in CFSv2, the smallest RMS differences between any rainfall products (Table 4.2) are observed for Lake Chad ranging from only 1.87 mm day^{-1} (between TRMM and ERA-Interim) to 2.01 mm day^{-1} (between CFSv2 and TRMM). In contrast, the largest RMS differences are

observed for Kainji reservoir ranging from 7.51 mm day^{-1} (between TRMM and ERA-Interim) to 12.50 mm day^{-1} (between CFSv2 and TRMM). Similarly, much smaller minimum (0.26 mm day^{-1}) and maximum (1.35 mm day^{-1}) evaporation RMS differences between CFSv2 and ERA-Interim are observed for Lake Chad and Lake Tana (Table 4.2). The smallest mean RMS differences are noticed between TRMM and ERA-Interim (3.85 mm day^{-1}), while the largest between CFSv2 and ERA-Interim (4.88 mm day^{-1}) over all six lakes and reservoirs. Overall, RMS differences can be considered similar among the three different rainfall products, thus net freshwater flux from ERA-Interim and bias corrected CFSv2 are chosen for the next step of forecasting lake levels.

4.6.2 Validation of Forecast Model-based Lake Level Estimates using Altimetry Observations

Here lake level observations obtained from three satellite radar altimetry products (ESA-DMU, GRLM and LEGOS) were used to validate two model-derived forecast lake levels of CFSv2 and ERA-Interim net freshwater flux. Both model forecast results show significant agreement with altimeter observations at a probability level of 0.05 for most lakes studied here (Fig. 4.3 and Fig. 4.4). Correlations range from negative -0.61 for Lake Tonle Sap to positive 0.44 for Kainji reservoir for ERA-Interim, and somewhat similar correlations from negative -0.44 for Lake Tana to positive 0.86 for Kainji reservoir for CFSv2, both significant at a probability level of 0.05 with respect to ESA-DMU over six lakes and reservoirs during a 90-day forecast period (Table 4.3 shows correlation among forecast models

and altimeter observations with a 95% confidence level interval). The highest correlation with altimeter observations is observed for Kainji reservoir in both model forecasts with r = 0.86 for CFSv2 and 0.44 for ERA-Interim with respect to ESA-DMU and r = 0.90 for CFSv2 and 0.50 for ERA-Interim with respect to GRLM (Table 4.3 and Table 4.4). Forecast results from both models with respect to LEGOS show similar results to those obtained with respect to ESA-DMU (Table 4.5). ERA-Interim gives smaller median correlation than CFSv2 (-0.15 versus 0.33) with respect to ESA-DMU for six lakes and reservoirs.

Few lakes experience insignificant correlations at a probability level of 0.05. For example, forecast model ERA-Interim with respect to ESA-DMU over Lake Malawi experiences significance at a probability level of 0.48. Similarly, forecast model CFSv2 over Lake Tonle Sap experiences significance at a probability level of 0.66. Both forecast models with respect to GRLM experience significant correlations at great probability levels (0.17-0.79) for most lakes. The fact that the ESA-DMU raw altimeter time series have only 3 original measurements during a 90-day period can be responsible for the significant lower correlations and unacceptable probability levels at some lakes. Overall, GRLM time series show lower correlations with less significant probability levels, even though contain slightly larger number of 9 original measurements. Higher time resolution observations (altimeter or *in situ* gauge) are necessary for further investigation.

A closer examination shows that the model-derived lake level estimates compared to altimeter observations experience RMS errors ranging from 1 cm for Lake Chad up to 2.80 m for Kainji reservoir in ERA-Interim and from 2 cm for Lake

Chad up to 2.22 m for Kainji reservoir in CFSv2 with respect to ESA-DMU (Table 4.3, 4.4 and 4.5 show RMS difference with standard error interval). Given RMS errors for six lakes and reservoirs are comparable to the observed altimeter errors itself (see Chapter 2 for altimeter error values). There is no overall best forecast model suitable for all lakes. The best model result varies here between ERA-Interim and CFSv2 for the six lakes and reservoirs.

Lake level estimates obtained from model forecasts experience bias with respect to altimeter observations over most six lakes and reservoirs. Positive bias indicates higher lake level produced by model forecast with respect to altimeter observations, which can range from 0 cm at Lake Chad up to 1.62 m at Kainji reservoir over a 90-day forecast period. In contrast, some lakes, such as Lake Chad and Lake Malawi, experienced lower values (negative bias) in model-based estimates of lake level with respect to altimeter observations during most of the 90-day forecast period (1 cm with respect to ESA-DMU at Lake Malawi and 9 cm with respect to GRLM at Lake Tana, respectively). These values can be acceptable as they do not exceed much of the RMS errors between the altimeter products (observed in Chapter 2) for most of the tropical lakes studied here. However, Kainji reservoir consistently shows the poorest result and experiences the largest RMS errors between the altimeter observations and between the forecast models with respect to altimeter observations. This can be due to the fact that the simple model used here cannot represent well tropical reservoirs with unknown anthropogenic influences.

4.7 Conclusions

The results of this study suggest that introduction of a simple 2-parameter hydrologic model into climate forecast models, such as the NCEP CFSv2, can be considered as a useful interim step until higher resolution climate forecast models are developed that can support more sophisticated full hydrologic system models for seasonal forecasts of lake levels. One factor that limits skill of the current numerical climate models is the bias in the model forecasts with respect to observations. A way of achieving skill, and to determine systematic errors in seasonal forecasts, is to implement an objective bias correction such as one performed in this study for a net freshwater flux.

The CFSv2 model bias, present because of systematic errors in the model hydrologic cycle, is determined with respect to ERA-Interim reanalysis. Over a set of six tropical lakes and reservoirs, net freshwater flux experiences small wet bias with a maximum of ~3 mm day^{-1} for Kainji reservoir, except for Lake Tana which experiences dry bias of -0.75 mm day^{-1}. After correcting for these, a simple hydrologic model is used for a single 90-day forecast that begins on January 1st, 2010. The resulting RMS error between forecast CFSv2 lake level estimates and altimeter observations after 90 days can range from 2 cm for Lake Chad to 2.22 m for Kainji reservoir.

Despite some simplifications associated with this 2-parameter model that could explain some of the mismatch between the model predictions and observations, it is shown that for most tropical lakes the skill of the bias corrected CSFv2 forecast and ERA-Interim forecast is significant. The quality of the results depends on the quality

of surface flux estimates. Forecast model estimates of lake level for 90-day forecasts maintain a relatively realistic mean state compared to those in observed lake level products. However, this simple model has shown that it cannot be applicable for tropical reservoirs with unknown anthropogenic influences (e.g. Kainji reservoir). In addition, for forecasting non-tropical lakes located in higher latitudes, the model would need to include additional parameters that can give information about the presence of ice and freezing periods.

Overall, these results offer a promising opportunity to easily and efficiently incorporate this simple hydrologic model into the predictive climate system model (e.g., CFSv2) for forecasting of tropical lake levels in the seasonal range (2-4 months) based on an output from the weather prediction center forecast models, yet unexplored until now. This type of model thus potentially represents a significant contribution to earth system modeling and can be easily used by climate modelers and by water management community. Future development of this topic includes increasing the number of tropical lakes and reservoirs distributed on other continents, and evaluating the forecast model outputs for other 90-day periods over multiple lead times.

4.8 Tables

Table 4.1 Bias for rainfall (P), evaporation (E), and net freshwater flux (P-E) in mm day^{-1}.

Lake	P (mm day^{-1})			E (mm day^{-1})	P-E (mm day^{-1})
	CFSv2-ERAI	CFSv2-TRMM	TRMM-ERAI	CFSv2-ERAI	CFSv2-ERAI
Chad	0.39	0.06	-0.32	-0.45	0.84
Kainji	0.97	1.22	0.25	-1.99	2.96
Tana	0.21	3.20	3.00	0.96	-0.75
Tanganyika	0.14	0.52	0.38	0.03	0.11
Malawi	0.46	-0.70	-1.16	0.31	0.15
Tonle Sap	0.01	-1.02	-1.03	-0.90	0.91

Table 4.2 RMS difference among product time series of rainfall (P) and evaporation (E) in mm day^{-1}.

	P (mm day^{-1})			E (mm day^{-1})
Lake	CFSv2 vs ERAI	CFSv2 vs TRMM	TRMM vs ERAI	CFSv2 vs ERAI
Chad	1.99	2.01	1.87	0.26
Kainji	12.50	12.50	7.51	1.20
Tana	8.17	8.71	9.25	1.35
Tanganyika	2.66	2.93	2.91	0.64
Malawi	4.12	3.04	2.81	0.92
Tonle Sap	5.63	4.79	4.79	1.07

Table 4.3 Correlation and RMS difference (m) among forecast model (ERA-Interim and CFSv2) and ESA-DMU altimeter observations of lake level during 3-month period. 95% confidence intervals are included for correlation. Standard error intervals are included for RMS difference.

	Correlation		RMS (m)	
Lake	Model-ERAI vs ESA-DMU	Model-CFSv2 vs ESA-DMU	Model-ERAI vs ESA-DMU	Model-CFSv2 vs ESA-DMU
Chad	-0.38 ± 0	0.44 ± 0	0.01 ± 0	0.02 ± 0
Kainji	0.44 ± 0.29	0.86 ± 0.29	2.26 ± 0.03	2.22 ± 0.03
Tana	-0.59 ± 0.01	-0.44 ± 0.01	0.09 ± 0	0.09 ± 0
Tanganyika	0.43 ± 0.01	0.21 ± 0.01	0.04 ± 0	0.05 ± 0
Malawi	0.08 ± 0.01	0.46 ± 0.01	0.05 ± 0	0.06 ± 0
Tonle Sap	-0.61 ± 0.05	-0.05 ± 0.04	0.42 ± 0	0.39 ± 0

Table 4.4 Correlation and RMS difference (m) among forecast model (ERA-Interim and CFSv2) and GRLM altimeter observations of lake level during 3-month period. 95% confidence intervals are included for correlation. Standard error intervals are included for RMS difference.

	Correlation		RMS (m)	
Lake	Model-ERAI vs GRLM	Model-CFSv2 vs GRLM	Model-ERAI vs GRLM	Model-CFSv2 vs GRLM
Chad	-0.37 ± 0	-0.13 ± 0	0.02 ± 0	0.03 ± 0
Kainji	0.50 ± 0.21	0.90 ± 0.21	1.40 ± 0.02	1.35 ± 0.02
Tana	0.38 ± 0.01	0.03 ± 0.01	0.09 ± 0	0.09 ± 0
Tanganyika	0.13 ± 0.01	0.26 ± 0.01	0.05 ± 0	0.06 ± 0
Malawi	0.15 ± 0.01	0.06 ± 0.01	0.08 ± 0	0.10 ± 0

Table 4.5 Correlation and RMS difference (m) among forecast model (ERA-Interim and CFSv2) and LEGOS altimeter observations of lake level during 3-month period. 95% confidence intervals are included for correlation. Standard error intervals are included for RMS difference.

	Correlation		RMS (m)	
Lake	Model-ERAI vs LEGOS	Model-CFSv2 vs LEGOS	Model-ERAI vs LEGOS	Model-CFSv2 vs LEGOS
Kainji	0.38 ± 0.34	0.79 ± 0.34	2.80 ± 0.04	2.77 ± 0.04
Tana	-0.68 ± 0.01	-0.60 ± 0.01	0.11 ± 0	0.11 ± 0
Tanganyika	0.47 ± 0.01	0.41 ± 0.02	0.09 ± 0	0.09 ± 0
Malawi	-0.22 ± 0.02	0.35 ± 0.02	0.19 ± 0	0.18 ± 0

4.9 Figures

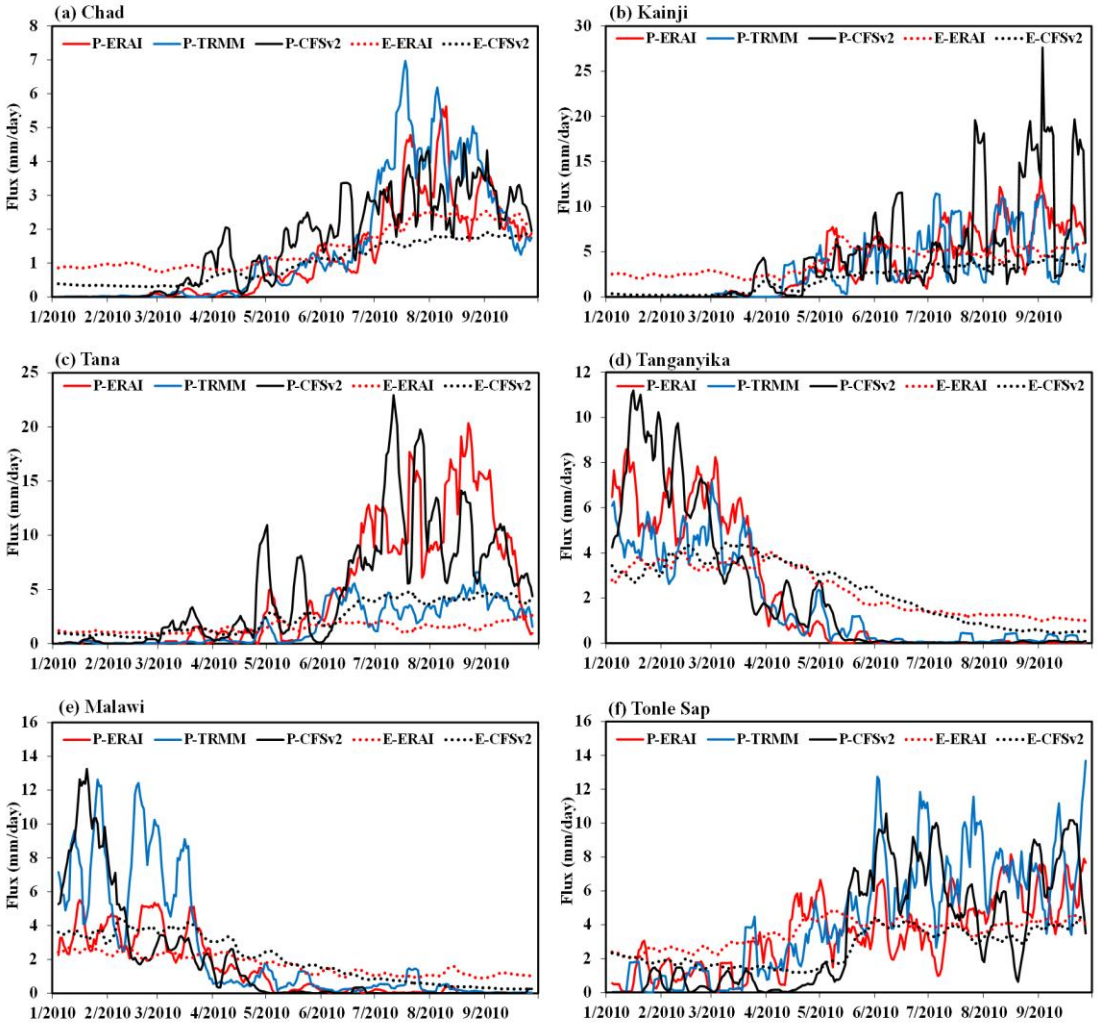

Figure 4.1 Comparison of rainfall and evaporation estimates (mm day^{-1}) for: ERA-Interim (red), TRMM (blue), and CFSv2 (black) rainfall; ERA-Interim (red dotted) and CFSv2 (black dotted) evaporation, averaged over the lake's catchment area, for six lakes: (a) Chad, (b) Kainji, (c) Tana, (d) Tanganyika, (e) Malawi, and (f) Tonle Sap during 1/2010-9/2010.

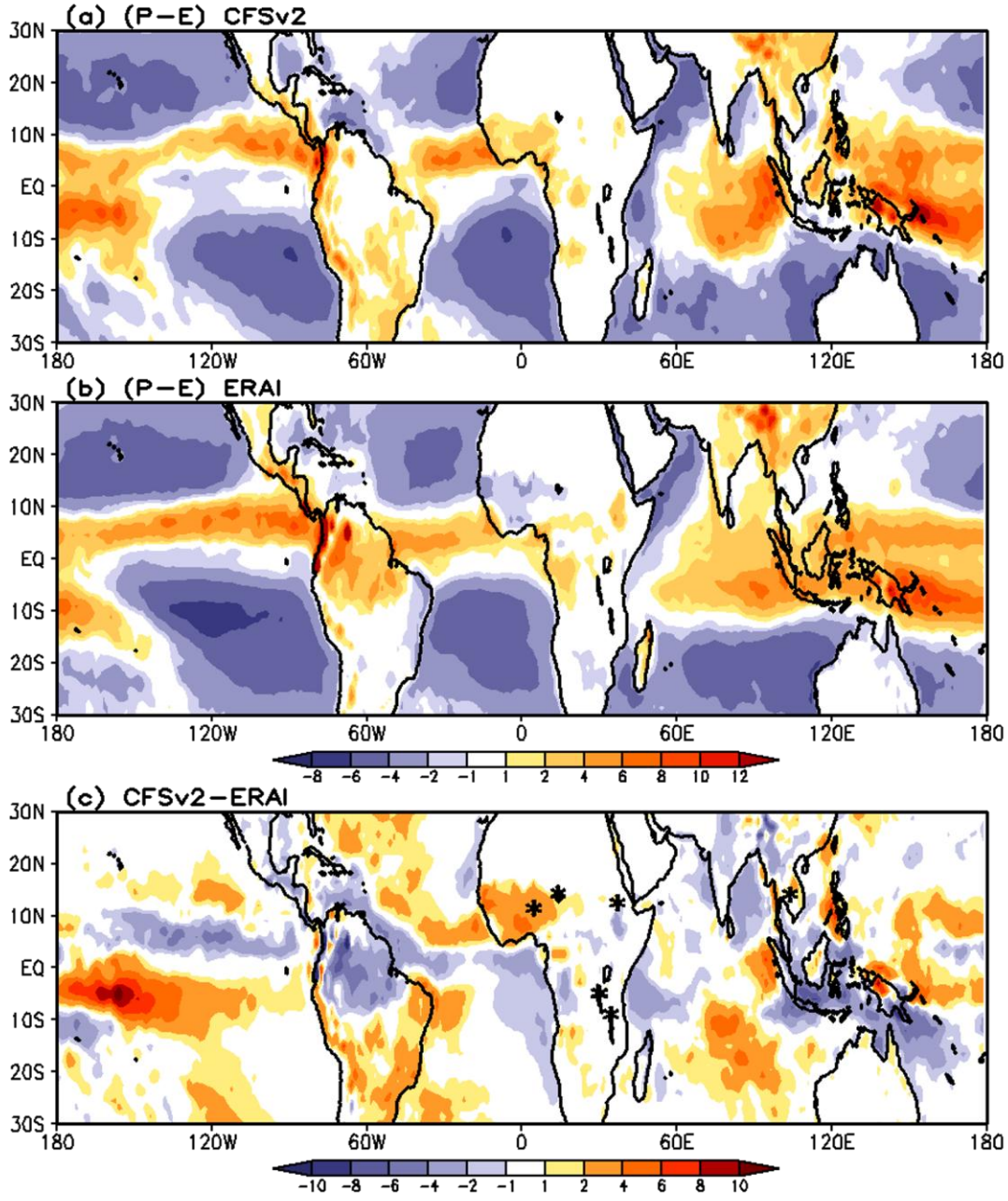

Figure 4.2 Mean distribution of P-E (mm day^{-1}) for: (a) CFSv2 reforecast, and (b) ERA-Interim reanalysis, and (c) their difference, over tropical latitudes during 9-month period (1/2010-9/2010). Stars in panel (c) indicate 6 lakes studied here.

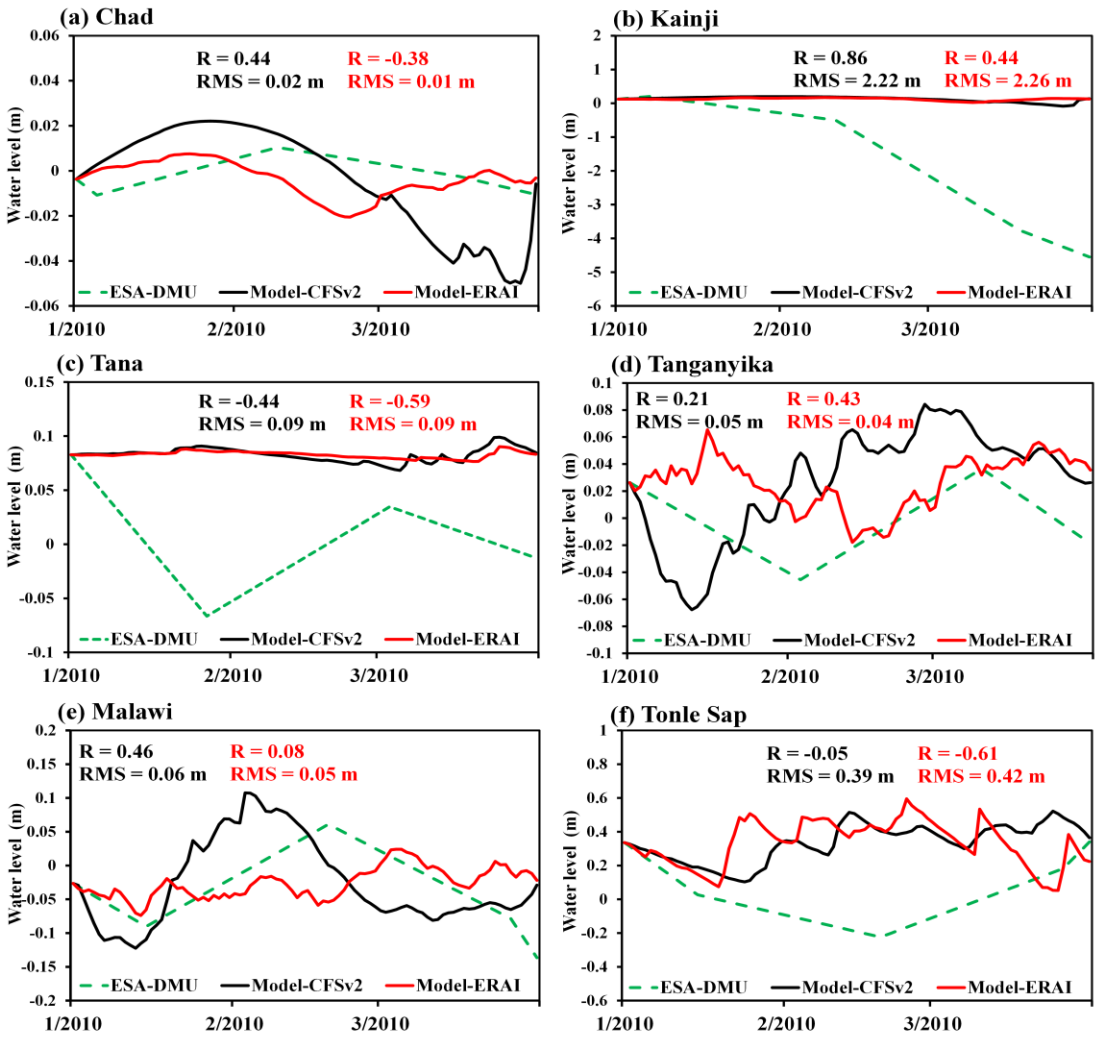

Figure 4.3 Comparison of water level estimates (m) of observed ESA-DMU (green dashed) with modeled CFSv2 (black) and ERA-Interim (red) lake level for six lakes: (a) Chad, (b) Kainji, (c) Tana, (d) Tanganyika, (e) Malawi, and (f) Tonle Sap during 1/1/2010-3/31/2010.

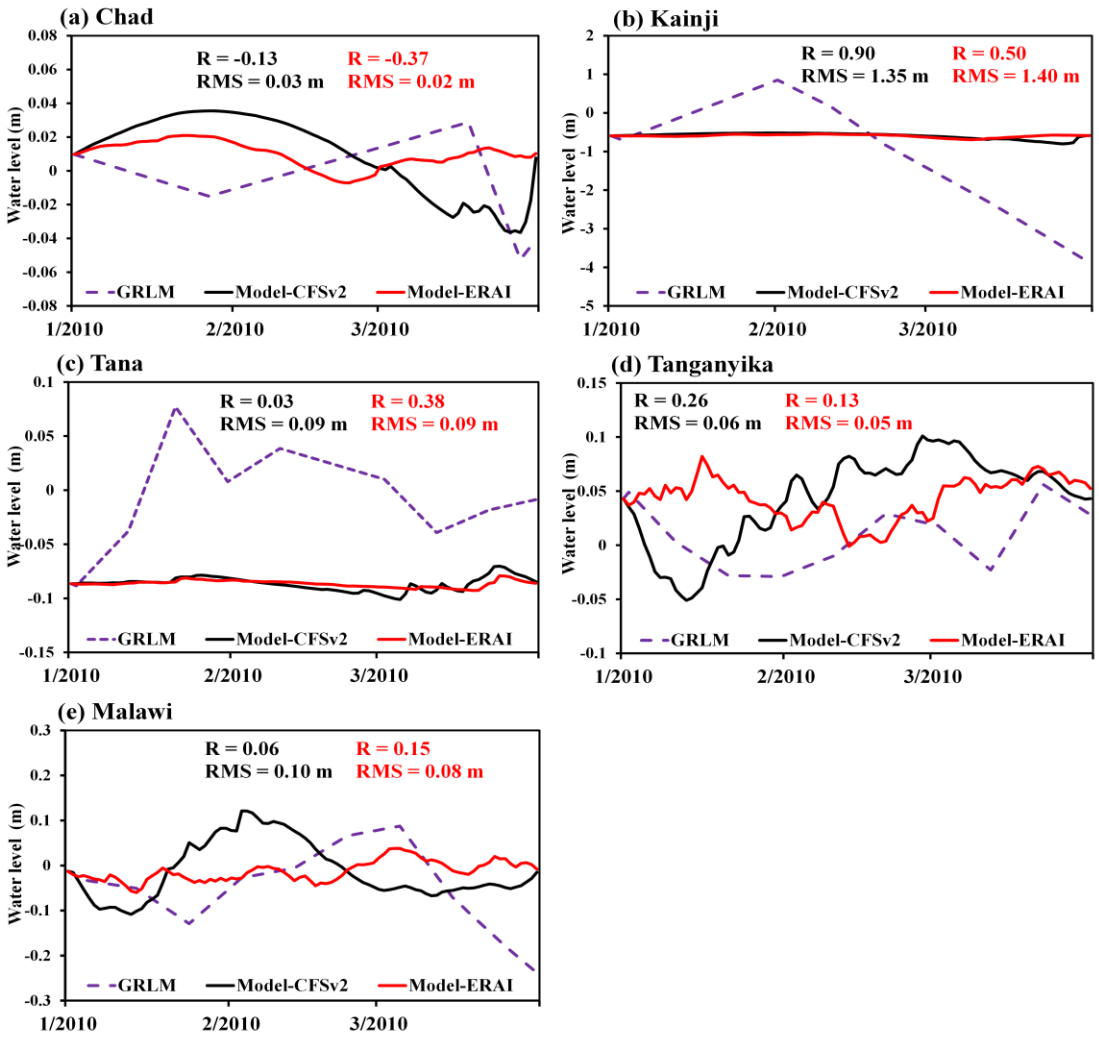

Figure 4.4 Comparison of water level estimates (m) of observed GRLM (purple dashed) with modeled CFSv2 (black) and ERA-Interim (red) lake level for five lakes: (a) Chad, (b) Kainji, (c) Tana, (d) Tanganyika, and (e) Malawi during 1/1/2010-3/31/2010.

Chapter 5: Summary and Concluding Remarks

This dissertation has a focus on: *validating satellite radar altimetry products*, *modeling*, and *forecasting* of water level in lakes and reservoirs. Targets are the tropical and global lakes and reservoirs at *intraseasonal*, *interannual* to *decadal* time-scales variations.

Chapter 2 has critically examined, validated and discussed three available continental water level products derived from satellite radar altimetry. The approaches used to generate these three products differ in methodology. Yet, all three radar altimetry products performed well for a sample of lakes and reservoirs of varying latitude, size, surface roughness, and surrounding terrain. This conclusion is based on treating *in situ* gauges as accurate estimators of lake and reservoir levels and thus differences between the altimeter products and the gauge time series provide estimates of the error in the altimeter time series. However, technical problems with gauges, data gaps, as well as unrepresentative siting (e.g., near the outlets of lakes and reservoirs) can easily increase the gauge error. Also, gauge time series are not publically available for many lakes and reservoirs, and if available are likely undocumented.

Examination of the internal error estimates shows some consistent patterns and reassuringly similar results from the three altimetry products. The North American Great Lakes show the smallest errors (<10 cm); while the largest errors, as determined by comparison to gauge time series, occur for the lakes that freeze (Lake Athabasca and Lake of the Woods). For these lakes the RMS differences between the

three products and gauge data are ≥50% of the lake level variability itself, most probably due to reduced performance of the radar altimeters when ice is present. However, even for the smaller lakes the error levels appear to be sufficiently low to detect climate variability in the two-decade available satellite radar altimeter record.

An extensive observational analysis of the climate effects of intraseasonal to interannual variations of water levels in a set of tropical lakes and reservoirs was presented in Chapter 3. This work explored the use of a simple empirical model in deriving lake level estimates from rainfall. The model parameters (delay time and catchment to lake area ratio) determined by the model provide important information regarding the hydrological properties of the lake basin. The ability to estimate these parameters is important since there are few published estimates of the delay time parameter and published estimates of the catchment to lake area ratio vary widely. The development of lake-level models driven by rainfall gives us a way to evaluate the accuracy of the rainfall products by using the lake catchment basins as if they are giant rain gauges.

Simplifications inherent in the simple empirical model used here likely explain much of the mismatch between the model predictions and observations. Besides many simplifications and assumptions used in this model, the quality of the results will highly depend on the quality of surface flux estimates. Evaluating the impact of these simplifications and developing more sophisticated models should open up new avenues for research.

Finally, the success of the models suggests a number of potential applications, including providing level estimates for basins where no ground-based or satellite-

based level data is available, and in developing lake level hindcasting/forecasting capabilities. It can be used by climate modelers and by the water management community, and thus potentially represents a significant contribution to earth system modeling.

It is noted that coupled climate models have systematic and coherent biases in simulating net freshwater flux (precipitation minus evaporation). An alternative approach to climate forecast models for the lake levels is analyzed in Chapter 4. The results of this work suggest that a simple 2-parameter hydrologic model can be introduced into climate forecast models and be considered a useful interim step until higher resolution climate forecast models are developed that may support more sophisticated full hydrologic system models for seasonal forecasts of lake levels. The bias in the model forecasts with respect to observations presents an important factor that limits skill of the current numerical climate models. This has to be accounted for in seasonal forecasts in order to achieve better skill and to determine systematic errors.

Despite some simplifications associated with this 2-parameter model, the bias corrected examined 90-day forecasts of water level for most tropical lakes give significant results and maintain a relatively realistic mean state with respect to those observed in lake level products. These novel results offer a promising opportunity to easily and efficiently incorporate this simple hydrologic model into the predictive climate system model for forecasting of lake levels in the sub-seasonal to seasonal range (2-4 months), and perhaps even interannual, based on output from the climate prediction center forecast models. This also offers a significant contribution to earth

system modeling. It is important to note that modeling and forecasting with this simple model works great for lakes, but it is not applicable for reservoirs with unknown anthropogenic influences. Future development of this work includes increasing the number of tropical lakes and reservoirs distributed globally, and examining the forecast model results of water levels in lakes for other time periods over multiple lead times.

Appendix A: Altimetric Lake Height Accuracy and Error Budget

A full explanation of the construction of altimetric lake height and the expected accuracy over the lakes and reservoirs based on the T/P Geophysical Data Records (GDR) was provided by Birkett (1995). To summarize for more recent Jason2/OSTM (Birkett and Beckley 2010, Dumont et al. 2009), the corrected altimetric range R_{corr} and the surface height H, with respect to the reference ellipsoid, are given by two Equations:

$$R_{corr} = R + A_{wet} + A_{dry} + A_{iono} + SSB \quad (A.1)$$

and

$$H = (Alt - R_{corr}) + T_{La} + T_E + T_P + T_L. \quad (A.2)$$

R is the altimetric range that has been corrected for calibration and instrument effects such as the center of gravity motion and the calibration and pointing angle errors. The Doppler shift and ultra-stable oscillator drift, related to the altimeter acceleration, are also included here. A_{wet}, A_{dry} and A_{iono} are the atmospheric corrections related to the water vapor and dry gases in the troposphere, and the free electron content in the ionosphere. SSB is the sea state bias, a combination of three effects: (i) an instrument-related tracker bias, (ii) the electromagnetic or embias, which relates to differences in radar echo contribution between the crests and troughs

of surface waves, and (iii) skewness, which is associated with deviations from the assumption that the probability density function of heights within the instrument footprint is symmetric.

In Eq. (A.2), Alt is the satellite altitude, and T_{La}, T_E, and T_L are the lake, earth, and loading tides associated with the lunar-solar forcing of the earth. T_P is the pole tide associated with variations in the Earth's rotation. For lake studies, an inverse barometric correction associated with the response of the water surface to atmospheric pressure is not applied, because in comparison with atmospheric pressure systems, the majority of lakes are small closed systems. A correction for geoid undulation (the EGM96 model within the Interim GDR (IGDR)) is also not applied as the focus is given on relative variations with time.

For large lakes and inland seas with wind-roughened unfrozen surfaces, three parameters: the radiometer-derived A_{wet}, the altimeter-derived dual-frequency A_{iono} and the model-derived SSB, mostly used for ocean surfaces, can be applicable here as well. Coastline interference and deviations of echo shape and power for the smaller or more sheltered lakes require the use of the alternate model-derived A_{wet} (ECMWF), A_{iono} (GIM), and assigns SSB = 0. No consideration is given to lake tides T_{La} within the Jason-2/OSTM IGDR. Except for the spring tides that can be ~8 cm for large lakes such as Lake Superior, lake tides in general can be assumed to be ~1–2 cm. However, without auxiliary data for each lake this term cannot be corrected for. The IGDR values for pole tide are based on the equilibrium pole tide. The Birkett (1995) repeat track method is flexible and partly manual. The various A_{wet} and A_{iono} options and the use of SSB are selected depending on the size of the target, the ground

track/coastline separation distance, the magnitude and variability of radar backscatter coefficient (σ°) and knowledge of winter ice conditions, and the validity of the correction. The Birkett et al. (2011) method for the GRLM Jason-2/OSTM products is more automated. It currently utilizes the AMR radiometer wet correction if valid (e.g., not set to the default value and <0), or if not, defaults to the ECMWF. It also applies the GIM ionospheric correction and the same scaling factor to the pole tide, and sets the SSB correction to zero. In both methods the lake elevations utilize the IGDR solution-1 load tide option and employ an identical range retracker (ocean or ice) for a given target.

Dumont et al. (2009) provide an estimated error analysis on the 1-Hz altimetric and geophysical parameters and corrections for average ocean conditions (2 m significant wave height and 11 dB σ°). Assuming similar values for the largest of lakes (Table A.1), overall root sum square (RSS) corrected range (R_{corr}) error is then 3–4.5 cm, depending on the range corrections chosen. Orbit altitude errors of 2.5 cm (IGDR) and combined tidal errors of ~1 cm place the RSS on an averaged 1-Hz lake height at ~4–5 cm. Some of the error contributions have already been confirmed by preliminary results from the Seattle 2009 Jason-2/OSTM Science Working Team (SWT) meeting. For example, the ocean-retracker range precision over the oceans is estimated at ~1.6 cm, the IGDR altitude error is <2.5 cm, and the error on A_{wet} is in the range of 0.1–0.8 cm. The values in Table A.1 can then be taken as first estimates, noting that the global altitude error is not thought to be highly geographically variable and its relative (repeat track) accuracy can be significantly better due to the removal of the time invariant, geographically correlated components.

The range precision R is a measure of the internal consistency or repeatability of the instrument and has an estimate of 1.7 cm. It is dominated by the error associated with estimating the location in the range window of a predefined point on the leading edge of the returned echo. For an ideal ocean echo, this point corresponds to the mean surface height in the altimeter footprint and is derived by interpolating across adjacent range bins of a given resolution. The altimeter response to lakes is not always similar to oceans and will change according to surface conditions. The range precision will thus vary on a lake-by-lake basis, noting extreme cases of super-calm water (specular echo) where the majority of echo power will be located in a single range bin of ~0.5 m resolution. Complex, multi-peaked echoes can also arise where islands, coastlines, and multiple small water targets are within the effective footprint, making the association of a range value to a single identifiable target difficult to achieve. In cases where the target can be easily identified, the range precision can be improved via averaging all available heights, from coast-to-coast, along the satellite ground track, effectively reducing the error by $1/\sqrt{N}$ where N is the number of valid measurements. This will not be the case for smaller targets where only a few 20-Hz height values are available, and in addition the overall height accuracy will be affected by the use of the model-derived A_{wet} and A_{iono}. The former depends in part on radiosonde measurements, and these can be sparse in many regions. For the latter, the GIM model may be in error by ~14% of the correction value, the error being strongly dependent on location, time of day, and solar activity (Scharroo and Smith 2010). Here we will assume a 3 cm (based on the historical T/P error budget; Birkett 1995) and 2 cm global average for the model-derived A_{wet} and A_{iono}, respectively.

Heavy rain events and the presence of lake ice in the footprint can cause a bias in the range measurement, and where possible such data must be identified and either highlighted or rejected.

Table A.1 Total error budget for 1-Hz IGDR lake height (from Birkett and Beckley 2010).

Contribution	RMS (cm)
Satellite orbit	2.5*
Range precision	(1.7)**
Wet troposphere correction, ECMWF/AMR	3/1.2
Dry troposphere correction	0.7
Ionosphere correction, GIM/DUAL	2.0/0.5
Earth + Pole + Loading tides	1
Sea state bias	2
Minimum total	4.04/5.26

*The removal of geographically correlated orbit error components via the use of repeat track techniques may reduce this value.
**Variable with surface roughness and target size.

Appendix B: Lake Model

Invoking conservation of mass for a lake catchment system leads to an approximate relationship between the lake level anomaly from its time mean (H), lake area (A_L), catchment area (A_C), anomalous net freshwater flux ($\tilde{P} - \tilde{E}$), and anomalous water loss (ε_t) at any given time (t) and space (x,y), from which begin with:

$$\frac{d}{dt}\left[\oiint H(x,y,t)dA_L\right] = \oiint [\tilde{P}(x,y,t-\delta t) - \tilde{E}(x,y,t-\delta t)]dA_C - \varepsilon_t . \qquad \text{(B.1)}$$

Assume H is independent of x and y, that A_L does not vary in time, and set $\varepsilon_t = 0$. We will assume that we have first removed the time mean precipitation and evaporation before applying these terms to (B.1) [e.g., $\tilde{P}(t) = P(t) - \overline{P}$]. Compute the time average of each term in (B.1):

$$\overline{\frac{d}{dt}[H(t)]} = \frac{1}{A_L}\overline{\oiint [\tilde{P}(x,y,t-\delta t) - \tilde{E}(x,y,t-\delta t)]dA_C} = 0. \qquad \text{(B.1a)}$$

So, we can replace H in (B.1) with its anomaly ($\tilde{H}$) relative to the time mean

$$\frac{d}{dt}[\tilde{H}(t)] = \frac{1}{A_L}\oiint [\tilde{P}(x,y,t-\delta t) - \tilde{E}(x,y,t-\delta t)]dA_C . \qquad \text{(B.2)}$$

Integrating (B.2) gives

$$\tilde{H}(t) = \frac{A_C}{A_L} \int_0^t [(\tilde{P}(\tau - \delta t) - \tilde{E}(\tau - \delta t)] d\tau + \tilde{H}(t = 0), \qquad \text{(B.3)}$$

where $\tilde{P}(t)$ is the average precipitation falling on the catchment area. Alternatively, we could assume $A_L = QH(t)$ in which case (B.2) becomes

$$QH^2(t) = \int_0^t A_C [\tilde{P}(\tau - \delta t) - \tilde{E}(\tau - \delta t)] d\tau + QH^2(t = 0), \qquad \text{(B.4)}$$

where now we need to write explicitly that $H(t) = \overline{H} + \tilde{H}(t)$. Define $A_{Lo} = 2Q\overline{H}$, and (B.4) becomes

$$\tilde{H}(t) + \frac{\tilde{H}^2(t)}{2\overline{H}} = \frac{A_C}{A_{Lo}} \int_0^t [\tilde{P}(\tau - \delta t) - \tilde{E}(\tau - \delta t)] d\tau + \tilde{H}(t = 0) + \frac{\tilde{H}^2(t = 0)}{2\overline{H}}. \qquad \text{(B.5)}$$

Note that (B.5) implies that correlating $\frac{A_C}{A_{Lo}} \int_0^t [\tilde{P}(\tau - \delta t) - \tilde{E}(\tau - \delta t)] d\tau$ with $\tilde{H}(t)$ can yield either a linear or quadratic relationship depending on level variability to mean level, $\sqrt{\overline{\tilde{H}^2}}\, \overline{H}^{-1}$.

Bibliography

Adler, R.F., G. J. Huffman, D. T. Bolvin, S. Curtis, and E. J. Nelkin, 2000: Tropical rainfall distributions determined using TRMM combined with other satellite and rain gauge information. *J. Appl. Meteor*., **39,** 2007–2023.

Alsdorf, D., C. Birkett, T. Dunne, J. Melack, and L. Hess, 2001: Water level changes in a large Amazon lake measured with spaceborne radar interferometry and altimetry. *Geophys. Res. Lett*., **28**, 14, 2671-2674.

Alsdorf, D., D. Lettenmaier, C. Vörösmarty, 2003: The need for global, satellite-based observations of terrestrial surface waters. *EOS Trans. AGU* **84**(29), 269.

Alsdorf, D. E., E. Rodriguez, and D. P. Lettenmaier, 2007: Measuring surface water from space. *Rev. Geophys.* **45**, RG2002.

Anyah, R. O., F. H. M. Semazzi, and L. Xie, 2006: Simulated physical mechanisms associated with climate variability over Lake Victoria basin in East Africa. *Mon. Wea. Rev.*, **134**, 3588-3609.

Anyamba, A., and J. R. Eastman, 1996: Interannual variability of NDVI Africa and its relation to El Niño-Southern Oscillation. *Int. J. Remote Sens.,* **1,** 2533-2548.

Argyilan, E. P., and S. L. Forman, 2003: Lake level response to seasonal climatic variability in the Lake Michigan-Huron system from 1920 to 1995. *J. Great Lakes Res.* **29**, 488-500.

Ashok, K., Z. Guan, and T. Yamagata, 2001: Impact of the Indian Ocean dipole on the relationship between the Indian monsoon rainfall and ENSO. *Geophys. Res. Lett.*, **28,** 4499–4502.

Avakyan, A. B. and V. B. Iakovleva, 1998: Status of global reservoirs: The position in the late twentieth century. *Lakes and Reservoirs: Res. Manage.*, **3,** 45-52.

Becker, M., W. Llowel, A. Cazenave, A. Güntner, and J.-F. Crétaux, 2010: Recent hydrological behaviour of the East African Great Lakes region inferred from GRACE, satellite altimetry and rainfall observations. *C. R. Geosci*. **342**, 223-233.

Benveniste, J., P. A. M. Berry, R. G. Smith, J. Freeman, L. Attwood, M. Milagro-Perez, and D. Serpe, 2007: River and Lake level data from Radar Altimetry in support of the Tiger initiative. Hydrospace07 workshop, Geneva, Switzerland, 12-14th November 2007.

Berry, P. A. M., 2002: A new technique for global river and lake height monitoring using satellite altimeter data. *Int. J. Hydropower Dams* **9**(6), 52–54.

Berry, P. A. M., J. D. Garlick, J. A. Freeman, and E. L. Mathers, 2005: Global inland water monitoring from multi-mission altimetry. *Geophys. Res. Lett.* **32**, 16401.

Berry, P. A. M., J. A. Freeman, R. G. Smith, and J. Benveniste, 2007: Near Real Time Global Lake and River Monitoring using the Envisat RA-2. In *Proceedings Envisat Symposium 2007,* Montreux, Switzerland, ESA SP-636.

Berry, P. A. M., and J. L. Wheeler, 2009: Jason2-ENVISAT exploitation, development of algorithms for the exploitation of Jason-2-ENVISAT

altimetry for the generation of a river and lake product. *Product Handbook*, **3**(5), De Montfort University Internal Report DMU-RIVL-SPE-03-110.

Berry, P. A. M., and J. Benveniste, 2010: Measurement of Inland surface water from multi-mission Satellite Radar Altimetry: sustained global monitoring for climate change. Chap. 29 in *Gravity, Geoid and Earth Observation*, International Association of Geodesy Symposia **135**, S. P. Mertikas, Eds., pp. 221-230, Springer Book Publications.

Betts, A. K., M. Köhler, and Y. Zhang, 2009: Comparison of river basin hydrometeorology in ERA-Interim and ERA-40 reanalyses with observations. *J. Geophys. Res*., **114,** D02101, doi:10.1029/2008JD010761.

Birkett, C. M., 1995: The contribution of TOPEX/Poseidon to the global monitoring of climatically sensitive lakes. *J. Geophys. Res*., **100,** 25179-25204.

Birkett, C. M., 1998: Contribution of the TOPEX NASA radar altimeter to the global monitoring of large rivers and wetlands. *Water Resour. Res*. **34**(5), 1223–1239.

Birkett, C. M., 2000: Synergistic remote sensing of Lake Chad: Variability of basin inundation. *Remote Sens. Environ*., **72,** 218-236.

Birkett, C. M., R. Murtugudde, and T. Allan, 1999: Indian Ocean climate event brings floods to East Africa's lakes and the Sudd Marsh. *Geophys. Res. Lett*., **26,** 1031-1034.

Birkett, C. M., L. A. K. Mertes, T. Dunne, M. H. Costa, and M. J. Jasinski, 2002: Surface water dynamics in the Amazon Basin: Application of satellite radar altimetry. *J. Geophys. Res*. **107 (D20**), 8059.

Birkett, C. M., and B. Beckley, 2010: Investigating the Performance of the Jason-2/OSTM Radar Altimeter over Lakes and Reservoirs. *Marine Geodesy* **33**(1), 204-238.

Birkett, C. M., C. Reynolds, B. Beckley, and B. Doorn, 2011: From Research to Operations: The USDA Global Reservoir and Lake Monitor. Chap. 2 in *Coastal Altimetry*, S. Vignudelli, A. G. Kostianoy, P. Cipollini, J. Benveniste, Eds., pp. 19-50, Springer Book Publications.

Birkinshaw, S. J., G. M. O'Donnell, P. Moore, C. G. Kilsby, H. Fowler, and P. A. M. Berry, 2010: Using satellite altimetry data to augment flow estimation technique on the Mekong River. *Hydrol. Process.* **24**, 3811-3825.

Bjerklie, D. M., S. L. Dingman, C. J. Vorosmarty, C. H. Bolster, and R. G. Congalton, 2003: Evaluating the potential for measuring river discharge from space. *J. Hydrol*. **278**, 17–38.

Calder, R.I., R. Hall, H. Bastable, H. Gunston, O. Shela, A. Chirwa, and R. Kafundu, 1995: The impact of land use change on water resources in sub-Saharan Africa: a modeling study of Lake Malawi. *J. Hydrol.*, **170,** 123–135.

Calmant, S., F. Seyler, and J. F. Crétaux, 2008: Monitoring continental surface waters by satellite altimetry. *Surv. Geophys*., **29**, 247-269.

Carmouze, J. P., J. R. Durand, C. Leveque, 1983: The lacustrine ecosystem during the "Normal Chad" period and the drying phase. *Lake Chad: Ecology and Productivity of a Shallow Tropical Ecosystem*, *Monogr. Biol*., Vol. 53, Dr. W. Junk Publishers, 527-560.

Charney, J. G., 1969: The intertropical convergence zone and the Hadley circulation of the atmosphere. *Proc. WMO/IUGG Symp. on Numerical Weather Prediction*, Tokyo, Japan, Japanese Meteorological Agency, 73–79.

Coe, M.T., and C. M. Birkett, 2004a: Calculation of river discharge and prediction of lake height from satellite radar altimetry: Example for the Lake Chad basin. *Water Resour. Res*., **40,** W10205, doi:10.1029/2003WR002543.

Coe, M.T., and C. M. Birkett, 2004b: Water resources in the Lake Chad basin: prediction of river discharge and lake height from satellite radar altimetry. *Water Resour. Res*. **40**(10), W10205.

Crétaux, J.-F., A. V. Kouraev, F. Papa, M. Bergé Nguyen, A. Cazenave, N. V. Aladin, and I. S. Plotnikov, 2005: Water balance of the Big Aral sea from satellite remote sensing and *in situ* observations. *J. Great Lakes Res.* **31**(4), 520-534.

Crétaux, J.-F., and C. Birkett, 2006: Lake studies from satellite radar altimetry. *C. R. Geosci.,* **338,** 1098-1112.

Crétaux, J.-F., S. Calmant, V. Romanovski, A. Shibuyin, F. Lyard, M. Berge-Nguyen, A. Cazenave, F. Hernandez, and F. Perosanz, 2009: An absolute calibration site for radar altimeters in the continental domain: Lake Issykkul in Central Asia. *J. Geod*. **83**(8), 723-735.

Crétaux, J.-F., and Coauthors, 2011a: SOLS: A lake database to monitor in near real time water level and storage variations from remote sensing data. *Adv. Space Res*., **47,** 1497-1507.

Crétaux, J.-F., S. Calmant, V. Romanovski, F. Perosanz, S. Tashbaeva, P. Bonnefond, D. Moreira, C. K. Shum, F. Nino, M. Bergé-Nguyen, S. Fleury, P. Gegout, R. Abarca Del Rio, and P. Maisongrande, 2011b: Absolute calibration of Jason radar altimeters from GPS kinematic campaigns over Lake Issykkul. *Marine Geodesy* **34**(3-4), 291-318.

Da Silva, J. S., S. Calmant, F. Seyler, O. Correa, R. Filho, G. Cochonneau, and W. J. Mansur, 2010: Water levels in the Amazon basin derived from the ERS 2 and ENVISAT radar altimetry missions. *Remote Sens. Environ.* **114**(10), 2160-2181.

De Oliveira Campos, I., F. Mercier, C. Maheu, G. Cochonneau, P. Kosuth, D. Blitzkow, and A. Cazenave, 2001: Temporal variations of river basin waters from Topex/Poseidon satellite altimetry. Application to the Amazon Basin. *C. R. Acad. Sci.* **333**, 633– 643.

Dumont, J. P., V. Rosmorduc, N. Picot, S. Desai, H. Bonekamp, J. Figa, J. Lillibridge, and R. Scharroo, 2009: *OSTM/Jason-2 products handbook.* Issue 1.3, CNES SALP-MU-M-OP-15815-CN, EUMETSAT EUM/OPS-JAS-MAN/08/0041, JPL OSTM-29-1237, NOAA/NESDIS Polar Series/OSTM J400.

Fearnside, P. M., 1989: Brazil's Balbina Dam: Environment versus the legacy of the pharaohs in Amazonia. *Environ. Manage.*, **13**, 401-423.

Frappart, F., S. Calmant, M. Cauhopé, F. Seyler, and A. Cazenave, 2006: Preliminary results of ENVISAT RA-2-derived water levels validation over the Amazon basin. *Remote Sens. Environ.* **100**(2), 252–264.

Fu, L. L., and A. Cazenave, 2001: *Satellite altimetry and earth sciences. A handbook of techniques and applications,* Inter. Geophys. Series **69**, pp. 463, Academic Press, San Diego, CA.

Fu, L. L., et al., 2003: Wide-swath altimetric measurement of ocean surface topography. *JPL Publ.* 03-002, pp. 67, Pasadena, CA.

Gana News Agency (2010).

Gana Media News (2010).

Getirana, A. C. V., M. P. Bonnet, E. Roux, S. Calmant, O. C. Rotunno Filho, and W. J. Mansur, 2009: Hydrological monitoring of large poorly gauged basins: a new approach based on spatial altimetry and distributed rainfall-runoff model. *J. Hydrol.* **1,** 4–5.

Glantz, M.H., R. W. Katz, and N. Nicholls, 1991: *Teleconnections Linking Worldwide Climate Anomalies: Scientific Basis and Societal Impact*. Cambridge University Press, 535 pp.

Gommenginger, C., P. Challenor, J. Gomez-Enri, G. Quartley, M. Strokosz, P. Berry, J. Garlick, D. Cotton, D. Carter, C. Roger, S. Haynes, I. LeDuc, M. Milagro, and J. Benveniste, 2006: New scientific applications for ocean, coastal, land and ice remote sensing with Envisat radar altimeter individual echoes. In *Proceedings 15 Years Progress Radar Altimetry Symposium*.

Gronewold, A. D., A. H. Clites, T. S. Hunter, and C. A. Stow, 2011: An appraisal of the Great Lakes advanced hydrologic prediction system. *J. Great Lakes Res*., **37**, 577-583.

Guyot, J.L., M. A. Roche, L. Noriega, H. Calle, and J. Quintanilla, 1990: Salinities and sediment transport in the Bolivian Highlands. *J. Hydrol.*, **113,** 147–162.

Huffman, G.J., R.F. Adler, D.T. Bolvin, G. Gu, E.J. Nelkin, K.P. Bowman, E.F. Stocker, and D.B. Wolff, 2007: The TRMM Multi-satellite Precipitation Analysis: Quasi-Global, Multi-Year, Combined-Sensor Precipitation Estimates at Fine Scale. *J. Hydrometeor*., **8**, 33-55.

Hughes, R. H., and J. S. Hughes, 1992: *A Directory of African Wetlands*. IUCN, 820 pp.

Inomata, H., and K. Fukami, 2008: Restoration of historical hydrological data of Tonle Sap Lake and its surrounding areas. *Hydrol. Processes,* **22,** 1337-1350.

International Great Lakes datum (IGLD) (1985).

International Lake Environment Committee, cited 1986: The United Nations Environment Program and Environment Agency, Government of Japan. World Lakes Database. [Available online at http://www.ilec.or.jp/database/database_old.html.]

Isiorho, S. A., G. Matisoff, and K. S. Wehn, 1996: Seepage relationships between Lake Chad and the Chad aquifer, *Ground Water*, **34**, 819– 826.

Janowiak, J.E., 1988: An investigation of interannual rainfall variability in Africa. *J. Climate*, **1,** 240-255.

Jimoh, O. D, 2008: Optimized operation of Kainji Reservoir. *J. Technol*., **12**, 34-42.

Jury, M. R., 2009: An Intercomparison of Observational, Reanalysis, Satellite, and Coupled Model data on Mean Rainfall in the Caribbean. *J. Hydrometeo*., **10**(2), 413-430.

Kebede, S., Y. Travi, T. Alemayehu, and V. Marc, 2006: Water balance of Lake Tana and its sensitivity to fluctuations in rainfall, Blue Nile basin, Ethiopia. *J. Hydrol.,* **316,** 233–247.

Kouraev, A. V., S. V. Semovski, M. N. Shimaraev, N. M. Mognard, B. Legresy, and F. Remy, 2007: Observations of lake Baikal ice from satellite altimetry and radiometry. *Remote Sens. Environ*. **108**, 240–253.

Kouraev, A. V., J.-F. Crétaux, S. A. Lebedev, A. G. Kostianoy, A. I. Ginzburg, N. A. Sheremet, R. Mamedov, E. A. Zhakharova, L. Roblou, F. Lyard, S. Calmant, and M. Bergé-Nguyen, 2011: Satellite Altimetry Applications in the Caspian Sea. Chap. 13 in *Coastal Altimetry*, S. Vignudelli, A. G. Kostianoy, P. Cipollini, J. Benveniste, Eds., pp. 331-366, Springer Book Publications.

LakeNet, cited 1997: World lakes network. [Available online at http://www.worldlakes.org/.]

Lee, H., C. K. Shum, K.-H. Tseng, J.-Y. Guo, and C.-Y. Kuo, 2011: Present-day lake level variation from Envisat altimetry over the Northeastern Qinghai-Tibetan plateau: links with precipitation and temperature. *Terr. Atmos. Ocean. Sci*. **22**(2), 169-175.

Magaña, V., J. A. Amador, and S. Medina, 1999: The midsummer drought over Mexico and Central America. *J. Climate*, **12**, 1577-1588.

Magome, J., H. Ishidaira, and K. Takeuchi, 2004: Monitoring water storage variation in Lake Tonle Sap by satellite for water resources management. *Proc. Int. Conf. on Advances in Integrated Mekong River Management*, Vientiane, Laos, Mekong River Comission, 335-338.

Maheu, C., A. Cazenave, and C. R. Mechoso, 2003: Water level fluctuations in the Plata Basin (South America) from Topex/Poseidon Satellite Altimetry. *Geophys. Res. Lett*. **30**(3), 1143–1146.

Marengo, J. A., and Coauthors, 2008: The drought of Amazonia in 2005. *J. Climate*, **21** (3), 495-516.

Medina, C. E., J. Gomez-Enri, J. J. Alonso, and P. Villares, 2008: Water level fluctuations derived from ENVISAT Radar altimetry (RA-2) and *in situ* measurements in a subtropical water body: lake Izabal (Guatemala). *Remote Sens. Environ*. **112**, 3604–3617.

Mekong River Commission, 2005: *Overview of the Hydrology of the Mekong Basin*. Mekong River Commission, 73 pp.

Mercier, F., A. Cazenave and C. Maheu, 2002: Interannual lake level fluctuations (1993-1999) in Africa from TOPEX/Poseidon: Connections with ocean-atmosphere interactions over the Indian Ocean. *Global Planet. Change*, **32,** 141-163.

Mertes, L. A. K., A. G. Dekker, G. R. Brakenridge, C. M. Birkett, and G. Létourneau, 2004: Rivers and lakes. In *Natural resources and environment manual of remote sensing*, S. L. Ustin, A. Rencz, Eds., **5**, Wiley, New York.

Misra, V., and Y. N. Zhang, 2007: The fidelity of NCEP CFS seasonal hindcasts over Nordeste. *Month. Weath. Rev*., **135**, 618-627.

Morris, C. S., and S. K. Gill, 1994: Variation of Great Lakes water levels derived from Geosat altimetry. *Water. Resour. Res.* **30**(4), 1009–1017.

Murtugudde, R., J. P. McCreary, and A. J. Busalacchi, 2000: Oceanic processes associated with anomalous events in the Indian Ocean with relevance to 1997-1998. *J. Geophys. Res*., **105,** 3295-3306.

Ngongondo, C., C.-Y. Xu, L. Gottschalk, and B. Alemaw, 2011: Evaluation of spatial and temporal characteristics of rainfall in Malawi: a case of data scarce region. *Theor. Appl. Climatol.* **106**, 79-93.

Nicholson, S.E., and J. Kim, 1997: The relationship of the El Niño-Southern Oscillation to African rainfall. *Int. J. Climatol.*, **17,** 117-135.

Nicholson, S.E., X. Yin, M. B. Ba, 2000: On the feasibility of using lake water balance model to infer rainfall: An example from Lake Victoria. *Hydrol. Sci. J.*, **45,** 75-95.

Nicholson, S.E., and Coauthors, 2003: Validation of TRMM and other rainfall estimates with a high-density gauge dataset for West Africa. Part II: Validation of TRMM rainfall products. *J. Appl. Meteorol*., **42,** 1355-1368.

Ricko, M., J. Carton, and C. Birkett, 2011: Climatic Effects on Lake Basins. Part I: Modeling Tropical Lake Levels. *J. Clim.* **24**, 2983-2999.

Ričko, M., C. M. Birkett, J. A. Carton, and J.-F. Crétaux, 2012: Intercomparison and Validation of Continental Water Level Products Derived from Satellite Radar Altimetry. Submitted to *J. App. Rem. Sens*, in review.

Roche, M. A., J. Bourges, J. Cortes and R. Mattos, 1992: Climatology and hydrology of the Lake Titicaca basin. *Lake Titicaca: A Synthesis of Limnological Knowledge, Monogr. Biol.*, Vol. 68, Kluwer Academic Publishers, 63-88.

Ropelewski, C. F. and M. S. Halpert, 1996: Quantifying Southern Oscillation-precipitation relationships. *J. Climate*, **9,** 1043–1059.

Ross, K., and R. McKellip, 2006: Verification and Validation of NASA-Supported Enhancements to PECAD's Decision Support Tools. NASA/John C. Stennis Space Center, Mississippi.

Sarch, M.-T., and C.M. Birkett, 2000: Fishing and farming at Lake Chad: responses to Lake level fluctuations. *Geogr. J.* **166**(2), 156-172.

Saha, S., S. Nadiga, C. Thiaw, J. Wang, W. Wang, Q. Zhang, H. M. van den Dool, H.-L. Pan, S. Moorthi, D. Behringer, D. Stokes, M. Pena, S. Lord, G. White, W. Ebisuzaki, P. Peng, P. Xie , 2006 : The NCEP Climate Forecast System. *J. Climate*, **19**, 3483-3517.

Saha, Suranjana, et. al., 2010: The NCEP Climate Forecast System Reanalysis. *Bull. Amer. Meteor. Soc*., **90**, 1015-1057.

Saha, S., S. Moorthi, X. Wu, J. Wang, S. Nadiga, P. Tripp, H-L. Pan, D. Behringer, Y-T. Hou, H. Chuang, M. Iredell, M. Ek, J. Meng, R. Yang, 2012: The NCEP Climate Forecast System Version 2. To be submitted to *J. Climate*.

Scharroo, R., and W. H. F. Smith, 2010: A GPS-based climatology for the total electron content in the ionosphere. Submitted to *J. Geophys. Res.*

Shum, C., Y. Yi, K. Cheng, C. Kuo, A. Braun, S. Calmant, and D. Chambers, 2003: Calibration of Jason-1 altimeter over Lake Erie. *Marine Geodesy*, **26**(3-4), 335–354.

Simmons, A., S. Uppala, D. Dee, and S. Kobayashi, 2007a: ERA-Interim: New ECMWF reanalysis products from 1989 onwards. *ECMWF Newsletter,* No. 110, ECMWF, Reading, United Kingdom, 25–35.

Simmons, A., S. Uppala and D. Dee, 2007b: Update on ERA-Interim. *ECMWF Newsletter,* No. 111, ECMWF, Reading, United Kingdom, 5.

Sombroek, W.G., 2001: Spatial and temporal patterns of Amazonian rainfall: Consequences for the planning of agricultural occupation and the protection of primary forests. *Ambio*, **30**, 388–396.

Swenson, S., and J. Wahr, 2009: Monitoring the water balance of Lake Victoria, East Africa, from space. *J. Hydrol*. **370**(1–4), 163–176.

Tapley, B. D., J. Ries, S. Bettadpur, D. Chambers, M. Cheng, F. Condi, B. Gunter, Z. Kang, P. Nagel, R. Pastor, T. Pekker, S. Poole, and F. Wang, 2005: GGM02—an improved Earth gravity field model from GRACE. *J. Geod.* **79**(8), 467–478.

Tonle Sap Biosphere Reserve Secretariat, cited 2006: Tonle Sap Biosphere Reserve (TSBR) environmental information database. [Available online at http://www.tsbr-ed.org/english/default.asp.]

Uppala, S., and Coauthors, 2004: ERA-40: ECMWF 45-year reanalysis of the global atmosphere and surface conditions 1957–2002. *ECMWF Newsletter,* No. 101, ECMWF, Reading, United Kingdom, 2–21.

Uppala, S. M., D. Dee, S. Kobayashi, P. Berrisford, and A. Simmons, 2008: Towards a climate data assimilation system: Status update of ERA-Interim. *ECMWF Newsletter*, No. 115, ECMWF, Reading, United Kingdom, 12-18.

Vallet-Coulomb, C., D. Legesse, G. Gasse, Y. Travi, and T. Chernet, 2001: Lake evaporation estimates in tropical Africa (Lake Ziway, Ethiopia). *J. Hydrol.*, **245,** 1-17.

Van Campo, E. and F. Gasse, 1993: Pollen- and diatom-inferred climatic and hydrological changes Sumxi Co basin (Western Tibet) since 13 000 yr B.P. *Quat. Res.*, **39,** 300-313.

Vijverberg, J., F. A. Sibbing and E, Dejen, 2009: Lake Tana: Source of the Blue Nile. *The Nile: Origin, Environments, Limnology and Human Use*, *Monogr. Biol*., Vol. 89, Springer, 163-192.

Vintzileos, A., and W. M. Thiaw, 2006: On the forecast of cumulative precipitation at subseasonal time-scales over the Sahel. *Geophys. Res. Lett*., **33**, 14, L14703.

World Meteorological Organization (WMO), 1994: Guide to hydrological practices. In *Data acquisition and processing, analysis, forecasting and other applications*, WMO-No.**168**, Geneva, Switzerland.

Xie, P., J.E. Janowiak, P. A. Arkin, R. F. Adler, A. Gruber, R. R. Ferraro, G. J. Huffman, and S. Curtis, 2003: GPCP pentad precipitation analyses: An experimental dataset based on gauge observations and satellite estimates. *J. Climate*, **16,** 2197-2214.

Xie, S. P. and J. A. Carton, 2004: Tropical Atlantic variability: Patterns, mechanisms, and impacts. *Earth Climate: The Ocean-Atmosphere Interaction, Geophys. Monogr*., Vol. 147, Amer. Geophys. Union, 121-142.

Yang, S., Y. D. Jiang, D. W. Zheng, et al. 2009: Variations of US Regional precipitation and simulations by the NCEP CFS: Focus on the Southwest. *J. Climate*, **22** (12), 3211-3231.

Yoo, J.-M., and J. A. Carton, 1990: Annual and interannual variation of the freshwater budget in the tropical Atlantic and the Caribbean Sea, *J. Phys. Oceanogr*., **20**, 831– 845.

Yua, A. W., M. A. Stephen, S. X. Li, G. B. Shaw, A. Seas, E. Dowdye, E. Troupaki, P. Liiva, D. Poulios, and K. Mascetti, 2010: Space laser transmitter development for ICESat-2 mission. In *Proceedings of SPIE* **7578**, 757809-1.

Yuan, X., E. F. Wood, L. Luo, and M. Pan, 2011: A first look at Climate Forecast System version 2 (CFSv2) for hydrological seasonal prediction. *Geophys. Res. Lett*., **38**, L13402.

Zhang, G., H. Xie, S. Duan, M. Tian, and D. Yi, 2011: Water level variation of Lake Qinghai from satellite and *in situ* measurements under climate change. *J. Appl. Remote Sens*. **5**, 053532.